Computing the ECH capacities for the rotating Kepler problem

Dissertation

zur Erlangung des akademischen Grades

DR. RER. NAT.

eingereicht an der

MATHEMATISCH-NATURWISSENSCHAFTLICH-TECHNISCHEN FAKULTÄT

DER UNIVERSITÄT AUGSBURG

von

Amin Mohebbi

am

Augsburg, Juli 2020

Betreuer:	Prof. Dr. Urs Frauenfelder, Universität Augsburg
Gutachter:	Prof. Dr. Felix Schlenk, Universität Neuchâtel
Gutachter:	Prof. Dr. Gabriele Benedetti, Universität Heidelberg
Tag der mündlichen Prüfung:	24.07.2020
Amin Mohebbi:	Computing the ECH capacities for the rotating Kepler problem

To Sahar and Victoria

Abstract

The rotating Kepler problem is a special case of *the restricted three body problem* such that the mass of one primaries in the R3BP is zero. The R3BP and the RKP have many applications in classical mechanics and dynamical systems. Since the Kepler problem gives us mathematical models to explain the moving of the planets, satellites, and their Orbits, we are interested to study the dynamics of them on the space in a rotating coordinate system which is independent of time via the RKP.

In this thesis, we are going to compute the ECH capacities for the RKP that by these capacities with the goal to find a sharp embedding obstruction between the symplectic 4-manifold belonging to the RKP and another symplectic 4-manifold.

In the first step, we will give an introduction to symplectic manifolds and the study of the Hamiltonian of the RKP, the Hillś region of the RKP and the periodic orbits of the RKP. In chapter 4, we will see the Ligon-Schaaf symplectomorphism and the Levi-Civita regularization then, in the next chapter, by using them we will define a *special concave toric domain* for the RKP which is a symplectic 4-manifold and we will find the weights of the SCTD of the RKP when the energy $c \leqslant -\frac{3}{2}$ via the extension of a new method to computing ECH capacities of a concave toric domain with the help of a new tree which is introduced in chapter 6. In the last step, we will use those weights and compute some ECH capacities of the RKP for $c \leqslant -\frac{3}{2}$ and more examples in the case $c = -\frac{3}{2}$.

To obtain the SCTD for the RKP, we assumed the Hamiltonian of the RKP as follows,

$$K = \frac{1}{2}|p|^2 - \frac{1}{|q|} + q_1 p_2 - q_2 p_1 \quad ; \quad (q, p) \in T^*(\mathbb{R}^2 \setminus \{0\}).$$

Then by applying the stereographic projection, the Ligon-Schaaf symplectomorphism and the Levi-Civita regularization respectively we got a convex function as

$$\tilde{K} : T^*\mathbb{C} \setminus \{0\} \longrightarrow \mathbb{R}$$
$$\tilde{K} = -\frac{1}{8\mu_1^2} + 2\mu_2,$$

for the energy $c \leqslant -\frac{3}{2}$. This function helps us to define the SCDT in the rotating coordinate system which is rotated by 45 degrees.

In the following, using the new tree, we will obtain the weights of the SCTD as functions which are only dependent on the energy in order to compute the ECH capacities for the RKP. Finally, we offer some theorems, properties of the weights and the ECH capacities of the RKP and examples for the fixed energy $c = -\frac{3}{2}$.

Acknowledgments

First of all, this thesis is dedicated to the memory of my beloved and honorable father. I would like to thank my father and mother for supporting me spiritually throughout my life. I am grateful to my wife for her patience and help. I would also like to thank my sister and brothers for their supports and helps.

Foremost, I would like to express my sincere gratitude to my supervisor Urs Frauenfelder for his continuous support of my Ph.D. study and research, as well as for his patience, motivation, enthusiasm, and immense knowledge. I was always inspired by his guidance during my research and writing of my thesis. I could not have imagined having a better supervisor for my Ph.D. study.

Besides my supervisor, I would like to thank the mathematical community at the University of Augsburg, and especially the sympathetic group, Kai Cieliebak, Alexandru Doicu, Christine Fischer, Pavel Hájek, Kathrin Helmsauer, Robert Nicholls, Lei Zhao, Seongchan Kim, Jennifer Gruber, Miguel Barbosa Pereira, Agustin Moreno Lopéz, Julius Natrup and Bowen Liu for their encouragement and support.

My sincere thanks go also to Filex Schlenk, Gabriele Benedetti and Edward Belbruno for their useful advice helping me better understand the mathematical subjects. Finally, I would like to thank Otto van Koert and the symplectic group at the University of Heidelberg for many interesting scientific discussions.

This work was funded by Deutsche Forschungsgemeinschaft(DFG).

Contents

Contents **viii**

1 Introduction **1**

1.1 The Rotating Kepler Problem and Regularization 1

1.2 The Concave Toric Domain 4

1.3 The ECH-capacities 7

1.4 Computing of ECH Capacities 8

2 Introduction to Symplectic Geometry **12**

2.0.1 Symplectic manifolds 12

2.0.2 Hamiltonian Vector Fields 13

2.0.3 Contact Manifold 14

2.1 Poisson bracket and Noether's theorem 15

2.2 The angular momentum and the Runge-Lenz vector 18

2.2.1 Angular Momentum 18

2.2.2 The Kepler problem and its integrals 19

2.2.3 The Runge-Lenz Vector 19

2.2.4 The Planar Kepler Problem 21

2.3 Mechanical Hamiltonian 22

2.4 Magnetic Hamiltonian 24

3 The Rotating Kepler Problem and its Periodic Orbits **25**

3.1 The Hamiltonian of the Rotating Kepler Problem 25

3.2 Hill's Region for the Rotating Kepler Problem 26

3.3 Periodic Orbits of the Rotating Kepler Problem 27

3.4 Periodic Orbits of the Second Kind 30

4 Regularization **34**

4.1 The Ligon-Schaaf Regularization 34

4.2 The Levi Civita Regularization 38

4.3 Levi-Civita Regularization and Uncoupled Harmonic Oscillators . . . 40

5 The Special Concave Toric Domain for The Rotating Kepler Problem 41
5.1 Introduction . . . 41
5.2 The Special Concave Toric Domain . . . 41

6 Construction of a New Tree and Slopes of Tori 48
6.0.1 The Calkin-Wilf tree . . . 48
6.1 The Stern-Brocot tree . . . 49
6.2 Introducing a New tree . . . 52
6.2.1 The New Tree . . . 52

7 Introduction to ECH Capacities 54
7.1 ECH capacities . . . 54
7.2 Concave toric domain . . . 56
7.3 Weight Expansions . . . 57

8 Computation of some ECH capacities for the RKP 65
8.1 Introduction to the computation . . . 65
8.2 The First Weight W_1 for the portion ω_1 in the SCTD $\mathcal{K}_c^b$ . . . 65
8.3 The Critical Energy Values and the Slopes of Weights . . . 68
8.4 The Higher Weights . . . 70
8.4.1 The Second Weight W_2 for the portion ω_{11} in the SCTD $\mathcal{K}_c^b$ . . . 70
8.4.2 The Third Weight W_3 for the portion ω_{111} in the SCTD $\mathcal{K}_c^b$ . . . 73
8.4.3 The Fourth weight W_4 for the region ω_{110} in the SCTD $\mathcal{K}_c^b$ . . . 77
8.4.4 The Fifth weight W_5 for the portion ω_{1100} in the SCTD $\mathcal{K}_c^b$ . . . 81
8.5 The Integrals of the Regions . . . 84

9 Appendix 1 90
9.1 The Restricted Three Body Problem . . . 90
9.2 Time Dependent Transformation . . . 91
9.3 The Circular Restricted Three Body Problem in the Rotating Frame . . . 92
9.3.1 The Lagrangian Points . . . 94
9.4 Hill's Region . . . 100

Bibliography 102

Chapter 1

Introduction

1.1 The Rotating Kepler Problem and Regularization

The rotating Kepler problem is the Kepler problem in rotating coordinates. It is a limit case of the restricted three body problem, where the mass of one of the primaries is zero. The Hamiltonian for the planar Kepler problem is

$$H : T^*(\mathbb{R}^2 \setminus \{0\}) \longrightarrow \mathbb{R} \tag{1.1.1}$$

$$H(q,p) = \frac{1}{2}|p|^2 - \frac{1}{|q|}. \tag{1.1.2}$$

Angular momentum

$$L : T^*\mathbb{R}^2 \longrightarrow \mathbb{R} \tag{1.1.3}$$

$$(q,p) \mapsto q_1p_2 - q_2p_1 \tag{1.1.4}$$

generates the rotation. Therefore the Hamiltonian for the rotating Kepler problem is

$$K : T^*(\mathbb{R}^2 \setminus \{0\}) \longrightarrow \mathbb{R} \tag{1.1.5}$$

$$K = \frac{1}{2}|p|^2 - \frac{1}{|q|} + q_1p_2 - q_2p_1 \quad ; \quad (q,p) \in T^*(\mathbb{R}^2 \setminus \{0\}).$$

Thus we can write the equation 1.1.5 as

$$K = H + L. \tag{1.1.6}$$

This Hamiltonian system is a completely integrable system in the sense of Arnold-Liouville.

Lemma 1. *The angular momentum is preserved under the flow of* X_H *and therefore* H *and* L *Poisson commute.*

Proof. The standard $SO(2)$ action acts Hamiltonianly on $T^*\mathbb{R}^2$ with the momentum map L. Thus the Hamiltonian for the central force is $SO(2)$-invariant, so the Noether theorem implies the results. □

Since H and L Poisson commute, we can write

$$\{K, L\} = \{H, L\} + \{L, L\} = 0. \tag{1.1.7}$$

Here, we want to explain an appropriate concave toric domain which allows us to compute some of the ECH capacities of the rotating Kepler problem for each energy level $c \leqslant -\frac{3}{2}$, where $-\frac{3}{2}$ is the critical value of the Hamiltonian K.

For this goal, first we need to introduce a global symplectic transformation, that is the Ligon-Schaaf regularization, which maps the solutions of the Kepler problem to geodesics on the sphere without reparametrizing time [4], [5].

We use the standard inner product $< x, y >$ of $x, y \in \mathbb{R}^2$ in order to identify $x \in \mathbb{R}^2$ with the linear form

$$y \longmapsto < x, y >, \qquad \text{on} \quad \mathbb{R}^2. \tag{1.1.8}$$

Thus we can identify the phase space P, i.e. the cotangent bundle of $\mathbb{R}^2 \setminus \{0\}$, with the set of (q, p) such that $q \in \mathbb{R}^2$, $q \neq 0$ and $p \in \mathbb{R}^2$.

Consider the equation of motion of the Kepler problem as

$$\begin{aligned} \dot{q} &= p \\ \dot{p} &= -|q|^{-3} q \end{aligned} \tag{1.1.9}$$

where $|q| = < q, q >^{\frac{1}{2}}$ for the Euclidean norm of $q \in \mathbb{R}^2$.

The right hand side of the equation 1.1.9 is the Hamiltonian vector field X_H with respect to the symplectic form $dp_1 \wedge dq_1 + dp_2 \wedge dq_2$ for the Hamiltonian function

$$H(q, p) = \frac{1}{2}|p|^2 - |q|^{-1}, \qquad (q, p) \in P, \tag{1.1.10}$$

which is the total energy of the system.

Define the open subset of P,

$$P_- := \{(q, p) \in P \,|\, H(q, p) < 0\} \tag{1.1.11}$$

consisting of the part of the phase space where the energy is negative.

The solutions of the Kepler system will be mapped to the geodesics of the unit sphere S of dimension 2 in $\mathbb{R}^3$ on which the rotation group $SO(3)$ acts naturally.

We consider the complement T of the zero section in the cotangent bundle of S as the phase space. We can describe T as the set of $(x, y) \in \mathbb{R}^3$ such that $< x, x >= 1$, $< x, y >= 0$ and $y \neq 0$.

The momentum mapping of the infinitesimal Hamiltonian action of $SO(3)$ on T is given by

$$\tilde{J} : (x, y) \longrightarrow x \wedge y. \tag{1.1.12}$$

Ligon and Schaaf [4] discovered a symplectomorphism from the phase space of the Kepler problem to the phase space of the geodesic flow on the sphere S^2, i.e.

$$\Phi_{LS} : H^{-1}(-\infty, 0) = P_- \longrightarrow T^*S^2 \setminus (S^2 \cup T^*_N S^2) = T \setminus (T^*_N S^2) \tag{1.1.13}$$

where $T^*_N S^2$ is the cotangent space at the north pole. In fact the map of Ligon and Schaaf works in every dimension. This symplectomorphism has the following properties.

Define the Delaunay Hamiltonian as,

$$\tilde{H}(x, y) := \frac{-1}{2|y|^2}, \qquad x, y \in T \tag{1.1.14}$$

where we recall that T is $T^*S^2 \setminus S^2$, i.e. the cotangent bundle of S^2 with the zero section removed.

Ligon and Schaaf showed that

$$\Phi^*_{LS} H = \tilde{H}, \tag{1.1.15}$$

and

$$\Phi^*_{LS} L = \tilde{J}_1 \tag{1.1.16}$$

where $\tilde{J} = (J_1, J_2, J_3)$ is the angular momentum on the cotangent bundle in the phase space T.

Because Φ^*_{LS} is a symplectomorphism which satisfies 1.1.15 it pulls back solutions of the Kepler problem with negative energy to geodesics on the sphere missing the north pole. We regularize the Kepler problem by adding the geodesics through the north pole. They correspond to collisions.

In the following, we abbreviate the Levi-Civita transformation by

$$\mathcal{L} : \mathbb{C}^2 \setminus \{0\} \longrightarrow T^*S^2 \setminus S^2. \tag{1.1.17}$$

The Levi-Civita transformation is a $2:1$ map which up to a constant factor is symplectic when we think of $\mathbb{C}^2$ as $T^*\mathbb{C}$. It pulls back the geodesic flow on S^2 to the flow of two uncoupled oscillators.

We introduce the following function

$$\mu = (\mu_1, \mu_2) : T^*\mathbb{C} \longrightarrow [0, \infty) \times \mathbb{R} \subset \mathbb{R}^2 \tag{1.1.18}$$

$$(u, v) \longmapsto \begin{cases} \frac{1}{2}(|u|^2 + |v|^2) \\ u_1 v_2 - u_2 v_1, \end{cases} \tag{1.1.19}$$

where μ can be thought of as the moment map for the torus action on $T^*(\mathbb{C})$ given.

Proposition 2. *Let $\mathcal{L}$ and Φ_{LS} be the Levi-Civita regularization and the Ligon-Schaaf regularization respec-*

tively. For the function

$$\mathcal{L}^*\Phi_{LS}^*(K) = \mathcal{L}^*\Phi_{LS}^*(H+L) : \mathbb{C}^2 \setminus (\mathbb{C}^2 \setminus \{0\}) \longrightarrow \mathbb{R},$$

we have the following formula

$$\mathcal{L}^*\Phi_{LS}^*(K) = -\frac{1}{8\mu_1^2} + 2\mu_2. \tag{1.1.20}$$

Proof. We will give the proof later in Chapter 5. □

1.2 The Concave Toric Domain

Proposition 3. *There exists a linear symplectomorphism between the symplectic manifold* $\mathbb{C} \oplus \mathbb{C}$ *and the cotangent bundle* $T^*\mathbb{C}$*. In other words, we have the linear symplectomorphism*

$$S : (\mathbb{C} \oplus \mathbb{C}, \omega_0) \longrightarrow (T^*\mathbb{C}, \omega_1). \tag{1.2.1}$$

Note that in Chapter 5 we will show the function $\mathcal{L}^*\Phi_{LS}^*(K)$ can be extend to $\mathbb{C}^2 \setminus \{0\}$ so we use the abbreviation

$$\tilde{K} : T^*\mathbb{C} \setminus \{0\} \longrightarrow \mathbb{R} \tag{1.2.2}$$

$$\tilde{K} := -\frac{1}{8\mu_1^2} + 2\mu_2, \tag{1.2.3}$$

for $c \leqslant -\frac{3}{2}$.

Define the first quadrant in $\mathbb{R}^2$ by

$$Q := [0,\infty) \times [0,\infty). \tag{1.2.4}$$

Moreover, we set

$$Q_{\frac{1}{2}} := \{(x,y) \in \mathbb{R}^2 : x \geqslant 0, |y| \leqslant x\}. \tag{1.2.5}$$

Suppose $\Omega \subset Q$ is a closed subset of the first quadrant, we give the definition of a concave toric domain which is defined by "K. Choi, D. Cristofaro-Gardiner, D. Frenkel, M. Hutchings, V. G. B. Ramos," [3] as follows,

$$X_\Omega := \nu^{-1}(\Omega) \tag{1.2.6}$$

where

$$\nu = (\nu_1, \nu_2) : \mathbb{C}^2 \longrightarrow [0,\infty) \times [0,\infty) \subset \mathbb{R}^2 \tag{1.2.7}$$

$$(z_1, z_2) \mapsto (\pi|z_1|^2, \pi|z_2|^2). \tag{1.2.8}$$

Note that ν is a moment map for the torus action $(\nu_1, \nu_2)(z_1, z_2) = (e^{i\theta_1} z_1, e^{i\theta_2} z_2)$ on $\mathbb{C}^2$. Alternatively we can write the symplectic 4-manifold with boundary X_Ω as

$$X_\Omega = \{z = (z_1, z_2) \in \mathbb{C}^2 | \pi(|z_1|^2, |z_2|^2) \in \Omega\}. \tag{1.2.9}$$

Definition 4. (Concave toric domain) We say that a toric domain X_Ω is a concave toric domain if Ω is a closed region bounded by the horizontal segment from $(0,0)$ to $(a,0)$, the vertical segment from $(0,0)$ to $(0,b)$ and the graph of a convex function $f : [0,a] \longrightarrow [0,b]$ with $f(0) = b$ and $f(a) = 0$, where $a > 0$ and $b > 0$.

Definition 5. (Special concave toric domain) A concave toric domain $X_\Omega \subset \mathbb{C}^2$ is called special if the function f satisfies additionally $f'(t) \geqslant -1$ for $t \in [0,a]$.

Define

$$\bar{S} : Q \longrightarrow Q_{\frac{1}{2}} \tag{1.2.10}$$

to be the rotation by 45 degree in clockwise direction combined with a dilation by $\frac{1}{\sqrt{2}\pi}$.

Note that

$$\begin{aligned} \bar{S}(\frac{1}{2\pi}(\nu_1 + \nu_2)) &= \mu_1 \\ \bar{S}(\frac{1}{2\pi}(\nu_1 - \nu_2)) &= \mu_2. \end{aligned} \tag{1.2.11}$$

So that we get following commutative diagram with S, $\bar{S}$, ν and μ as

$$\begin{array}{ccc} \mathbb{C} \oplus \mathbb{C} & \xrightarrow{S} & T^*\mathbb{C} \\ \nu \downarrow & & \downarrow \mu \\ Q & \xrightarrow{\bar{S}} & Q_{\frac{1}{2}} \end{array} \tag{1.2.12}$$

If we define

$$\Omega' := S^*(\Omega) \subset Q_{\frac{1}{2}}. \tag{1.2.13}$$

We obtain

$$X_{\Omega'} = \mu^{-1}(\Omega') = S(X_\Omega) \tag{1.2.14}$$

in $T^*\mathbb{C}$.

For the purpose of this thesis it is more convenient to think of a toric domain as a subset of $T^*\mathbb{C}$ instead of $\mathbb{C}^2$. We do this by using the above formula. In the following we think of Ω as a closed subset of $Q_{\frac{1}{2}}$ and omit the prime.

We next introduce the notation of a special concave toric domain

Remark 6. Using the above identification of $\mathbb{C}^2$ and $T^*\mathbb{C}$ and toric domain X_Ω is special concave if and only if

there exists a convex function

$$g : [a, b] \longrightarrow \mathbb{R}, \qquad 0 < a < b < \infty, \tag{1.2.15}$$

with properties $g(a) = a$, $g(b) = -b$ such that $\Omega \subset Q_{\frac{1}{2}}$ is bounded by the segment $\{(t, t) : t \in [0, a]\}, \{(t, -t) : t \in [0, b]\}$ and the graph of the convex function g.

Remark 7. In the following, we are working with $\Omega \subset Q_{\frac{1}{2}}$. If Ω satisfies the conditions of remark 1, we refer to $X_\Omega := \mu^{-1}(\Omega)$ as a special concave toric domain.

Assume $c \leqslant -\frac{3}{2}$, we define a closed subset of $Q_{\frac{1}{2}}$ by

$$\mathcal{K}_c := \mu(\tilde{K}^{-1}(-\infty, c)) \subset Q_{\frac{1}{2}}. \tag{1.2.16}$$

Note that $\mathcal{K}_c$ has two connected components, one bounded and one unbounded, i.e. we write

$$\mathcal{K}_c = \mathcal{K}_c^b \cup \mathcal{K}_c^u, \tag{1.2.17}$$

for $\mathcal{K}_c^b$ the bounded connected component and $\mathcal{K}_c^u$ the unbounded connected component. See the following figures,

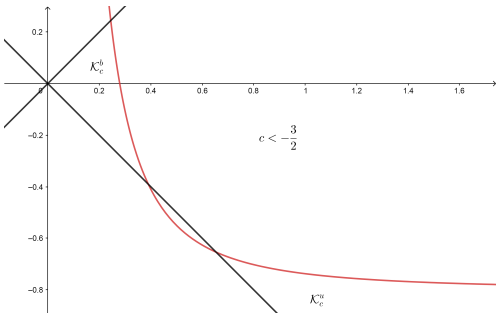

Figure 1.2.1: $c < -\dfrac{3}{2}$

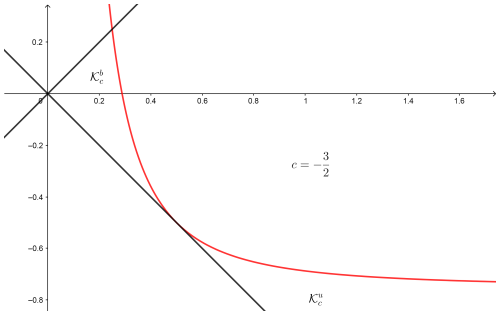

Figure 1.2.2: $c = -\dfrac{3}{2}$

Theorem 8. *For $c \leqslant -\frac{3}{2}$, we have*

$$\tilde{K}^{-1}((-\infty, c)) = X_{\mathcal{K}_c^b} \cup X_{\mathcal{K}_c^u} \subset T^*\mathbb{C} \tag{1.2.18}$$

and $X_{\mathcal{K}_c^b}$ is a special concave toric domain.

1.3 The ECH-capacities

In the first part of this chapter, we introduced the special concave toric domain $\mathcal{K}_c^b$. We obtained this domain for each energy value $c \leqslant -\frac{3}{2}$ (the critical value of K) after regularization with Φ_{LS} and taking double cover with $\mathcal{L}$. The energy hypersurface $K^{-1}(c)$ is pulled back to the boundary of the concave toric domain $\mathcal{K}_c$.

In this thesis, we are going to work on the bounded part of $\mathcal{K}_c$, that means the special concave toric domain $\mathcal{K}_c^b$ which lives in the coordinate space $Q_{\frac{1}{2}}$.

In the following diagram, we show the concave toric domain $\mathcal{K}_c$ for the energy $c \leqslant \frac{3}{2}$ and indicate the direct and the retrograde orbits on the graph for each level of the energy.

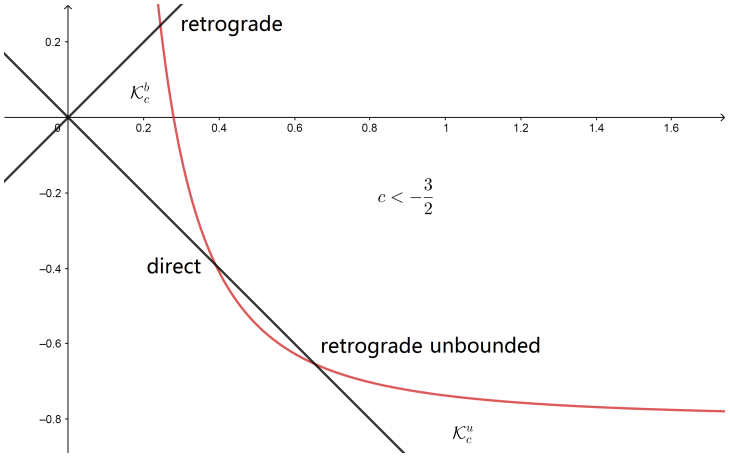

Figure 1.3.1: The direct and the retrograde orbits for an energy $c < -\frac{3}{2}$

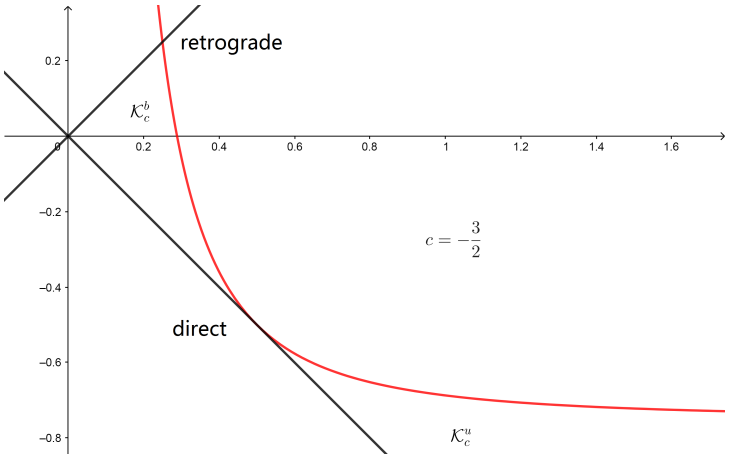

Figure 1.3.2: The direct orbit for the energy $c = -\frac{3}{2}$

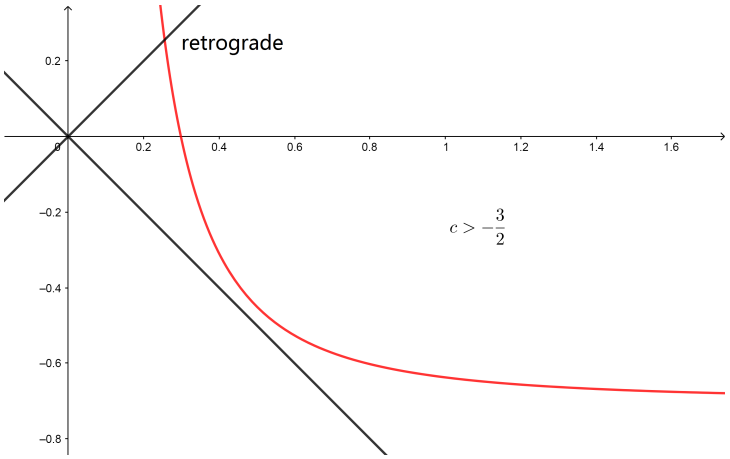

Figure 1.3.3: There is no direct for energy $c > -\frac{3}{2}$

As we can see from the graphs, it is impossible to define the concave toric domain when the energy is $c > -\frac{3}{2}$.

Given the special concave toric domain $\mathcal{K}^b_c$ in the standard coordinate space $\mathbb{C}^2 = \mathbb{R}^4$, this is a symplectic 4-manifold and we denote it by (X_Ω, ω_1). For the symplectic 4-manifold (X_Ω, ω_1) we want to compute the ECH capacities.

Given a compact 4-dimensional manifold with boundary (X, ω). The ECH capacities is a sequence of real numbers as

$$0 = c_0(X, \omega) \leqslant c_1(X, \omega) \leqslant \cdots \leqslant \infty \tag{1.3.1}$$

which give obstructions to embeddings between a symplectic 4-manifold with boundary into another and they satisfy some properties that will be given later.

1.4 Computing of ECH Capacities

First we will compute the weights for the special concave domain $\mathcal{K}^b_c$. Given the equation

$$-\frac{1}{8\mu_1^2} + 2\mu_2 - c = 0 \tag{1.4.1}$$

and let $\mu_1 = \mu_2$. Hence we have a cubic equation as

$$16\mu_1^3 - 8c\mu_1^2 + 1 = 0. \tag{1.4.2}$$

We compute the first and the second roots of the cubic equation and denote then by r_1 and r_2 respectively. Thus we have

$$r_1(c) =(\frac{c}{3}\cos(\frac{1}{3}\arccos(1+\frac{27}{4c^3})+\frac{2\pi}{3}))+\frac{c}{6}, \tag{1.4.3}$$

$$r_2(r_1) =r_2=-\frac{-1+\sqrt{1-4^3r_1^3}}{32r_1^2}. \tag{1.4.4}$$

Than we can write the first weight for the special domain $\mathcal{K}_c^b$ as

$$W_1(c)=\sqrt{2}r_1(c)=\sqrt{2}((\frac{c}{3}\cos(\frac{1}{3}\arccos(1+\frac{27}{4c^3})+\frac{2\pi}{3}))+\frac{c}{6}). \tag{1.4.5}$$

This weight corresponds to the node $\frac{1}{1}$ in the new tree which is introduced for the first time in Chapter 6 and the portion ω_1 in the special concave toric domain $\mathcal{K}_c^b$. For the higher weights, we need to define the T-periodic orbit for the RKP such as

Definition 9. A T-periodic orbit $\alpha:\mathbb{R}/T\mathbb{Z}\longrightarrow\mathbb{R}^4$ of the RKP is a k-fold covered ellipse in an l-fold covered coordinate system provided the following hold.

- There exists positive $l\in\mathbb{N}$ such that $T=2\pi l$, and
- the corresponding trajectory in the inertial coordinate system given by $\gamma(t):=\Phi_t^{-1}\alpha(t)$ is a k-fold covered ellipse of the standard Kepler problem.

The ellipses of positive eccentricity in an inertial system can form T^2 families of periodic orbits.

Given the torus comprised of k-fold covered ellipses in an l-fold covered rotating coordinates system we denote it with $T_{k,l}$. Some of these tori have special names. Namely, the torus $T_{2,1}$ is called Hekuba and the torus $T_{3,1}$ is called Hestia which play a prominent role in this thesis.

Consider a torus $T_{k,l}$, for all k and $l\in\mathbb{N}$. We find the critical energy value of T_{kl} with the following relation

$$c_{k,l}^+=-(\frac{1}{2}+\frac{l}{k})(\frac{k}{l})^{\frac{2}{3}}, \tag{1.4.6}$$

and the correspond slope with the torus $T_{k,l}$ and the energy $c_{k,l}^+$ with the relation

$$S_{k,l}=\frac{k+l}{-k+l}. \tag{1.4.7}$$

We can find the slopes correspond to tori $T_{k,l}$ for all $k,l\in\mathbb{N}$ by using the new tree which we introduce in Chapter 6.

Now given the asteroid Hekuba, i.e. the torus $T_{2,1}$. The critical energy value for the Hekuba is $c_{2,1}^+=-\sqrt[3]{4}$ and the slope correspond to the Hekuba is $S_{2,1}=-3$. Therefore we can compute the second weight for the ECH

capacities of the special concave domain $\mathcal{K}_c^b$ as

$$W_2(r_1) = \begin{cases} \sqrt{2}(r_2 - r_1) = \sqrt{2}(-\frac{-1+\sqrt{1-4^3 r_1^3}}{32 r_1^2} - r_1), & r_1 \leqslant \frac{1}{4}, \\ \sqrt{2}(\frac{3}{4\sqrt[3]{3}} + \frac{\sqrt[3]{9}}{8} + \frac{1}{2}(\frac{16 r_1^3 - 1}{16 r_1^2}) - r_1), & \frac{1}{4} \leqslant r_1 \leqslant \frac{1}{2}. \end{cases} \tag{1.4.8}$$

This weight corresponds to the node $\frac{1}{2}$ in the new tree and also the portion ω_{11} in the SCTD $\mathcal{K}_c^b$. For computing the second weight for the ECH capacities, we consider Hestia, i.e. the torus $T_{3,1}$. The critical energy value for Hestia is $c_{3,1}^+ = -\frac{5}{6}\sqrt[3]{9}$ and the slope corresponding to Hestia is $S_{3,1} = -2$. Thus we have the third weight for the ECH capacities of the special concave domain $\mathcal{K}_c^b$ corresponding to the portion ω_{110} as follows,

$$W_3(r_1) = \begin{cases} 0 & r_1 \leqslant x_2 \\ \sqrt{2} r_2(r_1) - (W_2(r_1) + W_1(r_1)) = \sqrt{2}(r_2(r_1) - x_2(r_1)), & x_2 \leqslant r_1 \leqslant x_3, \\ \sqrt{2} x_3 - (W_2(r_1) + W_1(r_1)) = \sqrt{2}(x_3(r_1) - x_2(r_1)), & x_3 \leqslant r_1 \leqslant \frac{1}{2}. \end{cases} \tag{1.4.9}$$

where r_2 is the second root of the cubic equation, x_2 is the intersection point of the slope -3 and the graph of the equation 1.4.1 and x_3 is the intersection point of the slope -2 and the graph of the equation 1.4.1 in the fourth quadrant of the standard coordinate system in $\mathbb{R}^2$.

Also we can find a relation for the fourth weight corresponds to the portion ω_{111} as follows,

$$W_4(r_1) = \begin{cases} \frac{1}{16(\sqrt[3]{\frac{1}{40}})^2} - \frac{1}{16 r_1^2} - 4 r_1 + 5(\sqrt[3]{\frac{1}{40}}) - W_2(r_1), & c_{3,2}^+ < c_{2,1}^+, \\ 0, & c_{2,1}^+ \leqslant c \leqslant -\frac{3}{2}. \end{cases} \tag{1.4.10}$$

Note that the weight $W_4(r_1)$ has special conditions that explained in Chapter 8.

We will proof in Chapter 8 that the weight $W_1(\mathcal{K}_c^b)$ is the largest weight of the SCTD for all $c \leqslant -\frac{3}{2}$. It even holds that

$$\frac{Area(\mathcal{K}_c^b - \omega_1)}{Area(\omega_1)} \leqslant \frac{1}{2}. \tag{1.4.11}$$

As a corollary we got for every $c - \frac{3}{2}$ the first weight W_1 corresponds to the first ECH capacities $c = -\frac{3}{2}$.

Finally in Chapter 8, by understanding all of the definition and properties of the weights we will compute the ECH capacities of the RKP. See the following table for the example. Note that we will show the weights $W_1, \cdots, W_5$ has the following order,

$$W_1 > W_4 > W_2 > W_5 > W_3 > W_k, \qquad \forall k \geqslant 6. \tag{1.4.12}$$

Rank	The ECH cap. for $\mathcal{K}^b_c$	The ECH cap. for $c = -\frac{3}{2}$
$c_1(\mathcal{K}^b_c)$	W_1	0.353554
$c_2(\mathcal{K}^b_c)$	$W_1 + W_4 = c_1 + W_4$	0.57732
$c_3(\mathcal{K}^b_c)$	$2W_1 = 2c_1$	0.707108
$c_4(\mathcal{K}^b_c)$	$2W_1 + W_4 = c_3 + W_2$	0.930874
$c_5(\mathcal{K}^b_c)$	$2W_1 + W_4 + W_2 = c_4 + W_2$	1.150121
$c_6(\mathcal{K}^b_c)$	$2W_1 + 2W_4 = 2c_2$	1.15464
$c_7(\mathcal{K}^b_c)$	$3W_1 + W_4 = 3c_1 + W_4$	1.284428
$c_8(\mathcal{K}^b_c)$	$3W_1 + W_4 + W_2 = c_7 + W_2$	1.503675
$c_9(\mathcal{K}^b_c)$	$3W_1 + 2W_4 = c_7 + W_4$	1.508194
$c_{10}(\mathcal{K}^b_c)$	$3W_1 + 2W_4 + W_2 = c_9 + W_2$	1.727441
$c_{20}(\mathcal{K}^b_c)$	$5W_1 + W_4 + W_2 + W_5$	2.2622493

Table 1.1: ECH capacities for $c = -\frac{3}{2}$

Chapter 2

Introduction to Symplectic Geometry

In this chapter, we will see some basic definitions and concepts of the Symplectic and the Contact geometry which are necessary in the following chapters. We will introduce the definition of symplectic manifolds, Hamiltonian flows and contact manifold and will give some of their properties. Then we will see some examples of them that will be useful in this thesis.

2.0.1 Symplectic manifolds

The archetypical example of a symplectic manifold is the cotangent bundle of a smooth manifold. We consider a finite dimensional C^∞ manifold N without boundary referred to as the configuration space and the cotangent bundle T^*N refereed to as the phase space. The cotangent bundle T^*N is endowed with a canonical 1-form $\lambda \in \Omega^1(T^*M)$ that is called the Liouville 1-form. Let $\dim N = n$ and take canonical coordinates $(q, p) = (q_1, \cdots, q_n, p_1, \cdots, p_n)$ of T^*N. Hence the Liouville 1-form becomes

$$\lambda(q, p) = \sum p_i dq_i. \tag{2.0.1}$$

The canonical symplectic form on T^*N is the exterior derivative of the Liouville 1-form, i.e.

$$\omega = d\lambda, \tag{2.0.2}$$

which in canonical coordinates is

$$\omega = \sum_{i=1}^{n} dp_i \wedge dq_i. \tag{2.0.3}$$

Motivated by this we define a symplectic manifold follows.

Definition 10. Define a symplectic manifold as a pair (M, ω) where M is a manifold and $\omega \in \Omega^2(M)$ is a two-form satisfying the following conditions

(i) ω is closed, i.e. $d\omega = 0$.

(ii) ω is non-degenerate, i.e. $\forall x \in M \;\; \xi \neq 0 \in T_xM \;\; \exists \; \eta \in T_xM \quad s.t. \;\; \omega(\xi \cdot \eta) \neq 0.$

The nondegeneracy of the symplectic form ω implies that M is even dimensional, i.e. $dimM = 2n$. Alternatively one can characterize the the nondegeneracy of ω by saying that

$$\omega \wedge \cdots \wedge \omega \qquad (n \;\; times) \tag{2.0.4}$$

never vanishes, thus M is orientable. Note that, using Darboux theorem, we can say all symplectic manifolds of the same dimension are locally symplectomorphism.

Let M be a symplectic manifold, a symplectomorphism $\psi \in Diff(M)$ is a diffeomorphism that preserve the symplectic form, i.e. ψ is a symplectomorphim if

$$\omega = \psi^*\omega, \tag{2.0.5}$$

and we denote the group of symplectomorphisms by $Symp(M, \omega)$ or for simplicity $Symp(M)$. In the general case we have

Definition 11. Assume that (M_1, ω_1) and (M_2, ω_2) are two symplectic manifolds. A symplectomorphism $\psi : M_1 \longrightarrow M_2$ is a diffeomorphism satisfying $\psi^*\omega_2 = \omega_1$.

Note that, because of nondegeneracy of ω, the linear map

$$T_qM \longrightarrow T_q^*M \tag{2.0.6}$$

$$v \mapsto \iota(v)\omega \tag{2.0.7}$$

is bijective.

2.0.2 Hamiltonian Vector Fields

Consider a symplectic manifold M and determine for any smooth function $H : M \longrightarrow \mathbb{R}$ a vector field $X_H : M \longrightarrow TM$ as

$$\iota(X_H)\omega = dH, \tag{2.0.8}$$

which is called the Hamiltonian vector field associated to the Hamiltonian function H.

Now if we assume M is closed then the vector field X_H generates an 1-parameter smooth group of diffeomorphisms $\phi_H^t \in Diff(M)$ with the following properties,

$$\frac{d}{dt}\phi_H^t = X_H \circ \phi_H^t, \qquad\qquad \phi_H^0 = id \tag{2.0.9}$$

This is named the Hamiltonian flow of H.

Using the identity

$$dH(X_H) = (\iota(X_H)\omega)(X_H) = \omega(X_H, X_H) = 0 \tag{2.0.10}$$

we can see that the vector field X_H is tangent to the level sets H =constant of H.

Using the above definitions we can give some essential properties of symplectomorphisms.

Proposition 12. *Let (M, ω) be a symplectic manifold.*

(i) The Hamiltonian flow ϕ_H^t is as a symplectomorphism, for every $t \in \mathbb{R}$.

(ii) For every Hamiltonian function $H : M \longrightarrow \mathbb{R}$ and every symplectomorphism $\psi \in \mathrm{Symp}(M, \omega)$ we have $X_{H\circ\psi} = \psi^* X_H$.

(iii) The Lie bracket of two Hamiltonian vector fields X_F and X_G is the Hamiltonian vector field $[X_F, X_G] = X_{\{F,G\}}$, where the Poisson bracket is defined by $\{F, G\} = \omega(X_F, X_G)$ which is explained in more detail in section 2.1.

Proof. McDuff, Salamon. Introduction to symplectic topology page 86 [6]. □

2.0.3 Contact Manifold

Unlike symplectic manifolds, contact manifolds are odd dimensional manifolds which have a contact form on it.

Given Σ is a $2n+1$-dimensional manifold and assume $\xi \in T\Sigma$ is a field of hyperplanes that is possibly integrable. For convenience, let ξ be transversally orientable, so we can assume ξ is the kernel of some 1-form α. We consider a vector field X as a section of ξ if and only if $\alpha(X) = 0$. This means that, $\alpha(X) = \alpha(Y) = 0$ is integrable if and only if $\alpha([X, Y]) = 0$ for all section $X \cdot Y : \Sigma \longrightarrow \xi$. Therefore ξ is integrable if and only if $\alpha \wedge (d\alpha)^n = 0$, then $d\alpha = 0$.

Definition 13. Let Σ be a manifold of dimension $2n+1$ and $\xi \subset T\Sigma$ be a transversally orientable hyperplane field, α is a 1-form with $\xi = \ker \alpha$ and $d\alpha$ is nondegenerate on ξ if and only if

$$\alpha \wedge (d\alpha)^n \neq 0, \tag{2.0.11}$$

the form α is called a contact form of the cotangent structure ξ.

Proposition 14. *Given the above definition,*

(i) Let α and α' are 1-forms such that $\xi = \ker \alpha = \ker \alpha'$. Then α is a contact form if and only if α' is.

(ii) If ξ is a contact structure then the symplectic bilinear form on ξ, induced by $d\alpha$ is independent of the choice of the contact form α up to a positive scaling function.

Proof. McDuff, Salamon. Introduction to symplectic topology, page 105 [6]. □

Notice: Two contact forms are equivalent if and only if they differ by a nonzero function on Σ, i.e. $0 < C^\infty(\Sigma)$ then two contact forms α and α' are equivalent if and only if $\alpha' = f\alpha$ where $f > 0$.

2.1 Poisson bracket and Noether's theorem

In this section we are going to study Poisson brackets and the Noether's theorem. For the first goal, we give the definition and some properties of the Poisson bracket.

Given a symplectic manifold (M, ω), and define the Possion bracket for the smooth function F and G by

$$\{F, G\} := \omega(X_F, X_G) = -dF(X_G) = dG(X_F) = -X_G(F) = X_F(G). \tag{2.1.1}$$

The Poisson bracket has the following dynamical interpretation. If we assume $\gamma(t)$ is a flow line of X_F, then

$$\frac{dG \circ \gamma(t)}{dt} = X_F(G) = \{F, G\}, \tag{2.1.2}$$

i.e. the Poisson bracket measures how far G is not invariant under the flow of F.

In particular, G is constant along orbits of X_F if and only if

$$\{F, G\} = \omega(X_F, X_G) = dF(X_G) \tag{2.1.3}$$

vanishes. The Poisson bracket is obviously antisymmetry. As the symplectic form ω is closed, the Poisson bracket satisfies in additional the Jacobi identity and therefore defines a Lie algebra structure on the space of smooth functions on M.

Lemma 15. *For smooth functions F and G on a symplectic manifold (M, ω), there is a relation between the Lie bracket and the Poisson bracket as follow*

$$[X_F, X_G] = X_{\{F,G\}}. \tag{2.1.4}$$

Proof. Rewrite the Lie bracket as follow

$$[X_F, X_G] = \mathcal{L}_{X_F} X_G = \frac{d}{dt}|_{t=0} (\phi_{X_F}^t)^* X_G = \frac{d}{dt}|_{t=0} X_{G \circ \phi_{X_F}^t}. \tag{2.1.5}$$

Since ϕ_H^t is a symplectomorphism, i.e. for every $t \in \mathbb{R}$, we have $(\phi_H^t)^* \omega = \omega$, the flow of X_F preserves the symplectic form, thus $\phi_{X_F}^t$ pulls back the Hamiltonian vector field of X_G to the Hamiltonian vector field of the pull

back of the Hamiltonian G. Therefore,

$$i_{[X_F,X_G]}\omega = \frac{d}{dt}|_{t=0}\omega(X_{G\circ\phi^t_{X_F}},.) \tag{2.1.6}$$

$$= \frac{d}{dt}|_{t=0}(-d(G\circ\phi^t_{X_F})) \tag{2.1.7}$$

$$= -d(\frac{d}{dt}|_{t=0}G\circ\phi^t_{X_F}) = -d(X_F(G)) = -d\{F,G\}. \tag{2.1.8}$$

□

Remark 16. Let (M,ω) be a symplectic manifold and consider a Darboux chart $(U,\omega = dp\wedge dq)$ for it. In a Darboux chart Poisson bracket for smooth functions F and G, is given by

$$\{F,G\} = \sum \frac{\partial F}{\partial p_i}\frac{\partial G}{\partial q^i} - \frac{\partial F}{\partial q_i}\frac{\partial G}{\partial p^i}. \tag{2.1.9}$$

We say a function L is an integral for a vector field X on a manifold M when $X(L) = 0$. In the following lemma we see a relation between integrals and Poisson brackets.

Lemma 17. *The function* G *is an integral of* X_F *if and only if* $\{F,G\} = 0$.

Proof. The function G is an integral if and only if $X_F(G) = 0$. This holds if and only if

$$0 = -dF(X_G) = \omega(X_F,X_G) = \{F,G\}. \tag{2.1.10}$$

□

Using the equality 2.1.4 and Lemma 17, we see that if $\{F,G\} = 0$, then we have $[X_F,X_G] = 0$. Note that the converse does not hold. For instance, consider the symplectic manifold $(\mathbb{R}^2,\omega_0 = dp\wedge dq)$ with the Hamiltonian $F = p$ and $G = q$, so $X_F = \partial_q$ and $X_G = -\partial_p$ and also $[X_f,X_G] = 0$. But G is linearly increasing under the flow of X_F. That means G is not an integral of X_F.

In the above example it is crucial that $\mathbb{R}^2$ is not compute. In the following lemma we see that if M is a closed manifold then the converse also works for the Hamiltonian F and G.

Lemma 18. *If* (M,ω) *is a closed symplectic manifold and* $F,G\in C^\infty(M,\mathbb{R})$ *are two smooth functions such that* $[X_F,X_G] = 0$. *Then* $\{F,G\} = 0$.

Proof. By Lemma 15,

$$X_{\{F,G\}} = [X_F,X_G] = 0. \tag{2.1.11}$$

In other words, the commutator of the two Hamiltonian vector fields vanishes. Without loss of generality, assume that M is connected (otherwise we treat each connected component of M separately). Therefore we conclude that

$$\{F,G\} = c, \tag{2.1.12}$$

where $c \in \mathbb{R}$ is a constant. Let $x \in M$. We want to know the behaviour of the flow of X_F through x. For that purpose we differentiate

$$\frac{d}{dt}G(\phi_F^t(x)) = dG(\phi_F^t(x))X_F(\phi_F^t(x)) = \{F, G\}(\phi_F^t(x)) = c. \tag{2.1.13}$$

We conclude that

$$G(\phi_F^t(x)) - G(x) = ct. \tag{2.1.14}$$

Since M is compact the function G is necessarily bounded. Therefore

$$c = 0. \tag{2.1.15}$$

It means F and G Poisson commute. □

We finish this section by stating the Noether theorem.

Theorem 19. *(Noether) Assume (M, ω) is a closed symplectic manifold and $F, G \in C^\infty(M, \mathbb{R})$. Then the following are equivalent.*

(i) G is an integral for the flow of F, i.e., $G(\phi_F^t(x))$ is independent of t for every $x \in M$.

(ii) The flow of G is a symmetry for F, i.e., $F(\phi_G^t(M))$ is independent of t for every $x \in M$.

(iii) F and G Poisson commute, i.e., $\{F, G\} = 0$.

(iv) The flow of X_F and X_G commute, i.e., $[X_F, X_G] = 0$.

Proof. The assertion (i) is a equivalent to assertion (ii) content of the lemma 17. Since the Poisson bracket is antisymmetric, the vanishing of $\{F, G\}$ is equivalent the vanishing of $\{G, F\}$, therefore the assertion (iii) is equivalent as well to assertion (ii). Finally from lemma 15 and lemma 18, the assertion (iii) is equivalent to assertion (iv). □

Noether's theorem motivates the notation of a momentum map. Namely suppose a Lie group G acts smoothly on a symplectic manifold (M, ω). A momentum map is a smooth map

$$\mu : M \longrightarrow \mathfrak{g}^* \tag{2.1.16}$$

where $\mathfrak{g}^*$ is the dual of the Lie algebra $\mathfrak{g}$ of G such that the following two conditions hold:

(i) $\forall \xi \in \mathfrak{g}$ define a vector field X_ξ on TM by

$$X_\xi(x) := \frac{d}{dt}\exp(t\xi), \qquad\qquad x \in M. \tag{2.1.17}$$

Then $X_\xi = X_{<\mu,\xi>}$.

(ii) μ is equivariant with respect to the given action $\mu : M \longrightarrow \mathfrak{g}^*$ of G on M and the coadjoint action of G on $\mathfrak{g}^*$.

Let smooth functions F and G. We can extend the above theorem for the Hamiltonian H. Take the Lie group G with the above acting and $H : M \longrightarrow \mathbb{R}$ is a Hamiltonian such that it is invariant under G. We have the following theorem

Theorem 20. *Each* $\xi \in \mathfrak{g} = \mathrm{Lie}(G)$ *gives an integral* H_ξ *of* X_H*, or equivalently* $\{H, H_\xi\} = 0$.

This is the Hamiltonian version of the theorem 19.

2.2 The angular momentum and the Runge-Lenz vector

In this section, we study central force problems, in particular the Kepler problem and its integrals.

2.2.1 Angular Momentum

Recall: We have seen the definition of the angular momentum for a Hamiltonian dynamical system on $T^*\mathbb{R}^3$ in Chapter 1 as follows.

Definition 21. Given H be a Hamiltonian dynamical system on $T^*\mathbb{R}^3$ and let $(q, p) \in \mathbb{R}^3 \times \mathbb{R}^3 = T^*\mathbb{R}^3$. Then we define the angular momentum L by

$$L := q \times p. \tag{2.2.1}$$

Note that in the whole of this thesis we will consider the dimension $n = 3$ and in all discussion dimension is 3.

Given the Hamiltonian

$$H = \frac{1}{2}|p|^2 + V(q) \tag{2.2.2}$$

on $(\mathbb{R}^3 - \{0\}) \times \mathbb{R}^n$ where the (smooth) function $V : \mathbb{R} \longrightarrow \mathbb{R}$ possibly with some singularity is only depend on the distance and we named it the potential for the central force.

Lemma 22. *The angular momentum is preserved under the flow of* X_H*. In other words, the components of the angular momentum* $L = (L_1, L_2, L_3)$ *satisfy* $\{H, L_i\} = 0$.

Proof. The standard $SO(3)$ action acts Hamiltonianly on $T^*\mathbb{R}^3$. Since the Hamiltonian for a central force is $SO(3)$-invariant, thus the proof can be done by Noether's theorem and theorem 20. □

2.2.2 The Kepler problem and its integrals

Consider the Hamiltonian for the spatial Kepler problem that we defined in the introduction as

$$H : T^*\mathbb{R}^3 \setminus \{0\} \longrightarrow \mathbb{R} \tag{2.2.3}$$

$$H = \frac{1}{2}|p|^2 - \frac{1}{|q|} \tag{2.2.4}$$

and take the symplectic form $\omega = dp \wedge dq$. Thus the equation of motion is

$$\dot{p} = -\frac{q}{|p|^3} \tag{2.2.5}$$

$$\dot{q} = p. \tag{2.2.6}$$

The Kepler problem is a completely integrable system. In the following we discuss the integrals of the Kepler problem and the rotating Kepler problem. The first integral of the Kepler problem which we are interested in is the angular momentum.

Lemma 23. *The angular momentum* L *is an integral of the Kepler problem.*

The Kepler problem has an obvious $SO(3)$ -symmetry, since the force in central, thus lemma 22 applies.

2.2.3 The Runge-Lenz Vector

The second interesting integral of the Kepler problem is the Runge-Lenz vector that we introduced.

Define the Laplace-Rung-Lenz vector (also called Runge-Lenz vector) by

$$A := p \times L - \frac{q}{|q|}. \tag{2.2.7}$$

This is an integral of the specific form of the central force in the Kepler problem as we show in the next Lemma.

Lemma 24. *The Runge-Lenz vector* A *is preserved under the flow of* X_H*. In other words, the components of* $A = (A_1, A_2, A_3)$ *satisfy* $\{H, A_i\} = 0$.

Proof. Take the time-derivative of A,

$$\dot{A} = \dot{p} \times L + \dot{L} - \frac{q}{|q|} + \frac{q}{|q|^2} \cdot \frac{q.\dot{q}}{|q|} \tag{2.2.8}$$

$$= -\frac{q}{|q|^3} \times (q \times q) - \frac{p}{|q|} + \frac{q}{|q|^3}(q.p) \tag{2.2.9}$$

$$= \frac{1}{|q|^3}(-q \times (q \times p) - (q \cdot q)p + (q \cdot p)q) \tag{2.2.10}$$

$$= 0. \tag{2.2.11}$$

In the second line we used the Hamiltonian equation and $\dot{L} = 0$, and in the last line we considered the following

well-known identity of vector product

$$(u \times v) \times w = (u \cdot w)v - (v \cdot w)u. \tag{2.2.12}$$

□

Unlike the preservation of the angular momentum, we can not see the preservation of the Runge-Lenz vector in an easy geometric way. It means we can not find a symmetry of the configuration space for the Runge-Lenz vector. To solve this problem, we should use a transformation into the geodesics flow of the round metric on S^3 which has an obvious $SO(4)$-symmetry.

For the planar case of the Kepler problem, the obvious symmetry is an $SO(2)$-symmetry and after regularization one get an $SO(3)$-symmetry.

Lemma 25. *The Runge-Lenz vector satisfies the identity*

$$|A|^2 = 1 + 2H.|L|^2. \tag{2.2.13}$$

Proof. We recall the equality $q \cdot (p \times L) = det(q, p, L) = (q \times p) \cdot L$ since p and L are orthogonal. So we have

$$|A|^2 = |p \times L|^2 - \frac{2}{|q|} q \cdot p \times L + (\frac{q}{|q|})^2 \tag{2.2.14}$$

$$= 1 + |p|^2|L|^2 - \frac{2}{|q|}|L|^2 \tag{2.2.15}$$

$$= 1 + 2(\frac{1}{2}|p|^2 - \frac{1}{|q|})|L|^2. \tag{2.2.16}$$

□

We can see that the Runge-Lenz vector A lies in a plane. To show that, we check that A is orthogonal to L

$$< A, L > = < p \times L, L > - < \frac{q}{|q|}, L > = 0. \tag{2.2.17}$$

That means the vector A lies in the plane $P_L = \{v \in \mathbb{R}^3 | < L, v > = 0\}$.

Here we want to describe the motion of a particle. We use a coordinate change, namely a rotation to move the L-vector to the z-axis. Then we have $L = (0, 0, l)$ for some $l > 0$ and so we can write the Runge-Lenz vector as

$$A = (|A| \cos g, |A| \sin g, 0), \tag{2.2.18}$$

where g is the angle called the argument of the perigee (perihelion).

We use the formula $< q \times L, q > = det(q, p, L)$ once move to get equalities

$$|q| + < A, q > = < \frac{q}{|q|} + q > + < A, q > \tag{2.2.19}$$

$$= < p \times L, q > = det(p, L, q) = < q \times p, L > = |L|^2. \tag{2.2.20}$$

Now if we write q in the polar coordinates

$$q = (r\cos\phi, r\sin\phi, 0). \tag{2.2.21}$$

and use the following identity

$$|q| + < A, q >= |L|^2. \tag{2.2.22}$$

We can compute the radius by

$$r = \frac{|L|^2}{1 + |A|\cos(\phi - g)} \tag{2.2.23}$$

where $f := \phi - g$ is the true anomaly and $|A|$ is the eccentricity.

2.2.4 The Planar Kepler Problem

In this section, we will describe the Kepler problem in dimension $n = 2$ which is named the planar Kepler problem.

We introduced the Hamiltonian of the Kepler problem in Chapter 1 as follows

$$H : T^*(\mathbb{R}^2 \setminus \{0\}) \longrightarrow \mathbb{R} \tag{2.2.24}$$

$$(q, p) \mapsto \frac{1}{2}|p|^2 - \frac{1}{|q|}. \tag{2.2.25}$$

We have seen in Chapter 2 that in the spatial Kepler problem, the angular momentum is a 3-dimensional vector, but in the planar case the first two components of the angular momentum vanish. Thus we have only the third component of the angular momentum. Therefore in this case, we get the angular momentum by

$$L : T^*\mathbb{R}^2 \longrightarrow \mathbb{R} \tag{2.2.26}$$

$$(q, p) \mapsto q_1p_2 - q_2p_1. \tag{2.2.27}$$

and Noether's theorem gives us the identity

$$\{H, L\} = 0, \tag{2.2.28}$$

since the angular momentum generates rotation. Thus we can say that the Kepler problem is rotationally invariant. The phase space of the planar Kepler problem is the 4-dimensional space $T^*\mathbb{R}^2 \setminus \{0\}$ as we discussed in Chapter 1, the Hamiltonian of the Kepler problem with the angular momentum is an integrable system.

If the energy is negative, the orbits of the planar Kepler problem are either ellipses or collision orbits.

The Kepler problem has two kind of symmetries. We used already one of them which is obtained by rotation and gives rise to the angular momentum. The second one is obtained the flows which only live on the phase space $T^*(\mathbb{R}^2 \setminus \{0\})$. The second symmetry does not arise from flows on the configuration space $\mathbb{R}^2 \setminus \{0\}$.

The preserve quantities of the second symmetry are two components of the Runge-Lenz vector. Here we give

the Runge-Lenz vector for the planar case and study its properties. In this case the third component of the vector vanishes. Thus for the other two components which we denote by A_1 and A_2 we can write the following formulas.

$$A_1, A_2 : T^*(\mathbb{R}^2 \setminus \{0\}) \longrightarrow \mathbb{R} \tag{2.2.29}$$

$$\begin{cases} A_1(q,p) = p_2(p_2q_1 - p_1q_2) - \frac{q_1}{|q|} = p_2L(q,p) - \frac{q_1}{|q|} \\ A_2(q,p) = -p_1(p_2q_1 - p_1q_2) - \frac{q_2}{|q|} = -p_1L(q,p) - \frac{q_2}{|q|} \end{cases} \tag{2.2.30}$$

Using lemma 24, the Poisson bracket of H with A_1 and A_2 vanishes, i.e.,

$$\{H, A_1\} = \{H, A_2\} = 0. \tag{2.2.31}$$

Thus we define the two dimensional vector $A = (A_1, A_2)$ as the Runge-Lenz vector for the planar Kepler problem. If we denote the energy of the system by c, by lemma 25, we have

$$A^2 = 1 + 2cL^2 \geqslant 0. \tag{2.2.32}$$

The length of the Runge-Lenz vector A corresponds to the eccentricity of the conic section. The above inequality becomes an equality if and only if the trajectory lies on a circle.

2.3 Mechanical Hamiltonian

Given (M, g) a Riemannian manifold and $f \in C^\infty(M, \mathbb{R})$ a smooth function on the configuration space we consider the Hamiltonian

$$H_f : T^*M \longrightarrow \mathbb{R} \tag{2.3.1}$$

$$(q,p) \mapsto \frac{1}{2}|p|_g^2 + f(q). \tag{2.3.2}$$

In the language of physics the above equation is the sum of the kinetic and potential energy. Let $M \subset \mathbb{R}^n$ be an open subset with Riemannian metric induced from the scaler to $\mathbb{R}^n$. Thus we have on $T^*M = M \times \mathbb{R}^n$

$$X_{H_f}(q,p) = \begin{bmatrix} p \\ \nabla f(q) \end{bmatrix}, \tag{2.3.3}$$

where ∇f is the gradient of f. Let $(q,p) \in T^*M \subset T^*\mathbb{R}^n$, if $q_p : \mathbb{R} \longrightarrow M$ be a solution of the second order ODE

$$\partial_t^2 q_p(t) = -\nabla f(q_p(t)) \tag{2.3.4}$$

and at the point 0 we have

$$q_p(0) = q, \qquad \partial_t q_p(0) = p. \tag{2.3.5}$$

Then the Hamiltonian flow of H_f is given by

$$\Phi_f^t(q,p) = (q_p(t), \partial_t q_p(t)). \tag{2.3.6}$$

We give some examples of Mechanical Hamiltonians that are important in this thesis such that we can refer them in the further chapters.

Example 26. *1: The first example is called the harmonic oscillator. Given a Hamiltonian by*

$$H : T^*\mathbb{R} \longrightarrow \mathbb{R} \tag{2.3.7}$$

$$(q,p) \mapsto \frac{1}{2}(p^2+q^2). \tag{2.3.8}$$

The flow of harmonic oscillator is

$$\Phi_H^t(q,p) = (q\cos t + p\sin t, -q\sin t + p\cos t). \tag{2.3.9}$$

The flow of the above harmonic oscillator is periodic of period 1.

2: Consider the cotangent bundle $T^*\mathbb{R}^2 = T^*\mathbb{R}\times T^*\mathbb{R}$ and the above harmonic oscillator. Now if we multiply two of this harmonic oscillator to each other. We can get the following Hamiltonian

$$H : T^*\mathbb{R}^2 \longrightarrow \mathbb{R} \tag{2.3.10}$$

$$(q,p) \mapsto \frac{1}{2}(q^2+p^2) = \frac{1}{2}(q_1^2+p_1^2) + \frac{1}{2}(q_2^2+p_2^2), \tag{2.3.11}$$

such that $H^{-1}(c)$ determine the level set or equivalently, energy hypersurface of the two uncoupled harmonic oscillator for the energy $c > 0$. This level set is a 3-dimensional sphere with radius $\sqrt{2c}$. In particular, the flow is periodic of period 1.

3: The third example is the Kepler problem. Consider the Hamiltonian of the Kepler problem and let $n = 2$ which is the planar Kepler problem. For $c \leqslant -\frac{3}{2}$ the Belburno-Moser-Ossipov and Ligon- Schaaf regularizations help us to embed the Hamiltonian flow of the Kepler problem to the geodesic flow of the 2-dimensional sphere. We will see in this thesis that the double cover of the geodesics flow on the round two dimensional sphere can be interpreted as the Hamiltonian flow of two uncoupled harmonic oscillators via Levi-Civita regularization.

4: For the next example, we will see the same results for the rotating Kepler problem in the further chapters which is one of the main topics of this thesis.

2.4 Magnetic Hamiltonian

The force for a mechanical Hamiltonian only depends on the position. But there are some important forces that depend on the velocity of the system. The magnetic Hamiltonians model these forces. For instance, the Lorenz force in the presence of a magnetic field or collision force.

We give the definition of a magnetic Hamiltonian. Given a Riemannian manifold (M, g) and an 1-form $A \in \Omega^1(M)$. If we denote the potential of the system by $f \in C^\infty(N, \mathbb{R})$. We can define the magnetic Hamiltonian by

$$H_{f,A} : T^*M \longrightarrow \mathbb{R} \tag{2.4.1}$$

$$(q, p) \mapsto \frac{1}{2}|p - A_p|_g^2 + f(q). \tag{2.4.2}$$

Chapter 3

The Rotating Kepler Problem and its Periodic Orbits

3.1 The Hamiltonian of the Rotating Kepler Problem

As we have seen in the Chapter 1, the Hamiltonian of the planar rotating Kepler problem is

$$\begin{aligned} K :& T^*(\mathbb{R}^2 \setminus \{0\}) \longrightarrow \mathbb{R} \\ K(q,p) &= \frac{1}{2}|p|^2 - \frac{1}{|q|} + q_1p_2 - q_2p_1, \qquad (q,p) \in T^*(\mathbb{R}^2 \setminus \{0\}) \end{aligned} \tag{3.1.1}$$

which is the sum of the Hamiltonian of the Kepler problem together with the angular momentum $L(q,p) = q_1p_2 - q_2p_1$.

We denoted in Chapter 1, $K = H + L$ and also we know that H and L Poisson commute. The Hamiltonian of the rotating Kepler problem is a special case of the Hamiltonian of the restricted three body problem

$$E(q,p) = \frac{1}{2}|p|^2 - \frac{\mu}{|q-\mu|} - \frac{1-\mu}{|q-e|} + q_1p_2 - q_2p_1 \tag{3.1.2}$$

where in the above Hamiltonian $\mu = 0$. We discuss the restricted three body problem with more details in the appendix 1.

In the language of physics, we can explain the Hamiltonian of the rotating Kepler problem as follows. Assume the moon has zero mass. We can say a satellite is just attracted by the earth like in the Kepler problem but the coordinates are rotating.

We complete the squares in 3.1.1 and obtain the magic Hamiltonian as follows

$$K(q,p) = \frac{1}{2}((p_1 - q_2)^2 + (p_2 + q_1)^2) - \frac{1}{|q|} - \frac{1}{2}|q|^2. \tag{3.1.3}$$

Now if we define the effective potential

$$U : \mathbb{R}^2 \setminus \{0\} \longrightarrow \mathbb{R} \tag{3.1.4}$$

$$U(q) = -\frac{1}{|q|} - \frac{1}{2}|q|^2, \tag{3.1.5}$$

then we can write

$$K(q,p) = \frac{1}{2}((p_1 - q_2)^2 + (p_2 + q_1)^2) + U(q). \tag{3.1.6}$$

Lemma 27. *The effective potential* U *of the rotating Kepler problem has a unique critical value* $-\frac{3}{2}$ *and its critical set consists of a circle of radius 1 around the origin.*

Proof. The effective potential is rotationally invariant. Therefore, its critical set is rotationally invariant as well. We write

$$U(q) = f(|q|). \tag{3.1.7}$$

For the function

$$f : (0,\infty) \longrightarrow \mathbb{R} \tag{3.1.8}$$

$$r \mapsto -\frac{1}{r} - \frac{1}{2}r^2. \tag{3.1.9}$$

The differential of f is

$$f'(r) = -\frac{1}{r^2} - r \tag{3.1.10}$$

and therefore f has a unique critical point at $r = 1$ with critical value

$$f(1) = -\frac{3}{2}. \tag{3.1.11}$$

□

Critical points of K and U are in bijection via the projection map $\pi|_{\mathrm{crit}(K)}$ 9.3.16 where $(q,p) \mapsto q$. The critical value of K coincides with the critical value of U at the same critical points. Thus we obtain the following corollary.

Corollary 28. *The Hamiltonian* K *of the rotating Kepler problem has a unique critical value* $-\frac{3}{2}$.

3.2 Hill's Region for the Rotating Kepler Problem

Define the Hill's region for the energy c by

$$\mathcal{K}_c := \pi(K^{-1}(c)) \subset \mathbb{R}^2 \setminus \{0\}. \tag{3.2.1}$$

where c is the Jacobian energy and π is the projection $(q,p) \mapsto q$. Alternatively, we can write the Hill's region as follows

$$\mathcal{K}_c = \{q | U(q) \leqslant -c\}. \tag{3.2.2}$$

Recall: Given the effective potential $U(q) = f(|q|)$. The unique critical value of this function is $-\frac{3}{2}$ at the point $r = -1$. Let $c < -\frac{3}{2}$, the Hill's region consist of two connected components such that one is bounded and the other one is unbounded. We denote the bounded component of the Hill's region by $\mathcal{K}_c^b$ and the unbounded component by $\mathcal{K}_c^b$.

Define the energy hypersurface lying over $\mathcal{K}_c^b$ by

$$\sum_c := \pi^{-1}(\mathcal{K}_c^b) \subset K^{-1}(c). \tag{3.2.3}$$

We apply the Moser regularization to the rotating Kepler problem and denote the regularized energy hypersurface by $\bar{\sum}$. This is a diffeomorphic to $\mathbb{R}P^3$.

Observe in general, there is no relation between periodic orbits of the inertial Kepler problem and periodic orbits of the rotating Kepler problem. More precisely, Let $\gamma : \mathbb{R} \longrightarrow \mathbb{R}^4$ be a solution of the inertial Kepler problem and assume $\Phi_t : \mathbb{R}^4 \longrightarrow \mathbb{R}^4$ is a time-dependent change of coordinates from the inertial problem to the rotating Kepler problem. Define $\alpha(t) := \Phi_t \gamma(t)$. Then $\alpha(t)$ solves the rotating Kepler problem. Since Φ_t is time-dependent, in general, α is not periodic. But there are two cases that periodic orbits of the inertial Kepler problem give rise to periodic orbits of the rotating Kepler problem.

Recall: The torus $T_{(2,1)}$ of periodic orbit of type $(2,1)$ is called Hekuba and $T_{(3,1)}$ Hestia. Since these orbits play an important role later in the analysis of ECH capacities of the RKP we give here explicitly their energy values

$$c^-_{2,1} = -\sqrt[3]{4}, \qquad\qquad c^-_{3,1} = -\frac{5}{6}\sqrt[3]{9}. \tag{3.2.4}$$

3.3 Periodic Orbits of the Rotating Kepler Problem

In this section we are going to study periodic orbits of the rotating Kepler problem. The rotating Kepler problem has two kind of periodic orbits that we explain here. The first kind are circles where the second kind are rotating ellipses.

To obtain the periodic orbits of the rotating Kepler problem. We can fix an energy and obtain a family of periodic orbits for the RKP that in this case the mass ratio μ is varying or we can fix μ and varying the energy and get a family of periodic orbits.

Given the Hamiltonian of the RKP as

$$K = H + L = \frac{1}{2}|p|^2 - \frac{1}{|q|} + q_1 p_2 - q_2 p_1 \tag{3.3.1}$$

Recall: The formula

$$A^2 = 1 + 2L^2c \tag{3.3.2}$$

where A is the Runge-Lenz vector whose length correspond to the eccentricity of the corresponding Kepler ellipse. Now if we substitute the Hamiltonian 3.3.1 on the equation 3.3.2, we have the following inequality

$$0 \leqslant 1 + 2H(K - H)^2 = 1 + 2K^2H - 4KH^2 + 2H^2 = P(K, H) \tag{3.3.3}$$

and denote the last equality with $p(K, H)$. The equality $p(K, H) = 0$ holds if and only if the eccentricity of the correspond periodic orbit vanish, i.e. when the periodic orbits are circular.

Here we give some essential properties of periodic orbits, than in the next section we will discuss the first and the second kind of periodic orbits.

From the Noether's theorem we know that $\{H, L\} = 0$, so $[X_H, X_L] = 0$. It means that X_H and X_L commute. Now take $K = H + L = H \diamondsuit L$ so we can write

$$\phi_K^t = \phi_H^t \circ \phi_L^t. \tag{3.3.4}$$

Now we can show how orbits for the energy $c < 0$ how look likes. Consider the q-component of an orbit of the Kepler problem and denote the Kepler ellipse by $\epsilon_\tau : [0, \tau] \longrightarrow \mathbb{R}^2$ where τ is its period. This is also a solution of the Kepler problem with negative energy.

Using the above solution of the Kepler problem we obtain us a solution for the RKP as

$$\epsilon_\tau^R(t) = e^{it}\epsilon_\tau(t) \tag{3.3.5}$$

which is not longer periodic. The angular momentum L generates the rotation in the q-plane and the p-plane. Thus there are two cases for orbits,

(i) ϵ_τ is a circle. In this case, ϵ_τ^R is periodic unless it is a critical point when $\tau = 2\pi$.

(ii) ϵ_τ is not circle. In this case it is a proper ellipse or a collision orbit that looks like a line.

We consider the orbit ϵ_τ which is an ellipse. In this case ϵ_τ^R is a periodic orbit if the following resonance relation is satisfied for some positive integers k and l such that

$$2\pi l = \tau k. \tag{3.3.6}$$

Thus periodic orbits for the RKP of the second kind have the following symmetry property.

Lemma 29. *Periodic orbits in the rotating Kepler problem of the second kind satisfy the following rotational*

symmetry

$$\epsilon_\tau^R(t+\tau) = e^{2\pi i l/k}\epsilon_\tau^R(t). \tag{3.3.7}$$

Proof. The resonance condition gives us the equality $\tau = 2\pi l/k$ and therefore we have

$$\epsilon_\tau^R(t+\tau) = e^{it+i\tau}\epsilon_\tau(t+\tau) = e^{2\pi i l/k}e^{it}\epsilon_\tau(t) = e^{2\pi i l/k}\epsilon_\tau^R(t). \tag{3.3.8}$$

□

In this part, we want to discuss about circular orbits when K is fixed. For this goal, define

$$p_K := p(K,\cdot). \tag{3.3.9}$$

This is a cubic equation in H and if we fix H then we define the function

$$p^H := p(\cdot, H), \tag{3.3.10}$$

which is a quadratic polynomial in K.

Let the critical value of K, $-\frac{3}{2}$, which is unique. At this critical value, the cubic equation is as follow

$$p_{-\frac{3}{2}}(K) = 2(K+2)(E+\frac{1}{2})^2 \tag{3.3.11}$$

i.e. $p_{-\frac{3}{2}}$ has a simple zero at -2 and a double zero $\frac{3}{2}$. We can compute the above zeros by using elementary calculation.

Recall: Given a cubic polynomial $p = ax^3 + bx^2 + cx + d$. For this polynomial we can write

$$\Delta(p) = b^2c^2 - 4ac^3 - 4b^3d - 27a^2d^2 + 18abcd. \tag{3.3.12}$$

From elementary calculus, we know that if $\Delta(p) > 0$ then the polynomial has three real roots and if $\Delta(p) = 0$ the polynomial has a double root and also if $\Delta(p) < 0$ the roots of the polynomial are one real and two complex conjugated.

Now consider the cubic polynomial p_K. The discriminate of this equation is

$$\Delta(p_K) = -32K^3 - 108. \tag{3.3.13}$$

The above discriminate vanishes at $K = -\frac{3}{2}$ and for $K < -\frac{3}{2}$ and $K > -\frac{3}{2}$ we have $\Delta(p_K) > 0$ and $\Delta(p_K) < 0$ respectively.

Let $K < -\frac{3}{2}$ and denote the above the roots of the cubic equation by $R^1(K)$, $R^2(K)$ $R^3(K)$ in $\mathbb{R}$ with order

$$R^1(K) < R^2(K) < R^3(K). \tag{3.3.14}$$

We have seen that for $K = -\frac{3}{2}$

$$R^1(-\frac{3}{2}) = -2, \qquad R^2(-\frac{3}{2}) = R^3(-\frac{3}{2}) = -\frac{1}{2}. \tag{3.3.15}$$

If $K > -\frac{3}{2}$ can extend R^1 to a continues function on the whole real line such that $R^1(K)$ be a unique real root of p_K. We take the quadratic equation

$$p^H(K) = 2HK^2 - 4H^2K + 2H^3 + 1. \tag{3.3.16}$$

Since $\Delta(p^K) = -8K$, for $K < 0$, p^K has precisely two real zeros. Therefore, the function R^1 and R^2 are monotone and R^3 is monotone decreasing such that

$$\lim_{K\to-\infty} R^1(K) = \lim_{K\to-\infty} R^2(K) = -\infty, \qquad \lim_{K\to-\infty} R^3(K) = \lim_{K\to\infty} R^1(K) = 0, \tag{3.3.17}$$

and their images are

$$imR^1|_{(-\infty,\frac{3}{2}]} = (-\infty, 2), \qquad imR^2 = (-\infty, \frac{1}{2}], \qquad imR^3 = [\frac{1}{2}, 0). \tag{3.3.18}$$

The circular orbits exist only if we have the identity $1 + 2HL^2 = 0$. That means, if the energy is negative, we have precisely two circular orbits whose angular momentum are differ by a sign, i.e. the circle is transverse backwards. Note that as an unparametrized simple orbit, a circular orbit in the (non-rotating) planar Kepler problem is determined uniquely by the energy K and the angular momentum L.

We know that the circular orbits are invariant under rotation. Thus a circular periodic orbit of the Kepler problem gives us a periodic orbits in the RKP.

Therefore, we can determine a periodic orbit of the RKP uniquely by the values of K and L. On the other hand, the angular momentum determined by H. Thus we can find a periodic orbit of the RKP by using K and H. Now if we fix values of K and H and also $p(K, H)$ be zero then a circular orbit exists. Hence form the above description, for $K < -\frac{3}{2}$, there exist three circular periodic orbits which they live on the bounded component. While for energy value $K > -\frac{3}{2}$, there exists a unique circular periodic orbit that lives on the unbounded component.

3.4 Periodic Orbits of the Second Kind

In the last section we discussed about the circular orbits and saw they are as well periodic orbits in the RKP. The second kind are of positive eccentricity respectively rotating collision orbits.

Now we want to describe the second kind of the periodic orbits of the RKP how they are bifurcate out of the circular periodic orbits of the RKP. A Kepler ellipse in the inertial system becomes an orbit in the rotating or synodical system. Since the period of the rotating coordinate system is 2π, if the orbit in the rotating system is

periodic of the period of the ellipses should be

$$\tau = \frac{2\pi l}{k} \tag{3.4.1}$$

where k and l relatively prime that in follow we explain what they are.

The positive integers l turns the coordinate system and k turns the ellipse. Note that these the periodic orbits are never isolated, since we can rotate them and make new periodic orbits. Thus we can say that the periodic orbits of the second kind appears in circle families.

Considering the periodic orbits as unparametrized simple orbits they appears in two dimensional torus families. Recall from Kepler's third law the following lemma.

Lemma 30. *The minimal period τ of a Kepler ellipse only depends on the energy and we have the relation*

$$\tau^2 = \frac{\pi^2}{-2c^2}. \tag{3.4.2}$$

We can get the energy of a period orbit from its period τ by the following formula

$$K_{k,l} = -\frac{1}{2}(\frac{k}{l})^{\frac{2}{3}}. \tag{3.4.3}$$

If we fix the Jacobi energy K, we can get the angular momentum in view of $L = H - K$ and if we have the energy and the angular momentum by using the relation

$$A^2 = 1 + KL^2, \tag{3.4.4}$$

we can compute the eccentricity of the ellipse. Therefore, we can determine periodic orbit of the second kind corresponds to relatively prime positive integer k and l we know the energy value c.

Now we are going to give astronomically description of periodic orbits of the second kind.

Consider the Sun-Jupiter system. Asteroids often follow periodic orbits in this system. For small integers k and l, the orbits corresponding to these integers have special names obtained form the asteroids lying on these orbits. For example, Hecuba: type (2,1), Hilda type (3,2), Thule: type (4,3), Hestia: type (3,1), Cybele: type (7,4).

In the general case, we denote the torus corresponding to the integers k and l by $T_{k,l}$. Thus using the function p^H , 3.3.10 for a periodic orbit of type (k, l) or equivalently $T_{k,l}$, we obtain the following relations

$$L_{k,l} = \sqrt{-\frac{1}{2K_{k,l}}} = (\frac{l}{k})^{\frac{1}{3}} \tag{3.4.5}$$

$$c^-_{k,l} = K_{k,l} - L_{k,l} = -\frac{1}{2}(\frac{k}{l})^{\frac{2}{3}} - (\frac{l}{k})^{\frac{1}{3}} = -(\frac{l}{k})^{\frac{1}{3}}(\frac{k+2l}{2l}) \tag{3.4.6}$$

$$c^+_{k,l} = K_{k,l} + L_{k,l} = -\frac{1}{2}(\frac{k}{l})^{\frac{2}{3}} + (\frac{l}{k})^{\frac{1}{3}} = (\frac{l}{k})^{\frac{1}{3}}(\frac{k+2l}{2l}) \tag{3.4.7}$$

Using the above notation consider a periodic orbit of type (k,l). The energy of this orbit is

$$c \in (c^-_{k,l}, c^+_{k,l}). \tag{3.4.8}$$

We can assume c as some kind of life-parameter of $T_{k,l}$ that is born at $c = c^-_{k,l}$ out of a $|k-l|$-fold covered circular periodic orbit.

For the energy $c \in (c^-_{k,l}, c_{k,l})$, the angular momentum of the orbit is less than zero and therefore the periodic orbit is direct, for $c = c_{k,l}$ the orbit is a collision and for the $c \in (c_{k,l}, c^+_{k,l})$ the angular momentum is bigger than zero and therefore the orbit is retrograde.

For the integers k and l, the orbit of type (k,l) is interior or exterior that explain in the following.

(i) If $k = l = 1$, the critical value of the RKP is $c^-_{k,l} = \frac{3}{2}$ and the exterior and interior direct orbits both collapse to the critical point.

(ii) If $k > l$, then $|L_{k,l}| < 1$ and the direct orbit is interior.

(iii) If $k < l$, then $|L_{k,l}| > 1$ and the direct orbit is exterior.

Now we are going to explain what happens when the energy c moves from $c^-_{k,l}$ to $c^+_{k,l}$. First let c increase, the eccentricity of $T_{k,l}$ starts to increase until the middle of the life of $T_{k,l}$ and the angular momentum for $T_{k,l}$in this part is negative. At the energy $c_{k,l} = \dfrac{c^-_{k,l} + c^+_{k,l}}{2}$ the eccentricity is equal to 1 and the orbit. After that eccentricity decreases and the angular momentum for $T_{k,l}$ is positive . Thus after the prograde attitude in the first part of life, the second part of life it changes to a retrograde attitude and finally $T_{k,l}$ dies at $c = c^+_{k,l}$ at the $k+l$-fold covered retrograde circular orbit.

Remark 31. There are three kinds of circular orbits for energy less than $-\dfrac{3}{2}$. Two of them live in the bounded component and one lives in the unbounded component of the Hill's region. In the bounded component of the Hill's region, there are two simply covered circular orbits.

We have defined the Hill's region $\mathcal{H}_c$. For the energy $c < -\dfrac{3}{2}$, this region has two connected components, one bounded and one unbounded.

The Runge-Lenz vector for a circular periodic orbit vanishes. We can see the radius of a circular periodic orbit is

$$r = L^2 = -\frac{1}{2H}. \tag{3.4.9}$$

From 3.3.18, we can see the circular periodic orbits corresponding to the energy values $R^1(c)$ and $R^2(c)$ have radius less than one while the radius of a circular periodic orbit correspond to the energy $R^3(c)$ is bigger than one. Therefore, the first two circular periodic orbits live in the bounded component of the Hill's region and the third one lives in the unbounded component of the Hill's region.

The circular periodic orbit corresponds to R^1 is referred as the retrograde circular periodic orbit and the circular periodic orbit corresponds to R^2 is referred to as the interior direct circular periodic orbit and finally the circular periodic orbit corresponds to R^3 referred to the exterior direct circular periodic orbit.

Chapter 4

Regularization

4.1 The Ligon-Schaaf Regularization

In this section, we are going to discuss the Ligon-Schaaf regularization which is a symplectomorphism that maps the solutions of the planar Kepler problem to the geodesics on the sphere S^2. Unlike the Moser-Belbruno-Osipov regularization, the Ligon-Schaaf regularization is a symplectomorphism without reparametrizing time. As the Moser-Belbruno-Osipov regularization, the Ligon-Schaaf regularization covers both positive and negative energy of the system but in this thesis we restrict ourself only to the negative part of the energy.

The Ligon-Schaaf regularization works for each dimension n as the Moser-Belbruno-Osipov regularization but here we just take the dimension $n = 2$ and apply our conditions on 2 dimensional space.

We use the 2-form $y \mapsto < x, y >$ on $\mathbb{R}^2$ where $< x, y >$ is the standard inner product. Using this form we identify $x \in \mathbb{R}^2$ with a vector in the dual space and also can obtain the cotangent bundle of $\mathbb{R}^2 \setminus \{0\}$ as the set of (q, p) such that $q, p \in \mathbb{R}^2$ for $q \neq 0$ and that is the phase space P.

As we have seen in Chapter 1, the equation of motion of the Kepler problem is

$$\begin{aligned} \dot{q} &= p \\ \dot{p} &= -|q|^{-3} q, \end{aligned} \tag{4.1.1}$$

where $q, p \in \mathbb{R}^2$.

Consider the Hamiltonian of the Kepler problem

$$H(q, p) = \frac{1}{2}|p|^2 - \frac{1}{|q|}, \tag{4.1.2}$$

which is the total energy of the system. With help of this Hamiltonian, the right hand side of the equation 4.1.1 becomes the Hamiltonian vector field X_H.

Define the eccentricity vector as

$$A(q, p) := |q|^{-1} q - |p|^2 q + < q, p > p. \tag{4.1.3}$$

The components of this vector are constants of motion such as the angular momentum $L(q,p)$. If we let $e = \sqrt{(A)^2}$, then by work of Gyorgyi, we can see that the norm of the eccentricity vector A is equal to eccentricity of a orbit e and there exists a direct relation between elliptical orbits $0 \leqslant e < 1$ and the eccentricity vector A as follow

$$e^2 = |A|^2 = 1 + 2H. \tag{4.1.4}$$

We consider an open subspace of P which lives on the negative part of the energy and denote it as

$$P_- = \{(q,p) \in P \mid H(q,p) < 0\}, \tag{4.1.5}$$

which is defined already in Chapter 1.

Now we are going to describe situations that can have elliptical and collision orbits in our Hamiltonian system. There are two cases which depend on the Hamiltonian and the angular momentum.

For the first case, assume $H < 0$ and $L \neq 0$. Therefore, the solutions of the system are the elliptical orbits of eccentricity e such that $0 \leqslant e < 1$ and for the second case assume $H < 0$ and $L = 0$, then the solutions of the system are collision orbits. That means the solutions run into the origin with infinite speed in finite positive and negative time.

Take the angular momentum $L = q_1p_2 - q_2p_1$. We discussed the Poisson bracket in Chapter 2. We write the vector A as $A = (A_1, A_2)$,

$$\{L, A_1\} = -A_2 \tag{4.1.6}$$

$$\{L, A_2\} = A_1 \tag{4.1.7}$$

$$\{A_1, A_2\} = -2HL.$$

Note that in the above equalities for case n are as follows,

$$\{l_{ij}, A_k\} = \delta_{jk}A_i - \delta_{ik}A_j \tag{4.1.8}$$

$$\{A_i, A_j\} = -2Hl_{ij}. \tag{4.1.9}$$

Define the eccentricity vector by

$$\eta := \nu\varepsilon \tag{4.1.10}$$

where $\nu := (-2H)^{\frac{1}{2}}$. Hence we can write the Poisson bracket relations in 4.1.6 in term of η as follow

$$\{L, \eta_1\} = -\eta_2 \tag{4.1.11}$$

$$\{L, \eta_2\} = \eta_1 \tag{4.1.12}$$

$$\{\eta_1, \eta_2\} = L. \tag{4.1.13}$$

We have the above equities for the case n as follows

$$\{l_{ij}, \eta_k\} = \delta_{jk}\eta_i - \delta_{ik}\eta_j \tag{4.1.14}$$

$$\{\eta_i, \eta_j\} = l_{ij}. \tag{4.1.15}$$

If we think of L as η_3. We can recover precisely the Lie algebra of $SO(3)$.

We define $J = (L, \eta_1, \eta_2)$ from P_- the dual of the Lie algebra $SO(3)$ as the momentum map of an infinitesimal Hamiltonian action of $SO(3)$ on P_-. Note that if we assume the Lie subalgebra $SO(2)$. Then we can extend this infinitesimal action to the standard infinitesimal rotation.

Now we can describe, how we can map the solutions of the Kepler problem to the geodesics on the sphere S^2 in $\mathbb{R}^3$ such that the rotation group $SO(3)$ acts naturally.

Here we define the phase space for the geodesics on the sphere S^2.

Definition 32. The cotangent bundle of S^2 can be identified with vectors $(x, y) \in \mathbb{R}^3 \times \mathbb{R}^3$ such that $< x, x >= 1$ and $< x, y >= 0$. The zero section corresponds to the element $(x, 0)$ where $< x, x >= 1$. We denote by T the complement of the zero section.

Now we define the angular momentum map of the infinitesimal Hamiltonian action of $SO(3)$ on T by

$$\tilde{J} : (x, y) \longrightarrow x \wedge y. \tag{4.1.16}$$

With the above notation, we show that the image of the Kepler solutions are geodesics with time rescaled under the Ligon-Schaaf map factor that depends only on the energy. In other words, the Kepler solutions are mapped to the solution curve of the Delaunay Hamiltonian which is defined as follows

$$\tilde{H}(x, y) = -\frac{1}{2} \cdot \frac{1}{|y|^2} = -\frac{1}{2} \cdot \frac{1}{|\tilde{J}|^2} \tag{4.1.17}$$

where $(x, y) \in T$. Note that the components of $\tilde{J}$ are also constant along the geodesics in T. Now we can define the Ligon-Schaaf regularization and give its properties.

The Ligon-Schaaf regularization is a symplectomorphism that maps the phase space P_- into the phase space T. We denote this symplectomorphism by $\Phi = \Phi_{LS}$ and define it as

$$\Phi = \Phi_{LS} : P_- \longrightarrow T \tag{4.1.18}$$

$$\Phi(q, p) := ((\sin\phi)\mathcal{A} + (\cos\phi)\mathcal{B}, -\nu(\cos\phi)\mathcal{A} + \nu(\sin\phi)\mathcal{B}), \tag{4.1.19}$$

where

$$\mathcal{A} = \mathcal{A}(q, p) := (|q|^{-1}q - < q, p > p, \nu^{-1} < q, p >), \tag{4.1.20}$$

$$\mathcal{B} = \mathcal{B}(q, p) := (\nu^{-1}|q|p, |p|^2|q| - 1), \tag{4.1.21}$$

and

$$\phi = \phi_{LS}(q,p) := \nu^{-1} < q,p > . \tag{4.1.22}$$

To compute the solutions of the Kepler problem on the sphere S^2, we need to use the properties of the Ligon-Schaaf symplectomorphism which we listed as follows

(i) Let e_3 be the third standard basis vector in $\mathbb{R}^3$, which is the north pole of the sphere S^2. Then Φ is an analytic diffeomorphism from P_- onto the open subset T_- of T consisting of all $(x,y) \in T$ such that $x \neq e_3$.

(ii) Φ is a symplectomorphism.

(iii) If γ is a solution curve of the Kepler vector field X_H in P_-, then $\Phi \circ \gamma$ is a solution curve of the Delaunay vector field $X_{\tilde{H}}$ in T.

(iv) It holds that $J = \tilde{J} \circ \Phi$.

Using the Ligon-Schaaf symplectomorphism, we can define the action of g on P_- as an action on T. To show this action let $g \in SO(3)$ and denote the obvious action g on T by g_T and the action g on P_- by g_{P_-}. Hence we define

$$g_{P_-}(q,p) := \Phi^{-1} \circ g_T \circ \Phi(q,p), \qquad (q,p) \in P_-. \tag{4.1.23}$$

To have this action well-define, the x-component of $\Phi(q,p)$ is not allow to be equal to $g_T^{-1}(e_3)$. But the set T is equal to P_- if and only if when $g \in SO(2)$. Note that the action of $SO(3)$ on P_- is not globally defined since the preimage of the fiber over the north pole e_3 in T is missing. Element in this fiber correspond to collisions. Moreover, note that this fiber is a Lagrangian submanifold.

Now we are going to give a condition that the identity $J = \tilde{J} \circ \Phi$ holds for a general map Φ.

Proposition 33. *Suppose Φ is a map from P_- to T. Φ satisfies $J = \tilde{J} \circ \Phi$ if and only if there exists an $\mathbb{R}/2\pi\mathbb{Z}$-valued function ϕ on P_- such that $\Phi = \Phi_\phi$.*

Proof. In paper [5]. □

By the symplectomorphism Φ, we can also map the fibers of J into the fibers of $\tilde{J}$. Therefore, we map the image of J into the images of $\tilde{J}$, and the equality appears if and only if the image of Φ is included in all fibers of $\tilde{J}$.

Now if we accept this description, we can give the following lemma.

Lemma 34. *Assume $\mathcal{C} := \{j \in \wedge^2\mathbb{R}^3 | \operatorname{rank} j = 2\}$. We have $J(P_-) = \mathcal{C} = \tilde{J}(T)$. A fiber of J is equal to an X_H-orbit in P_-. A fiber of $\tilde{J}$ is equal to an $X_{\tilde{H}}$-orbit in T, which in turn is equal to an orbit of the circle action $\alpha \longrightarrow \Gamma_\alpha$ in T defined by*

$$\Gamma_\alpha(x,y) = ((\cos\alpha)x + |y|^{-1}(\sin\alpha)y, -|y|(\sin\alpha)x + (\cos\alpha)y), \tag{4.1.24}$$

where $(x, y) \in T$ *and* $\alpha \in \mathbb{R}/2\pi\mathbb{Z}$.

Proof. In paper [5]. □

4.2 The Levi Civita Regularization

In this section, we will discuss about the Levi-Civita regularization. We will see in the next chapters how this regularization and the Ligon-Schaaf symplectomorphism can help us to map the solutions of the Kepler problem for fixed negative energy to the geodesics of the sphere S^2 and then to S^3 in the complex space $\mathbb{C}^2$. Note that a geodesic on S^2 is determined only by a point in S^2 and a unique direction, i.e. a point in the unit tangent space of S^2 which is diffeomorphic to $\mathbb{R}P^3$. Observe that S^3 is the double cover of $\mathbb{R}P^3$. Note that, in the language of physics, we can explain this double cover of the geodesics flow on S^2 as a Hamiltonian flow of two uncoupled Harmonic oscillators.

The Levi-Civita regularization is a 2:1 map from $\mathbb{C}^2 \setminus \{0\}$ to $T^*S^2 \setminus S^2$.

We denote the regularization with $\mathcal{L}$ and define it as follows

$$\begin{aligned} \mathcal{L} : \mathbb{C}^2 \setminus (\mathbb{C} \times \{0\}) &\longrightarrow T^*\mathbb{C} \setminus \mathbb{C} \\ (u, v) &\mapsto (\frac{u}{\bar{v}}, 2v^2) \end{aligned} \tag{4.2.1}$$

where $\bar{v}$ is the complex conjugate of v. Note that this regularization depends complex number in 2-dimensional space, i.e. $\mathbb{C}^2$. But the regularizations that were discovered by Moser-Belbruno-Osipov and Ligon- Schaaf work in every dimension.

In this section we consider a 2-dimensional space and discuss the Levi-Civita transformation. This transformation gives us a covering map with degree 2. To find this covering map, we extend the Levi-Civita regularization $\mathcal{L}$ defined above by 4.2.1 to the cotangent bundle T^*S^2 as follows,

$$\mathcal{L} : \mathbb{C}^2 \setminus \{0\} \longrightarrow T^*S^2 \setminus S^2 \tag{4.2.2}$$

where $\mathbb{C}$ is assumed to be a chart of S^2 via stereographic projection at the north pole.

First of all, we try to find an appropriate symplectic form for $\mathbb{C}^2$. This form identified $\mathbb{C}^2$ with $T^*\mathbb{C}$. Let $(p, q) \in T^*\mathbb{C} = \mathbb{C} \times \mathbb{C}$ such that p is the base coordinate and q is the fiber coordinate. We have the following 1-form on $\mathbb{C}^2$,

$$\lambda_{\mathbb{C}^2} = \frac{1}{2}(u_1 du_2 - u_2 du_1 + v_1 dv_2 - v_2 dv_1). \tag{4.2.3}$$

This 1-form gives us the standard symplectic form on $\mathbb{C}^2$

$$\omega_{\mathbb{C}^2} = -d\lambda_{\mathbb{C}^2} = du_1 \wedge du_2 + dv_1 \wedge dv_2. \tag{4.2.4}$$

On the other hand, if we use a Liouville 1- form for $T^*\mathbb{S}^2$ namely 1-form

$$\lambda = q_1 dp_1 + q_2 dp_2 = Re(q d\bar{p}). \tag{4.2.5}$$

then its pull-back under the Levi-Civita map is

$$\begin{aligned}\lambda_{\mathcal{L}}(u,v) :=& \mathcal{L}^*\lambda(u,v) && (4.2.6)\\ =& Re(2v^2 d(\frac{\bar{u}}{v})) && (4.2.7)\\ =& 2Re(v^2(\frac{d\bar{u}}{v} - \frac{\bar{u}dv}{v^2})) && (4.2.8)\\ =& 2Re(vd\bar{u} - \bar{u}dv) && (4.2.9)\\ =& 2(v_1 du_1 - u_1 dv_1 + v_2 du_2 - u_2 dv_2). && (4.2.10)\end{aligned}$$

Now we take the exterior derivative of $\lambda_{\mathcal{L}}(u,v)$. Hence we endow $T^*\mathbb{C}$ with the symplecic form

$$\omega_{\mathcal{L}} = 4(dv_1 \wedge du_1 + dv_2 \wedge du_2). \tag{4.2.11}$$

From the above computation we can say that $\mathcal{L}$ is a 2:1 symplectic map from $(T^*\mathbb{C}, \omega_{\mathcal{L}})$ to $(T^*S^2 \setminus S^2, d\lambda)$.

However, note that the symplectic form $\omega_{\mathcal{L}}$ and $\omega_{\mathbb{C}^2}$ are different. Namely the subspaces $\mathbb{C}\times\{0\}$ and $\{0\}\times\mathbb{C}$ with the symplectic form $\omega_{\mathcal{L}}$ are Lagrangian and with the symplectic form $\omega_{\mathbb{C}^2}$ are symplectic submanifolds. But the two symplectic forms have the radial vectors field as a common Liouville vector field. It means, if we define the Liouville vector field $X_{\mathcal{L}}$ implicitly by

$$\iota_{X_{\mathcal{L}}}\omega_{\mathcal{L}} = \lambda_{\mathcal{L}} \tag{4.2.12}$$

then

$$X_{\mathcal{L}} = \frac{1}{2}(u_1\frac{\partial}{\partial u_1} + u_2\frac{\partial}{\partial u_2} + v_1\frac{\partial}{\partial v_1} + v_2\frac{\partial}{\partial v_2}) \tag{4.2.13}$$

which is also a Liouville vector field for $\omega_{\mathbb{C}^2}$. The standard Liouville vector field on T^*S^2 is defined as

$$\iota_X d\lambda = \lambda \tag{4.2.14}$$

where λ is the Liouville 1-form, or explicitly

$$X = q\frac{\partial}{\partial q} \tag{4.2.15}$$

for the fiber variables q. Since we can observe pull back commutes with the exterior derivative we obtain

$$\mathcal{L}^*X = X_{\mathcal{L}}. \tag{4.2.16}$$

In particular, this implies the following lemma.

Lemma 35. *A closed haypersurface $\Sigma \subset T^*S^2$ is fiberwise star-shaped if and only if $\mathcal{L}^{-1}\Sigma \subset \mathbb{C}^2$ is star-shaped.*

Remark: The unit cotangent bundle S^*S^2 is diffeomorphic to the 3-dimensional projective space $\mathbb{R}P^3$. On the other hand, we can find a diffeomorphism between the unit cotangent bundle S^*S^2 and a fiberwise star-shaped

hypersurface in T^*S^2 by fiberwise projection.

Corollary 36. *There exists a diffeomorphism between a fiberwise star-shaped hypersurface in* T^*S^2 *and the projective space* $\mathbb{R}P^3$ *if* $\mathcal{L}^{-1}\Sigma \subset \mathbb{C}^2$ *is star-shaped.*

Note that, a star-shaped hypersurface in $\mathbb{C}^2$ is diffeomorphic to the 3-dimensional sphere S^3 which is a twofold cover of $\mathbb{R}P^3$.

4.3 Levi-Civita Regularization and Uncoupled Harmonic Oscillators

In this section, we will focus on the twofold cover created by the Levi-Civita regularization. In the previous section, we showed that there exists a 2:1 map between $\mathbb{C}^2 \setminus \{0\}$ and $T^*S^2 \setminus S^2$.

Recall: A fiberwise star-shaped haypersurface in T^*S^2 is diffeomorphic to $\mathbb{R}P^3$. Thus we have a diffeomorphism $T^*S^2 \longrightarrow \mathbb{R}P^3$ and we know that star-shaped hypersurface in $\mathbb{C}^2$ is diffeomorphic to S^3 and this is also a twofold cover of $\mathbb{R}P^3$. Therefore for every fiberwise star-shaped hypersurface in T^*S^2 we can find a double cover on $\mathbb{C}^2$.

Remark: This double cover energy hypersurface is an important tool that we will use in the following chapters to find a concave toric domain for the rotating Kepler problem.

As an example of the Levi-Civita regularization, we can apply the Levi-Civita regularization to the Kepler problem. To this deal, first we need to substitute the values $2v^2$ and $\frac{u}{\bar{v}}$ instead of q and p in the Hamiltonian of the Kepler problem for the energy value c. Thus we have a new Hamiltonian for the Kepler problem with respect to u and v as

$$H(u,v) = \frac{|u|^2}{2|v|^2} - \frac{1}{2|v|^2} - c. \tag{4.3.1}$$

We can define

$$H'(u,v) := |v|^2 H(u,v) = \frac{1}{2}(|u|^2 - c|v|^2 - 1). \tag{4.3.2}$$

If we look at the level sets for energy zero

$$\Sigma := H^{-1}(0) = H'^{-1}(0) \tag{4.3.3}$$

we see that this level set is a three dimensional sphere for energy negative c.

The Hamiltonian flow of H' on Σ is just a representation of the Hamiltonian flow H on Σ. Note that the new Hamiltonian flow is periodic and physically it is the flow of two uncoupled harmonic oscillators.

In the next chapter we will apply the composition of the Levi-Civita map and the Ligon-Schaaf map to the rotating Kepler problem.

Chapter 5

The Special Concave Toric Domain for The Rotating Kepler Problem

5.1 Introduction

In this chapter, we will introduce an appropriate concave toric domain for the rotating Kepler problem. To this purpose, we use the stereographic projection and transfer the cotangent bundle of $\mathbb{R}^2$ to the cotangent bundle of S^2.

Consider the Ligon-Schaaf symplectomorphism. Recall that the Ligon-Schaaf symplectomorphism interchanges the Hamiltonian of the Kepler problem with Delaunay Hamiltonian. Therefore, we get the solutions of the Kepler problem as geodesics on the cotangent bundle T^*S^2. Angular momentum generate the rotating. Therefore the Hamiltonian of the rotating Kepler problem is obtained by adding angular momentum to the Kepler problem. As explained before the Ligon-Schaaf symplectomorphism interchanges angular momentum on the plane with a component of angular momentum on the sphere. Therefore the Ligon-Schaaf symplectomorphism pull back the Hamiltonian of the rotating Kepler problem to a Hamiltonian defined on the cotangent bundle of S^2 minus its zero section. The Levi-Civita map is a 2:1 map between $\mathbb{C}^2$ minus the origin and the cotangent bundle of S^2 minus the zero section.

For the next part, we assume the phase space T of the geodesics solutions of the RKP. Then by the Levi-Civita regularization, we map them to the space $\mathbb{C}^2$. This map gives us a double cover such that we can define a special concave toric domain which is an appropriate concave toric domain for the rotating Kepler problem.

5.2 The Special Concave Toric Domain

There are some steps for computing the concave toric domain of the RKP that we give in the following.

Let the unit sphere S^2 and denote the north pole of it in $\mathbb{R}^3$ with $N = (0, 0, 1)$. Take a point $x = (x_1, x_2, x_3)$ on

S^2 and a covector on the tangent space of S^2 at x with $y = (y_1, y_2, y_3)$ such that

$$x \neq N, \qquad x \cdot x = 1, \qquad x \cdot y = 0. \tag{5.2.1}$$

Using the stereographic projection transformation, we embed map the cotangent bundle of the space $\mathbb{R}^2$ to the cotangent bundle of the sphere S^2. In other words, we have

$$T^*\mathbb{R}^2 \longrightarrow T^*S^2 \tag{5.2.2}$$

$$(q, p) \mapsto (x, y), \tag{5.2.3}$$

such that we have the following equalities

$$\begin{aligned} x_k =& \frac{2q_k}{(q^2+1)}, \qquad x_3 = \frac{(q^2-1)}{(q^2+1)} \\ y_k =& \frac{(q+1)p_k}{2} - (q \cdot p)q_k, \qquad y_3 = q \cdot p \end{aligned} \tag{5.2.4}$$

where $k = 1, 2$.

Note that these are canonical transformations in the sense that the symplectic forms $\sum_{k=1}^{2} dq_k \wedge dp_k$ and the restriction of $\sum_{k=1}^{3} dx_k \wedge dy_k$ to T^*S^2 match.

Recall that the Hamiltonian of the Kepler problem is given by

$$H : T^*\mathbb{R}^2 \longrightarrow \mathbb{R} \tag{5.2.5}$$

$$(q, p) \mapsto \frac{1}{2}\|p\|^2 - \frac{1}{\|q\|} \tag{5.2.6}$$

where $\| \, . \, \|$ is the norm with respect to the standard metric.

In the chapter 5 we introduced the Delaunay Hamiltonian which is given by

$$\tilde{H}(x, y) = -\frac{1}{\|2y^2\|} \tag{5.2.7}$$

where $\| \, . \, \|$ is the norm with respect to the round geometric of S^2. Note that the Hamiltonian flow of the Delaunay Hamiltonian is a reparametrized geodesic flow on S^2.

Using the Stereographic projection 5.2.4, the Delaunay Hamiltonian becomes

$$\tilde{H}(q, p) = -\frac{2}{(|q|+1)^2|p|^2}. \tag{5.2.8}$$

The property

$$\Phi_{LS}^* H = \tilde{H}, \tag{5.2.9}$$

of the Ligon-Schaaf symplectomorphism guarantees that the Ligon-Schaaf symplectomorphism maps the Hamiltonian vector field of the Kepler Hamiltonian to the Hamiltonian vector field of the Delaunay Hamiltonian.

As explained in Chapter 5, the Ligon-Schaaf symplectomorphism interchanges angular momentum in $\mathbb{R}^2$ with the first component of angular momentum on S^2. Therefore in view of 5.2.8, after applying Ligon-Schaaf and stereographic projection the Hamiltonian of the rotating Kepler problem becomes

$$K(q,p) = \tilde{H}(q,p) + L(q,p) = -\frac{2}{(|q|+1)^2|p|^2} + q_1p_2 - q_2p_1. \tag{5.2.10}$$

If we interpret q and p as complex numbers, i.e. $q = q_1 + iq_2$ and $p = p_1 + ip_2$. We can rewrite 5.2.10 as

$$K(q,p) = \tilde{H}(q,p) + L(q,p) = -\frac{2}{(|q|+1)^2|p|^2} + Im(\bar{q}\cdot p). \tag{5.2.11}$$

Note that the Levi-Civita transformation is a $2:1$ map which up to a constant factor is symplectic when we think of $\mathbb{C}^2$ as $T^*\mathbb{C}$. It pulls back the geodesic flow on S^2 to the flow of two uncoupled oscillators.

We plug $\frac{u}{\bar{v}}$ and $2v^2$ into the relation 5.2.10 instead of q and p respectively. Then get the following identity

$$\begin{aligned}\tilde{H}(u,v) + L(u,v) &= -\frac{2}{(|\frac{u}{\bar{v}}|+1)^2(|2v^2|)^2} + Im(\frac{\bar{u}}{\bar{v}}\cdot 2v^2) \\ &= -\frac{2}{2(|u|^2+|v|^2)^2} + 2Im(\bar{u}v) \\ &= -\frac{1}{2(|u|^2+|v|^2)^2} + 2(u_1v_2 - u_2v_1).\end{aligned} \tag{5.2.12}$$

To simplify expression 5.2.12, we introduce the function

$$\mu : T^*\mathbb{C} \longrightarrow [0,\infty)\times\mathbb{R} \subset \mathbb{R}^2 \tag{5.2.13}$$

$$(u,v) \mapsto \begin{cases} \frac{1}{2}(|u|^2+|v|^2)^2 \\ u_1v_2 - u_2v_1. \end{cases} \tag{5.2.14}$$

This is the momentum map of the torus action on $T^*\mathbb{C}$.

Note that in view of the elementary inequality

$$|ab| \leqslant \frac{1}{2}(a^2+b^2) \tag{5.2.15}$$

it follows that $|\mu_2| \leqslant \mu_1$.

Componentwise we have

$$\mu_1 := \frac{|u|^2+|v|^2}{2}, \qquad \mu_2 := u_1v_2 - u_2v_1. \tag{5.2.16}$$

If we use the above definitions and plug them in the relation 5.2.12 the following proposition follows when K denotes the Hamiltonian of the rotating Kepler problem.

Proposition 37. *Given the Ligon-Schaaf symplectomorphism and the Levi-Civita regularization, the pull*

back of K *becomes*

$$\mathcal{L}^*\Phi_{LS}^*(K) = -\frac{1}{8\mu_1^2} + 2\mu_2. \tag{5.2.17}$$

Proof. This follows from the discussion above. □

To continue, we show that the symplectic manifold $\mathbb{C}\oplus\mathbb{C}$ and the cotangent bundle $T^*\mathbb{C}$ are symplectomorphic.

Proposition 38. *There exists a linear symplectomorphism between the symplectic manifold* $\mathbb{C}\oplus\mathbb{C}$ *and the cotangent bundle* $T^*\mathbb{C}$. *In other words, we have the linear symplectomorphism*

$$S : (\mathbb{C}\oplus\mathbb{C}, \omega_0) \longrightarrow (T^*\mathbb{C}, \omega_1). \tag{5.2.18}$$

Proof. Consider the symplectic form on $T^*\mathbb{C}$ as

$$\omega_1 = du_1 \wedge dv_1 + du_2 \wedge dv_2. \tag{5.2.19}$$

Let $(z_1, z_2) \in \mathbb{C}^2$ such that $z_1 = x_1 + iy_1$ and $z_2 = x_2 + iy_2$. We define the following linear map

$$S : \mathbb{C}^2 \longrightarrow T^*\mathbb{C} \tag{5.2.20}$$

as

$$\begin{aligned} u_1 &\longrightarrow \frac{1}{\sqrt{2}}(y_1 - y_2) \\ u_2 &\longrightarrow \frac{1}{\sqrt{2}}(x_1 + x_2) \\ v_1 &\longrightarrow \frac{1}{\sqrt{2}}(x_2 - x_1) \\ v_2 &\longrightarrow \frac{1}{\sqrt{2}}(y_1 + y_2) \end{aligned} \tag{5.2.21}$$

To prove that S interchanges the symplectic forms ω_0 and ω_1 we compute using 5.2.21. Thus we have

$$\begin{aligned} S^*(\omega_1) &= S^*(du_1 \wedge dv_1 + du_2 \wedge dv_2) \\ &= (\frac{1}{\sqrt{2}}(dy_1 - dy_2) \wedge \frac{1}{\sqrt{2}}(dx_2 - dx_1)) + (\frac{1}{\sqrt{2}}(dx_1 - dx_2) \wedge \frac{1}{\sqrt{2}}(dy_1 + dy_2)) \\ &= dx_1 \wedge dy_1 + dx_2 \wedge dy_2 \\ &= \omega_0. \end{aligned} \tag{5.2.22}$$

□

We extend the function 5.2.17 to $T^*\mathbb{C} \setminus \{0\}$ and define

$$\tilde{K} : T^*\mathbb{C} \setminus \{0\} \longrightarrow \mathbb{R} \tag{5.2.23}$$
$$\tilde{K} := -\frac{1}{8\mu_1^2} + 2\mu_2.$$

Now we use the above function and obtain a Concave Toric Domain for the RKP on a coordinate system which is rotated in view of Proposition 38. To define this CTD, we make the following abbreviations.

Denote the first quarter in $\mathbb{R}^2$ by $Q := [0,\infty) \times [0,\infty)$ and define

$$Q_{\frac{1}{2}} := \{(x,y) \in \mathbb{R}^2 : x \geqslant 0, |y| \leqslant x\}. \tag{5.2.24}$$

Assume $\Omega \subset Q$ is a closed set on the first quarter in $\mathbb{R}^2$. A toric domain is defined by

$$X_\Omega := \nu^{-1}(\Omega), \tag{5.2.25}$$

where

$$\nu = (\nu_1, \nu_2) : \mathbb{C}^2 \longrightarrow Q \subset \mathbb{R}^2 \tag{5.2.26}$$
$$(z_1, z_2) \mapsto (\pi|z_1|^2, \pi|z_2|^2). \tag{5.2.27}$$

Note that ν is a momentum map for the torus action

$$(\nu_1, \nu_2)(z_1, z_2) = (e^{i\theta_1} z_1, e^{i\theta_2} z_2) \tag{5.2.28}$$

on $\mathbb{C}^2$.

Also we can define the symplectic 4-manifold with boundary X_Ω as

$$X_\Omega := \{z = (z_1, z_2) \in \mathbb{C}^2 \mid \pi(|z_1|^2, |z_2|^2) \in \Omega\}. \tag{5.2.29}$$

We give the definition of the Hutchings CTD and then we define the special concave toric domain for the RKP and compare the both definitions with each other.

Definition 39. (The Hutchings CTD) We say that a toric domain X_Ω is a concave toric domain if Ω is a closed region bounded by the horizontal segment from $(0,0)$ to $(a,0)$, the vertical segment from $(0,0)$ to $(0,b)$ and graph of a convex function $f : [0,a] \longrightarrow [0,b]$ with $f(0) = b$ and $f(a) = 0$, where $a > 0$ and $b > 0$.

Definition 40. (The Special Concave Toric Domain) A concave toric domain $X_\Omega \subset \mathbb{C}^2$ is called special if the function f satisfies the additional property $f'(t) \geqslant -1$ for $t \in [0,a]$.

Define $\bar{S}$ by

$$\bar{S} : Q \longrightarrow Q_{\frac{1}{2}} \tag{5.2.30}$$

which is a clockwise 45 degree rotation composed with a $\frac{1}{\sqrt{2}\pi}$ dilation.

Given the above definition and the momentum maps on the torus actions $T^*\mathbb{C}$ and $\mathbb{C}^2$. We have the following relations between the momentum maps μ and ν,

$$\begin{aligned}\bar{S}(\frac{1}{2\pi}(\nu_1+\nu_2)) =&\mu_1\\ \bar{S}(\frac{1}{2\pi}(\nu_1-\nu_2)) =&\mu_2.\end{aligned}$$

Using these equalities and the relations S, $\bar{S}$, μ and ν, the diagram

$$\begin{array}{ccc}\mathbb{C}\oplus\mathbb{C} & \xrightarrow{S} & T^*\mathbb{C}\\ \nu\downarrow & & \downarrow\mu\\ Q & \xrightarrow{\bar{S}} & Q_{\frac{1}{2}}\end{array} \tag{5.2.31}$$

commutes. We define a new concave domain Ω' as

$$\Omega' := S^*(\Omega)\subset Q_{\frac{1}{2}} \tag{5.2.32}$$

such that

$$X_{\Omega'} = \mu^{-1}(\Omega') = S(X_\Omega) \tag{5.2.33}$$

in $T^*\mathbb{C}$.

For the purposes of this thesis and for more simplicity, we assume that the concave toric domain is a subset of $T^*\mathbb{C}$ instead of $\mathbb{C}^2$ and we think of Ω is a closed subset of $Q_{\frac{1}{2}}$ and miss the prime.

Using the new convention a special concave toric domain can be defined as follows.

Remark 41. Using the above identification of $\mathbb{C}^2$ and $T^*\mathbb{C}$ a toric domain X_Ω is special concave toric domain if and only if there exists a convex function

$$g : [a,b]\longrightarrow\mathbb{R},\qquad 0<a<b<\infty, \tag{5.2.34}$$

with properties $g(a)=a$, $g(b)=-b$ such that $\Omega\subset Q_{\frac{1}{2}}$ is bounded by the segment $\{(t,t) : t\in[0,a]\},\{(t,-t) : t\in[0,b]\}$ and the graph of the convex function g.

Remark 42. In the following, we are working with $\Omega\subset Q_{\frac{1}{2}}$. If Ω satisfies the conditions of remark 41 we refer to $X_\Omega := \mu^{-1}(\Omega)$ as a special concave toric domain.

Assume $c\leqslant -\frac{3}{2}$, we define a closed subset of $Q_{\frac{1}{2}}$ by

$$\mathcal{K}_c := \mu(\tilde{K}^{-1}(-\infty,c))\subset Q_{\frac{1}{2}}. \tag{5.2.35}$$

Note that if $c < -\frac{3}{2}$ then $\mathcal{K}_c$ has two connected components, one bounded and one unbounded, i.e. we write

$$\mathcal{K}_c = \mathcal{K}_c^b \cup \mathcal{K}_c^u, \tag{5.2.36}$$

for $\mathcal{K}_c^b$ the bounded connected component and $\mathcal{K}_c^u$ the unbounded connected component.

For $c = -\frac{3}{2}$ the two sets become connected as a singularity which is the point $(\frac{1}{2}, -\frac{1}{2})$.

Theorem 43. *For $c \leqslant -\frac{3}{2}$, we have*

$$\tilde{K}^{-1}(-\infty, c) = X_{\mathcal{K}_c^b} \cup X_{\mathcal{K}_c^u} \subset T^*\mathbb{C} \tag{5.2.37}$$

and $X_{\mathcal{K}_c^b}$ is a special concave toric domain.

Proof. After all these transformations this now follows immediately from 5.2.23, since the function from $(0, \infty) \longrightarrow \mathbb{R}$

$$x \mapsto \frac{1}{16x^2}$$

is convex. □

See the graphs of the SCTD for the energies $c \leqslant -\frac{3}{2}$, $c = -\frac{3}{2}$ and $c > -\frac{3}{2}$ in Figures 1.3.1, 1.3.2 and 1.3.3 respectively.

Chapter 6

Construction of a New Tree and Slopes of Tori

In this chapter we will study the Calkin-Wilf and the Stern-Brocot tree and then we introduce a new tree for the coordinate system rotated by 45 degree. From the new tree we can read off the slopes and critical energy values and also specify the tori correspond to these slopes that we need them in the computation of the ECH capacities of the RKP.

6.0.1 The Calkin-Wilf tree

The Calkin-Wilf tree is a labelled complete infinite binary tree where the labels are rational and are obtained by a recursive formula. In fact, there is a one-to-one correspondence between rational number and the labels of the nodes. For $a, b \in \mathbb{N}$, the iteration relation is

$$\frac{a}{b} \mapsto \frac{a}{a+b} \quad \text{and} \quad \frac{a+b}{b}. \tag{6.0.1}$$

We call fractional numbers $\frac{a}{a+b}$ even and fraction numbers $\frac{a+b}{b}$ odd and put them on the left and the right hand sides below the root $\frac{a}{b}$ respectively.

We draw this tree by induction. We define the labelling of the root $\frac{1}{1}$ for the first stage and generate the $n+1$-stage by the set of the previous n-th stages by using 6.0.1. Now for the first stage, we start from the root $\frac{1}{1}$ and attribute numbers $\frac{1}{2}$ and numbers $\frac{2}{1}$ to its children and put them on the left and the right hand sides below the root $\frac{1}{1}$. For the next stage we take the root $\frac{a}{b}$ and put the fraction numbers $\frac{a}{a+b}$ and $\frac{a+b}{b}$ to the left and the right and sides below the root $\frac{a}{b}$ and make a new level of the tree.

Remark 44. We denote the left hand child of a root by its zero child and the right hand child of a root by its 1 child and call them the even and odd child of a root respectively.

Thus the Calkin-Wilf tree is

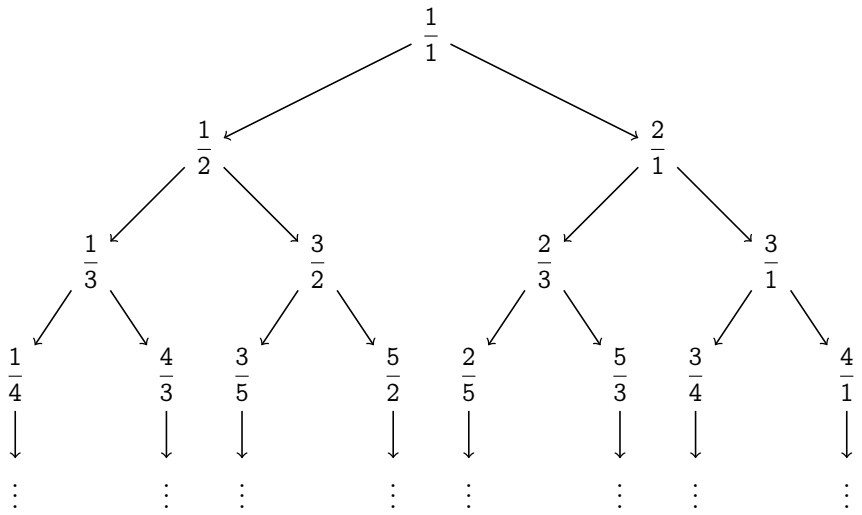

Remark 45. In the Calkin-Wilf tree, each positive rational number appears once and only once each of which represented as a reduced fraction.

We can write the Calkin-Wilf tree line by line as

$$\frac{1}{1}, \frac{1}{2}, \frac{2}{1}, \frac{1}{3}, \frac{3}{2}, \frac{3}{1}, \frac{1}{4}, \frac{4}{3}, \frac{3}{5}, \frac{5}{2}, \frac{2}{5}, \frac{5}{3}, \frac{4}{1}, \cdots \tag{6.0.2}$$

by using the iteration relation

$$x_1 = 1, \qquad x_{n+1} = (2[x_n] + 1 - x_n)^{-1} \tag{6.0.3}$$

where $[x]$ is the floor number of x, see [7]. It means the largest integer number less than or equal to x.

6.1 The Stern-Brocot tree

Here we give the Stern-Brocot tree which was introduced by Moritz Stern 1858 and Achille Brocot 1861. As the Calkin-Wilf tree, the Stern-Brocot tree is a complete infinity binary tree whose nodes are labelled by a unique rational number.

We can obtain this tree by induction and a mediant method whose definition we give in the following.

Definition 46. A mediant is a fraction such that its numerator is the sum of the numerators of two other fraction and its denominator is the sum of the denominators of two other fraction.

The Stern-Brocot tree constructed by induction that the level zero comes from pseudofractions $\frac{0}{1}$ and $\frac{1}{0}$. We describe how we can get other levels by induction. To generate a new level, we give an increasing order to vertices on the previous level and then by using the mediants, we find new terms of the new level. Finally we write the new term increasingly on a line and generate the new level of the Stern-Brocot tree.

In other words,

Stage -1: We start with the auxiliary labels $\frac{0}{1}$ and $\frac{1}{0}$ lowest to highest terms. Stage -1, we do not really consider as part of the tree but this level is used in the inductive constructive of the tree.

Stage 0: The root is $\frac{1}{1}$ which can be interpreted as mendiant of stage -1.

Stage 1: We add the mediant of the boundaries.

Stage n+1: We add the mediants of all consecutive fraction in the tree including the boundaries from the lowest to highest.

Therefore we have the Stern-Brocot tree as follow

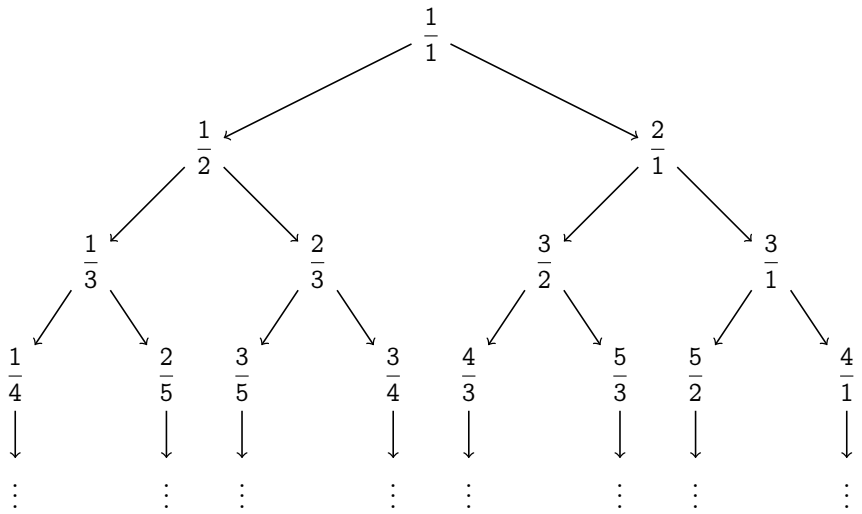

Note that we should always start form the fractional numbers $\frac{0}{1}$ and $\frac{1}{0}$ as level -1.

In this tree every rational number appears but just once.

Proposition 47. *At any stage of the Stern-Brocot tree, the consecutive fractions* $\frac{p}{q} < \frac{p'}{q'}$ *have the property*

$$qp' - pq' = 1. \tag{6.1.1}$$

Proof. Proof by induction. □

Proposition 48. *At any stage* n*, the sum of the numerator and the denominator of a newborn is at least* $n + 1$.

Proof. Proof by induction. □

We can offer another method to find the labels of the Stern-Brocot tree. Here we show that the Calkin-Wilf tree and the Stern-Brocot tree are related to each other by duality.

Recall: An infinite complete binary tree is a tree with the property that every node has two children.

Since both trees are labelled infinite complete binary trees, in view of the last property, the nodes can be expressed as finite binary sequences, like 101001 or 001010011. Here the root is 1. In the example of the Stern-Brocot tree,

$$\mathrm{Node}(1) = \frac{1}{1} \tag{6.1.2}$$

$$\mathrm{Node}(10) = \frac{1}{2} \tag{6.1.3}$$

$$\mathrm{Node}(101) = \frac{2}{3} \tag{6.1.4}$$

$$\vdots \tag{6.1.5}$$

For νa finite binary sequence we define the corresponding label of the Calkin-Wilf tree by k_ν, i.e.

$$k_1 = \frac{1}{1} \tag{6.1.6}$$

$$k_{10} = \frac{1}{2} \tag{6.1.7}$$

$$k_{101} = \frac{3}{2} \tag{6.1.8}$$

$$\vdots \tag{6.1.9}$$

Similarly, we denote the labels od the Stern-Brocot tree by σ_ν. So that

$$\sigma_1 = \frac{1}{1} \tag{6.1.10}$$

$$\sigma_{10} = \frac{1}{2} \tag{6.1.11}$$

$$\sigma_{101} = \frac{2}{3} \tag{6.1.12}$$

$$\vdots \tag{6.1.13}$$

If V is the set of all finite binary sequences, i.e. the nodes of our infinite complete binary tree, then the bit-reversal isomorphism is the bijection $B : V \longrightarrow V$ which reads every binary sequence backwards. For example,

$$B(10100011000) = 00011000101. \tag{6.1.14}$$

Using this bijection, we can obtain the labels of the Stern-Brocot tree form the labels od the Calkin-Wolf tree and vica versa by formulas

$$k_{B(\nu)} = \sigma_\nu, \qquad \sigma_{B(\nu)} k_\nu. \tag{6.1.15}$$

6.2 Introducing a New tree

In this section, we are going to introduce a new tree which is an important tree in this thesis and help us to find slopes and critical energy values of tori and asteroids in the SCTD.

Using these slopes on the SCTD, we will get information about the tori, their critical energies and critical points which are important to compute the ECH capacities of the RKP. The critical energy value of a torus or a asteroid is smallest energy for which the torus or asteroid appear first.

Note that, we will see that the critical energies and the critical points of tori and asteroids determined uniquely.

In the following, we explain how to get the new tree by using the Stern-Brocot tree and the relation of slopes for troi $T_{k,l}$. In the next chapter, we will see the relation of the critical energy of a torus $T_{k,l}$, the critical point of the torus and give their examples.

6.2.1 The New Tree

We define a new tree by interpreting the labels the Stern-Brocot tree as slopes and rotate them 45 degree in clockwise direction. We denote the nodes of the Stern-Brocot tree by the fractional number $\frac{k}{l}$ and we can write them as a matrix $\begin{bmatrix} k \\ l \end{bmatrix}$. Since we consider the new tree in the rotated coordinates, we multiply the matrix of the node $\frac{k}{l}$ by $\begin{bmatrix} 1 & 1 \\ -1 & 1 \end{bmatrix}$ which corresponds to a rotation by 45 degree and a dilation by $\sqrt{2}$ which does not influence the slope. Namely

$$\begin{bmatrix} 1 & 1 \\ -1 & 1 \end{bmatrix} \begin{bmatrix} k \\ l \end{bmatrix} = \frac{k+l}{-k+l}. \tag{6.2.1}$$

Now therefore we replace the label $\frac{k}{l}$ in the Stern-Brocot tree by the label $\frac{k+l}{-k+l}$. If we do the above method for all nodes of the Stern-Brocot tree, then we get the new tree such that the nodes of the new tree are the slopes of the the tori $T_{k,l}$ in the SCTD. The new tree is

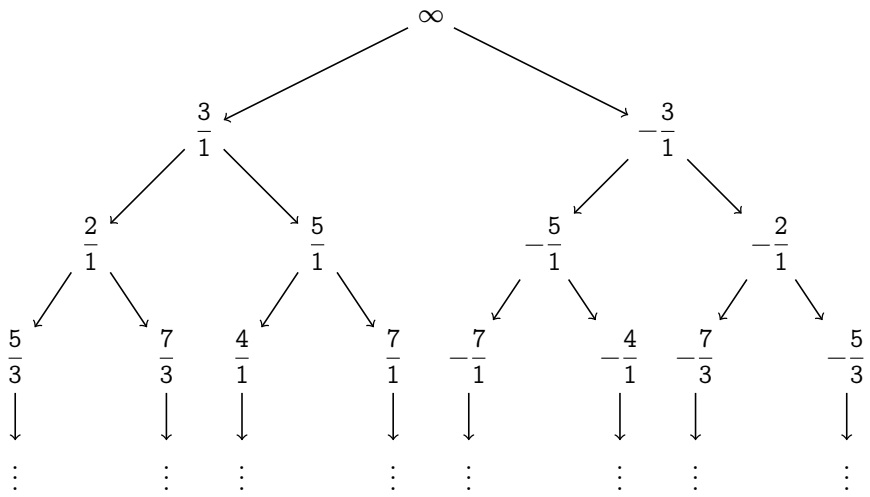

The Stern-Brocot tree is an infinity complete tree and the nodes of that correspond to tori $T_{k,l}$ where $k, l \in \mathbb{N}$. Therefore using the nodes of the new tree we can determine the slopes of all tori in the SCTD.

Denote the slope of a torus $T_{k,l}$ by $S_{k,l}$ in the SCTD. We compute the slope of the torus $T_{k,l}$ using the relation

$$S_{k,l} = \frac{k+l}{-k+l} \tag{6.2.2}$$

on the SCTD.

We can find the slopes of all tori $T_{k,l}$ by the above relation on the SCTD which are determined uniquely by a rational number.

Chapter 7

Introduction to ECH Capacities

ECH capacities were introduced by" K. Choi, D. Cristofaro-Gardiner, D. Frenkel, M. Hutchings, V. G. B. Ramos,"[3]. In this chapter we recall ECH capacities which give obstructions to symplectic embeddings of one symplectic 4-manifold with boundary into another. For concave toric domains, there is an algorithm how to compute ECH capacities due to [3].

In the first section, we recall the definition and some properties of ECH capacities. In the second section, we recall the definition of a concave toric domain. In the third section, we explain the algorithm how to obtain ECH capacities for a concave toric domain using the Stern-Brocot tree. As far as we know this is the first time that the connection between the algorithm due to [3] and the Stern-Brocot tree is made explicit.

7.1 ECH capacities

Suppose (X, ω) is a compact symplectic 4-manifold. This manifold can have boundary and corners. ECH capacities are defined for the manifold (X, ω) as a sequence of real numbers

$$0 = c_0(X, \omega) \leqslant c_1(X, \omega) \leqslant c_2(X, \omega) \leqslant \cdots \leqslant \infty \tag{7.1.1}$$

which have useful properties as follows.

(Monotonicity) If there exists a symplectic embedding

$$(X, \omega) \longrightarrow (X', \omega'). \tag{7.1.2}$$

Then for all k, we have inequality

$$c_k(X, \omega) \leqslant c_k(X', \omega'). \tag{7.1.3}$$

(Conformality) For $r > 0$ it holds true that

$$c_k(X, r\omega) = rc_k(X, \omega). \tag{7.1.4}$$

(Disjoint Union)

$$c_k(\bigsqcup_{i=1}^{n}(X_i, \omega_i)) = \max_{k_1+k_2+\cdots+k_n=k} \sum_{i=1}^{n} c_{k_i}(X_i, \omega_i). \tag{7.1.5}$$

(Ellipsoid) Let $a, b > 0$ and define the ellipsoid by

$$E(a, b) := \{(z_1, z_2) \in \mathbb{C}^2 | \frac{\pi|z_1|^2}{a} + \frac{\pi|z_2|^2}{b} \leqslant 1\}. \tag{7.1.6}$$

We can write $c_k(E(a, b)) = N(a, b)$, where $N(a, b)$ denotes the sequence of all nonnegative integer linear combinations of a and b arranged in nondecreasing order and index k starting from zero.

Note that in the remaining chapters of this thesis we will use the standard symplectic form on $\mathbb{C}^2 = \mathbb{R}^4$.

If we let $a = b$, then we abbreviate

$$E(a, b) = E(a, a) =: B(a) \tag{7.1.7}$$

that is called a ball with radius $\sqrt{\frac{a}{\pi}}$. We apply the identity $a = b$ on the ellipsoid property and get a similar property as the ellipsoid property for a ball with radius $\frac{a}{\pi}$, i.e.

$$c_k(B(a)) = ad \tag{7.1.8}$$

where d is the unique nonnegative integer such that

$$\frac{d^2 + d}{2} \leqslant k \leqslant \frac{d^2 + 3d}{2}. \tag{7.1.9}$$

McDuff showed that there exists a symplectic embedding $int(E(a, b)) \longrightarrow E(a', b')$ if and only if $N(a, b)_k \leqslant N(a', b')_k$ for all k. Therefore ECH capacities give a sharp obstruction to symplectic embeddings one of (open) ellipsoid into another.

Define the polydisk

$$P(a, b) = \{(z_1, z_2) \in \mathbb{C}^2 \,:\, \pi|z_1|^2 \leqslant a,\ \pi|z_1|^2 \leqslant b\}. \tag{7.1.10}$$

We use ECH capacities and give a sharp obstruction which is symplectically embedding by

$$E(a, b) \overset{s}{\hookrightarrow} P(a', b'). \tag{7.1.11}$$

In genera case, the inverse of the above embedding is not hold, i.e. ECH capacities give not a sharp obstruction to embedding $P(a', b')$ into $E(a, b)$.

Example 49.

- *Assume there exist a symplectic embedding as*

$$P(1,1) \overset{s}{\hookrightarrow} E(a, 2a) \tag{7.1.12}$$

the ECH capacities give us the equality $a \geqslant 1$.

- *If there exist a symplectic embedding*

$$P(1,2) \overset{s}{\hookrightarrow} \mathrm{int}B(a). \tag{7.1.13}$$

Then ECH capacities only imply that $a \geqslant 2$. *This embedding shown by Hindi-Lisi that* $a \geqslant 3$ *recently.*

Definition 50. A symplectic embedding $\phi : (X, \omega) \longrightarrow (X', \omega')$ is optimal if there does not exist a symplectic embedding $(X, r\omega) \longrightarrow (X', \omega')$ for any $r > 1$.

By the monotonicity and conformality properties of ECH capacities, for some k, if we have $0 < c_k(X, \omega) = c_k(X', \omega')$ and if there exist a symplectic embedding $(X, \omega) \longrightarrow (X', \omega')$. Then this symplectic embedding is optimal.

7.2 Concave toric domain

One of the main result of this thesis is computing an appropriate concave toric domain for the rotating Kepler problem that we have already done in chapter 6. There are strong relations between the SCTD and Hutchings concave toric domain and also there are similar (although not exactly the same) algorithms for computing the ECH capacities of both domains. In this chapter we give the computing method of the Hutchings CTD with an example and will extend it in the next chapter to compute the ECH capacities of the RKP in the SCTD.

For this purpose, first we give the definition of the Hutchings concave toric domain and then we compute the weights for it. Suppose Ω is a domain in the first quadrant of the plane $\mathbb{R}^2$. The " toric domain" is defined by

$$X_\Omega := \{z \in \mathbb{C}^2 \mid \pi(|z_1|^2, |z_2|^2) \in \Omega\}. \tag{7.2.1}$$

We denote by ν the map

$$\nu : X_\Omega \longrightarrow \pi \tag{7.2.2}$$

$$z \mapsto \pi(|z_1|^2, |z_2|^2) \tag{7.2.3}$$

which is called momentum map. The concave toric domain as introduced by Hutchings is

Definition 51. A concave toric domain is a domain X_Ω where Ω is the closed region bounded by the horizontal segment from $(0,0)$ to $(a,0)$, the vertical from $(0,0)$ to $(b,0)$ and the graph of a convex function $f : [0,a] \longrightarrow [0,b]$

with $f(0) = b$ $f(a) = 0$. The concave toric domain X_Ω is rational if f is piecewise linear and f' is rational wherever it is defined.

Example 52. *Given a triangle with vertices* $(0,0)$, $(a,0)$ *and* $(0,b)$ *on the standard coordinate space in* $\mathbb{R}^2$. *This concave toric domain is an ellipsoid such as* $E(a,b)$.

By work of McDuff (Cor. 2.5) [8], we known that the ECH capacities of an ellipsoid $E(a,b)$ with $\frac{a}{b}$ rational are equal to the ECH capacities of a certain ball packing of the ellipsoid. For instance, a finite disjoint union of balls whose interior symplectically embeds into the ellipsoid filling up all of its volume. Therefore we should find this finite disjoint union of balls. To find this balls union, we give a new notation and call it weight expansion of the pair (a,b). Note that we can apply ECH capacities of concave toric domains for all a and b as well.

7.3 Weight Expansions

Let X_Ω be a CTD, the weight expansion of Ω is a finite (or infinite) unordered list of (possibly repeated) positive real number $W(\Omega) = (a_1, a_2, \cdots, a_n)$ defined inductively. Here we explain how to get these weights.

Remark 53. By the Stern-Brocot tree, we can relate every weight to a node of the Stern-Brocot tree. On the other hand, these nodes correspond to tori $T_{k,l}$ and we can find their slopes by the formula

$$S^{CTD}_{k,l} = -\frac{k}{l}. \tag{7.3.1}$$

They are determined uniquely for portions of a CTD.

Recall: A node of the Stern-Brocot tree is called even or odd if we write it by a sequence of 0 and 1 such that the sequence ends with 0 or 1 respectively.

We denote portions of a CTD with $\Omega_{i_1 i_2 \cdots i_j}$ where $i_1, i_2, \cdots, i_j \in \{0,1\}$. Each portion like $\Omega_{i_1 i_2 \cdots i_j}$ is related to the node $N_{i_1 i_2 \cdots i_j}$ in the Stern-Brocot tree. We consider the above notations and compute weights of the CTD.

For the easiest case, let Ω be a triangle with vertices $(0,0), (0,a)$ and $(a,0)$. The weight of Ω is equal to a, i.e. $W^{CDT}(\Omega) = a$.

Otherwise, let $a > 0$ be the largest real number such that the triangle with vertices $(0,0), (0,a)$ and $(a,0)$ is contained in Ω. We name this triangle Ω_1. Thus we have the torus $T_{1,1}$ and the slope $S^{CTD}_{1,1} = -1$ for this portion. Refer to chapter 4 on tori and periodic orbits, $T_{1,1} = \nu^{-1}(\nu_{1\Omega_1}, \nu_{2\Omega_1})$. Hence the first weight of the CTD is

$$W^{CTD}(\Omega_1) = a. \tag{7.3.2}$$

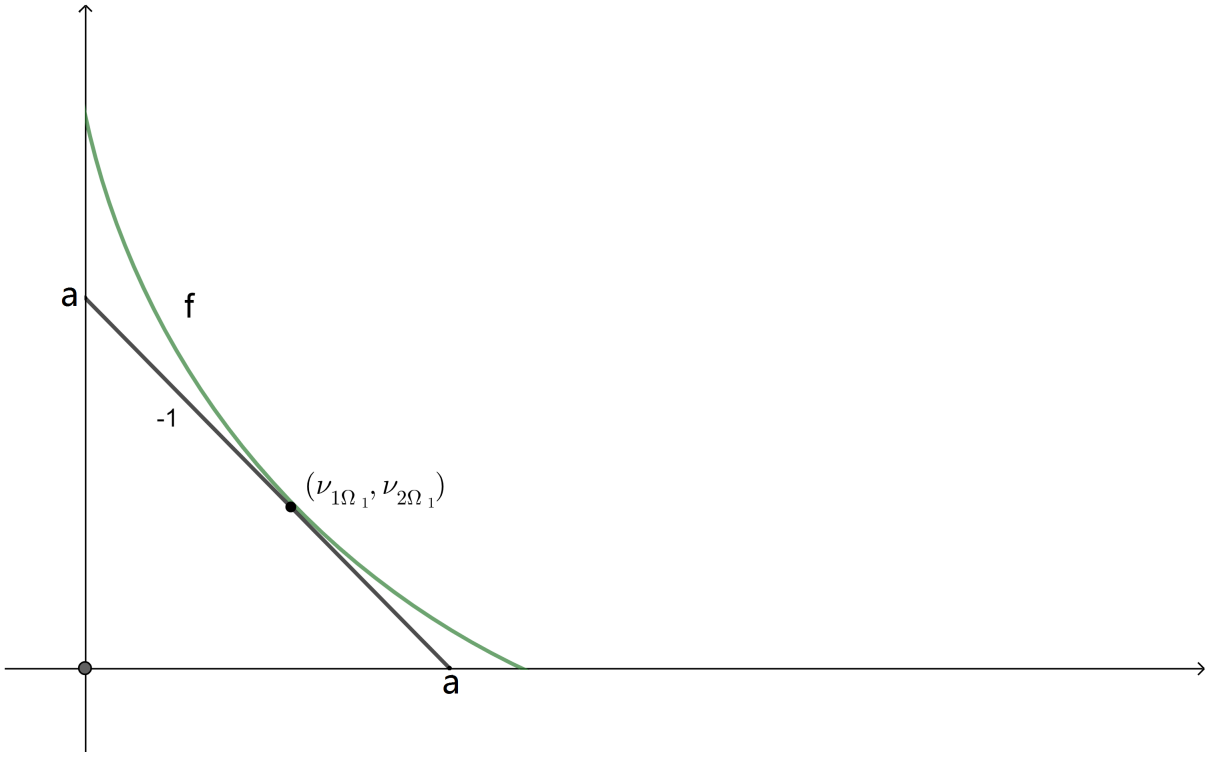

Figure 7.3.1: The portion for the first weight $W^{\mathrm{CTD}}(\Omega_1)$

Denote the tangent point of the line $x + y = a$ and the graph of f with $(\nu_{1\Omega_1}, \nu_{2\Omega_1})$ and call it the critical point of Ω_1. See Figure 7.3.1

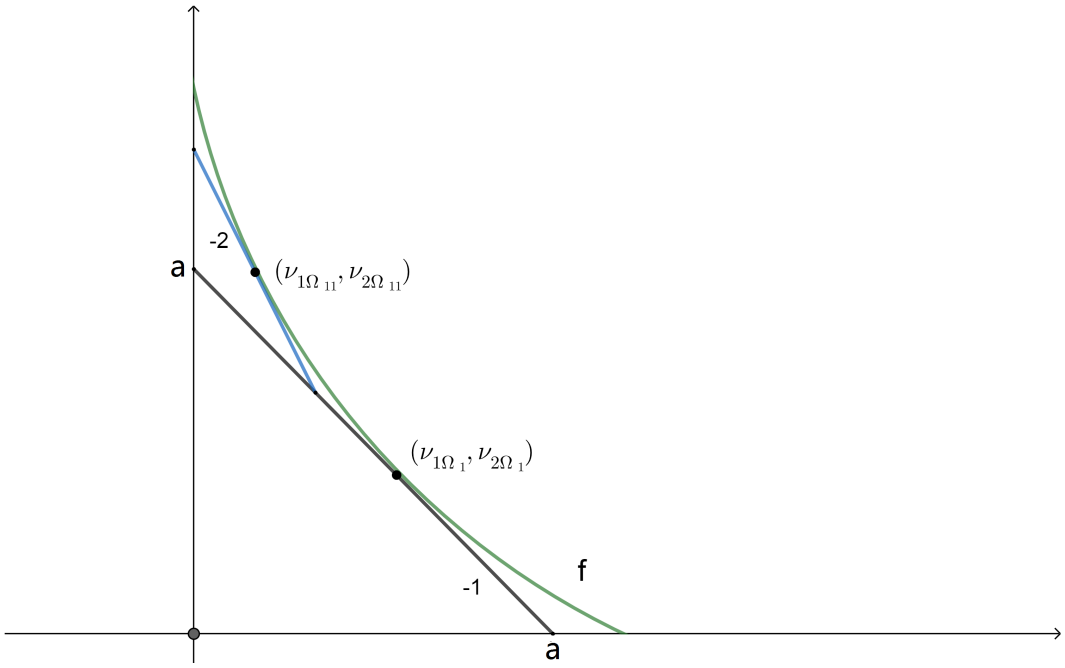

Figure 7.3.2: The portion for the weight $W^{\mathrm{CTD}}(\Omega_{11})$

Assume the portion Ω_{11} of Ω is the portion between the line $x+y=a$ and the graph of the function f above the point $(\nu_{1\Omega_1}, \nu_{2\Omega_1})$. Because of the index, we say this portion is odd. Its node in the Stern-Brocot tree is $\frac{k}{l}=\frac{2}{1}$ and its slope satisfies

$$S_{2,1}^{CTD} = -\frac{2}{1} = -2. \tag{7.3.3}$$

Also the critical point $(\nu_{1\Omega_{11}}, \nu_{2\Omega_{11}})$ of this portion is the tangent point of the slope $S_{2,1}^{CDT} = -2$ in the graph of the function f. On the other hand, we have

$$T_{2,1} = \nu^{-1}(\nu_{1\Omega_{11}}, \nu_{2\Omega_{11}}). \tag{7.3.4}$$

If we denote the intersection point of the slope $S_{2,1}^{CTD} = -2$ and y axis with (x_2, y_2). Then we can write the second weight the CTD by

$$W^{CTD}(\Omega_{11}) = y_2 - W(\Omega_1). \tag{7.3.5}$$

See Figure 7.3.2.

Now denote the portion below the critical point $(\nu_{1\Omega_1}, \nu_{2\Omega_1})$ between the line $x+y=a$ and the graph of the function f by Ω_{10}. Due to the index, this is an even portion of the CTD Ω. This portion is related to the node $N_{1,0}$ in the Stern-Brocot tree which is $\frac{k}{l}=\frac{1}{2}$ and the torus is $T_{1,2} = \nu^{-1}(\nu_{1\Omega_{10}}, \nu_{2\Omega_{10}})$ where $(\nu_{1\Omega_{10}}, \nu_{2\Omega_{10}})$ is the critical point of the portion Ω_{10}. The slope of this portion is

$$S_{1,2}^{CTD} = -\frac{1}{2}. \tag{7.3.6}$$

If we define the intersection point of the slope $S_{1.2}^{CTD}$ and the x axis with (x_3, y_3), then the third weight of the CTD will be

$$W^{CTD}(\Omega_{10}) = x_3 - W^{CTD}(\Omega_1). \tag{7.3.7}$$

See Figure 7.3.3

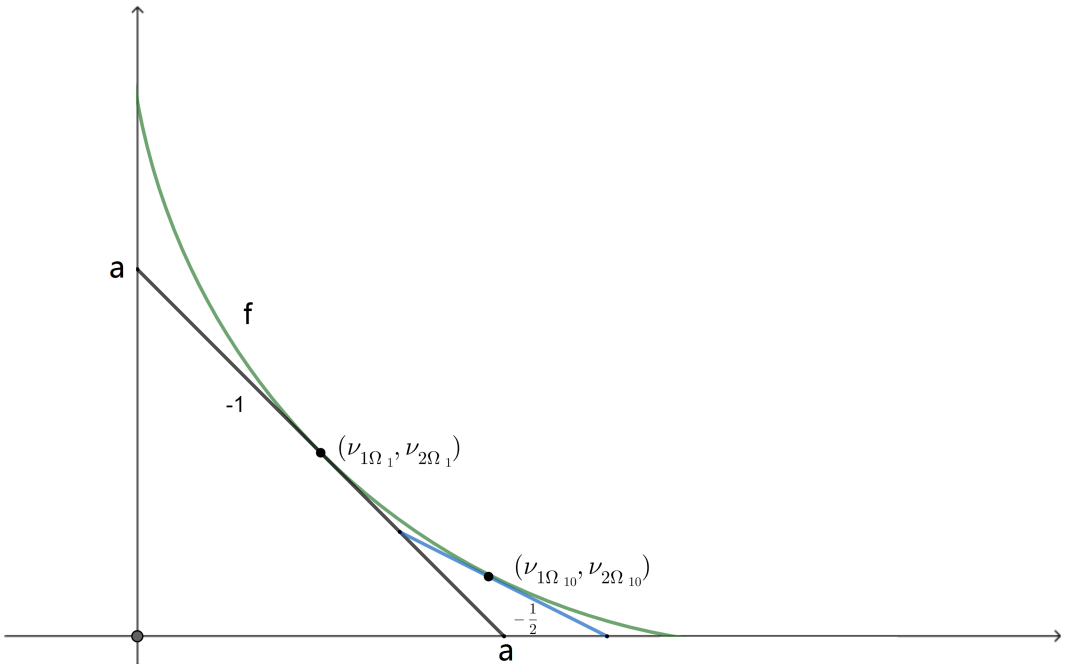

Figure 7.3.3: The portion for the weight $W^{\mathrm{CTD}}(\Omega_{10})$

Remark 54. If we want to use slopes correspond to portions $\Omega_{i_1,\cdots,i_j}$. There are two special cases for a slope corresponds to a portion $\Omega_{i_1,\cdots,i_j}$.

The first case appears when a slope $_{k,l}$ corresponds to the even portion $\Omega_{i_1,\cdots,i_k,0}$ has no tangent point with the graph of the equation f in the domain of the portion $\Omega_{i_1,\cdots,i_k,0}$ which is defined, i.e. the tangent point of the graph of the equation f and the line corresponds to the slope $S_{k,l}$ be out side of the CTD. In this case, we consider the intersection point of the graph of the equation and the x-axis and then we draw the slope $S_{k,l}$ from this intersection point.

Example 55. *In follow, we see the first case for the slopes* $S_{1,1}$ *and* $S_{1,2}$,

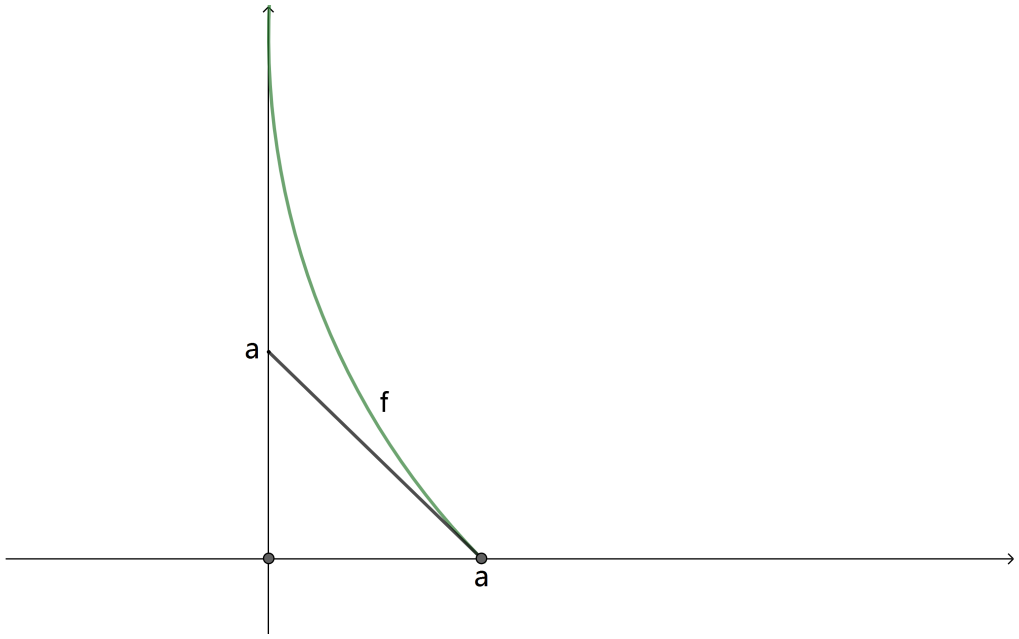

Figure 7.3.4: The first case for the slope $S_{1,1}$

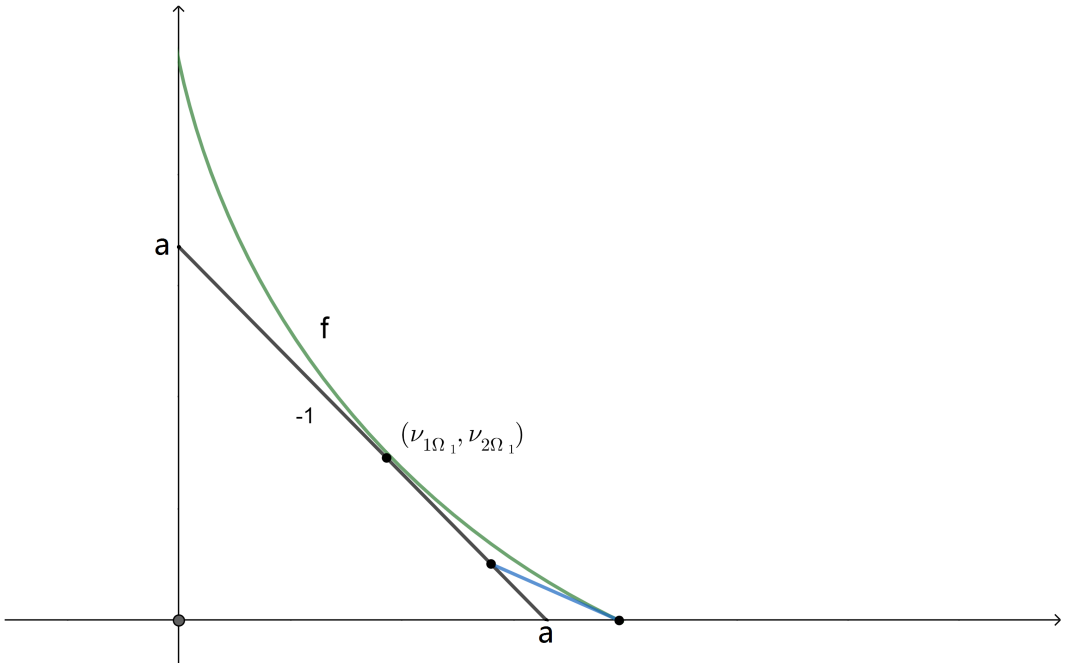

Figure 7.3.5: The first case for the slope $S_{1,2}$

Notice: The first case happens only when the portion $\Omega_{i_1,\cdots,i_k,0}$ has bounded by the x-axis.

The second case appears when a slope $S_{k,l}$ corresponds to an odd portion like $\Omega_{i_1,\cdots,i_k,1}$ has no tangent point in the domain of the portion $\Omega_{i_1,\cdots,i_k,1}$, i.e. the tangent point of the graph of the equation f and the line corresponds to the slope $S_{l,k}$ be outside of the CTD. In this case, we consider the intersection point of the graph of the equation f and the y-axis and then draw the slope $S_{k,l}$ form the intersection point for the portion $\Omega_{i_1,\cdots,i_k,1}$ in the CTD.

Example 56. *We can see the second case for the slopes* $S_{1,1}$ *and* $S_{2,1}$ *in the following figures*

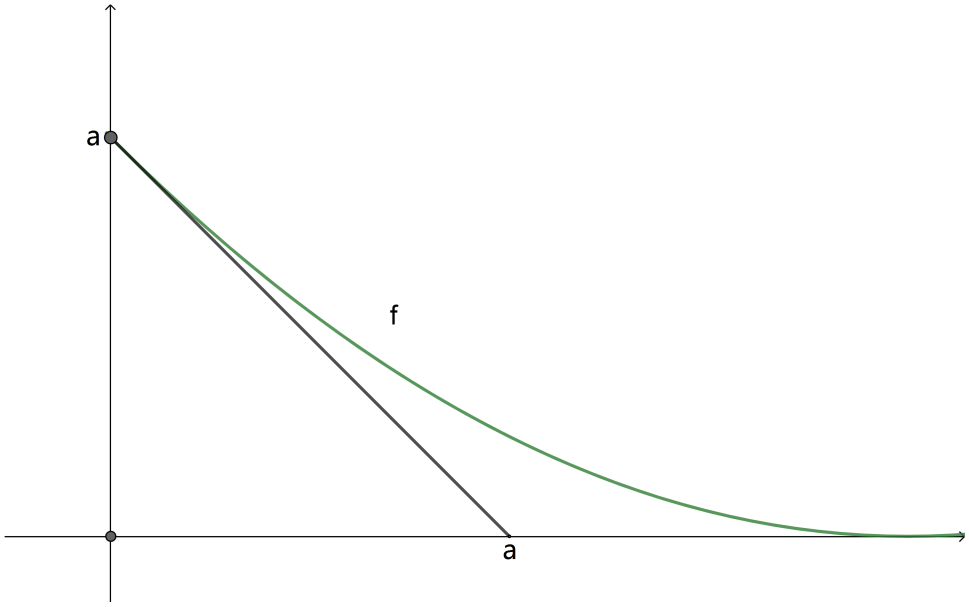

Figure 7.3.6: The second case for the slope $S_{1,1}$

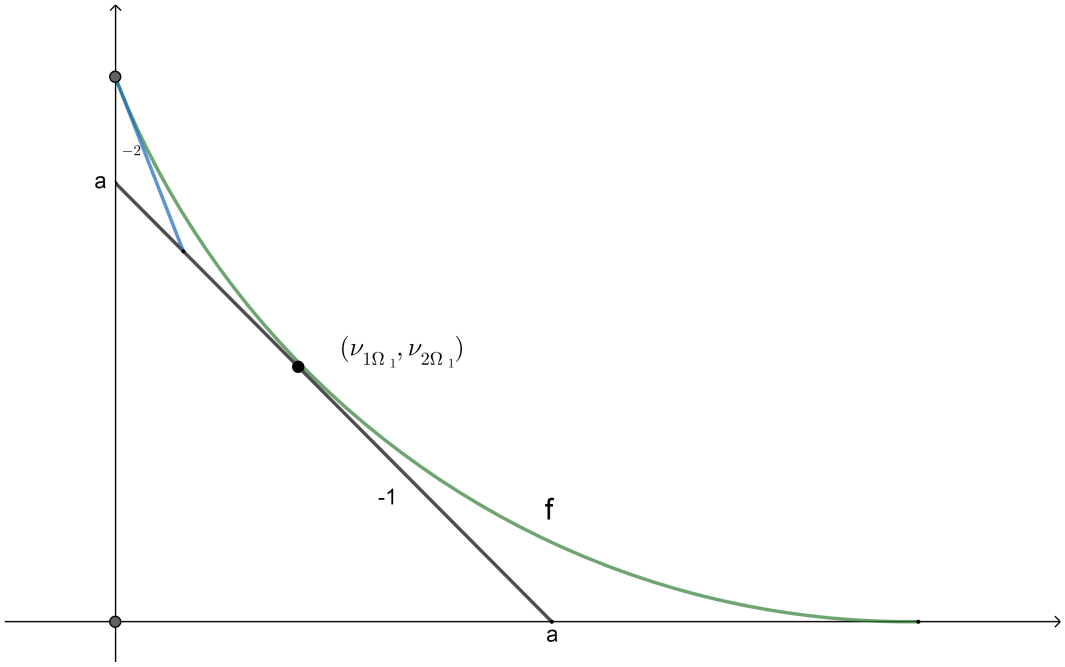

Figure 7.3.7: The second case for the slope $S_{2,1}$

Note that the second case happens only as the odd portion $\Omega_{i_1,\cdots,1_k,1}$ has bounded by the y-axis.

We can follow the method in paper [3] and convert the portion Ω_{11} to the standard shape, namely the same shape as Ω_1 by multiplication with the matrix $\begin{bmatrix} 1 & 0 \\ 1 & 1 \end{bmatrix} \in SL_2(\mathbb{Z})$ and a transformation. But the final results are the same as the above results.

We can convert the portion Ω_{10} to the standard shape namely the same as the portion Ω_1 by multiplication the portion of Ω_{10} with the matrix $\begin{bmatrix} 1 & 1 \\ 0 & 1 \end{bmatrix} \in \mathrm{SL}_2(\mathbb{Z})$ and a translation. Then we have a right angled shape for this portion.

Following the above ways we compute recursively the higher weights $\Omega_{100}, \Omega_{101}, \Omega_{110}, \Omega_{111}, \Omega_{1000}, \Omega_{1001}, \cdots$ for the CTD.

We give an order to the weight expansion $(a_1, a_2, \cdots, a_n)$ as follow. Let V is a finite binary sequence. We define

(i)

$$\begin{aligned} a_1 &:= \max\{W(\Omega_v) \ : \ v \in V\} \\ n_1 &:= \#\{v \in V \ : \ W(\Omega_v) = a_1\} \\ a_i &= a_1 \quad \text{for } 1 \leqslant i \leqslant n_1, \end{aligned}$$

(ii)

$$\begin{aligned} a_{n_1+1} &:= \max\{W(\Omega_v) \ : \ v \in V \text{ and } \ W(\Omega_v) < a_1\} \\ n_2 &:= \#\{v \in V \ : \ W(\Omega_v) = a_{n_1+1}\} \\ a_i &= a_{n_1+1} \quad \text{for } n_1 + 1 \leqslant i \leqslant n_1 + n_2, \end{aligned}$$

recursively

(iii)

$$\begin{aligned} a_{n_k+1} &:= \max\{W(\Omega_v) \ : \ v \in V \text{ and } \ W(\Omega_v) < a_1\} \\ n_{k+1} &:= \#\{v \in V \ : \ W(\Omega_v) = a_{n_k+1}\} \\ a_i &= a_{n_k+1} \quad \text{for } \sum_{j=1}^{k} n_j + 1 \leqslant i \leqslant \sum_{j=1}^{k+1} n_j. \end{aligned}$$

Now we should note that $a_1 \geqslant a_2 \geqslant a_3 \geqslant \cdots$ and we define $W^{\mathrm{CTD}}(\Omega_{i_1 i_2 \cdots i_j}) = 0$ when $\Omega_{i_1 i_2 \cdots i_j} = \emptyset$.

Remark 57. In the case when Ω is a rational triangle, the weight expansion is determined by continued fraction expansion of the slope of the diagonal and in particular $W(\Omega)$ is finite.

Note in the case when X_Ω is rational its weight expansion is finite.

Theorem 58. *Given X_Ω a rational concave toric domain and its weight expansion be $(a_1, \cdots, a_n)$. The ECH capacities of X_Ω are given by*

$$c_k(X_\Omega) = c_k(\coprod_{i=1}^{n} B(a_i)). \tag{7.3.8}$$

In view of the disjoint union property, the formula 7.1.8, and the above theorem, the ECH capacities of a disjoint union of balls is

$$c_k(\coprod_{i=1}^{n} B(a_i)) = \max\{\sum_{i=1}^{n} a_i d_i \mid \sum_{i=1}^{n} \frac{d_i^2 + d_i}{2} \leqslant k\} \tag{7.3.9}$$

where $d_1, d_2, \cdots, d_n$ are nonnegative integers. Note that because of $a_1 \geqslant a_2 \geqslant \cdots \geqslant a_n$ it holds that $d_i = 0$ whenever $i > k$. Therefore 7.3.9 is equivalent to the formula

$$c_k(\coprod_{i=1}^{n} B(a_i)) = \max\{\sum_{i=1}^{k} a_i d_i \mid \sum_{i=1}^{k} \frac{d_i^2 + d_i}{2} \leqslant k\}. \tag{7.3.10}$$

In particular,

$$c_k(\coprod_{i=1}^{n} B(a_i)) = c_k(\coprod_{i=1}^{k} B(a_i)). \tag{7.3.11}$$

If the weight expansion of a concave toric domain is infinite, as in our example, the following generalization of the theorem 58 holds.

Lemma 59. *If X_Ω be a concave toric domain with the weight expansion $a_1 \geqslant a_2 \geqslant \cdots \geqslant a_n$, then*

$$c_k(X_\Omega) = c_k\left(\coprod_{i=1}^{k} B(a_i)\right). \tag{7.3.12}$$

Proof. See the paper [3]. □

Chapter 8

Computation of some ECH capacities for the RKP

8.1 Introduction to the computation

In this chapter, we are going to compute some of the ECH capacities of the rotating Kepler problem for the energy $c \leqslant -\frac{3}{2}$ on the special concave toric domain $\mathcal{K}_c^b$ by using the definitions of the previous chapters.

For this goal, we consider the special concave toric domain $\mathcal{K}_c^b$ of the rotating Kepler problem which we have obtained in the chapter 4.

Let $c \leqslant -\frac{3}{2}$ and consider the equation

$$\mu_2 = \frac{1}{16\mu_1^2} + \frac{c}{2}. \tag{8.1.1}$$

8.2 The First Weight W_1 for the portion ω_1 in the SCTD $\mathcal{K}_c^b$

For computing the first weight, we find the intersection point of the graph of equation 8.1.1 and the line $\mu_2 = \mu_1$. If we plug in the equality $\mu_2 = \mu_1$ in the equation 8.1.1, then we get the following cubic equation

$$-16\mu_1^3 + 8c\mu_1^2 + 1 = 0. \tag{8.2.1}$$

We will find the roots of the equation 8.2.1 by using the trigonometric method. For this deal, we need to convert the equation 8.2.1 to the standard form. Thus we have the following equation

$$\mu_1^3 - \frac{1}{2}c\mu_1^2 - \frac{1}{16} = 0. \tag{8.2.2}$$

For convenience, we define A_1, A_2 and A_3 as

$$A_1 := -\frac{1}{2}c, \qquad A_2 := 0, \qquad A_3 := -\frac{1}{16}. \tag{8.2.3}$$

Now we follow the steps of the trigonometry method. Set

$$B_1 := \frac{3A_2 - A_1^2}{9} = \frac{-c^2}{36} \tag{8.2.4}$$

$$B_2 := \frac{9A_2A_1 - 27A_3 - 2A_1^3}{54} = \frac{27 + 4c^3}{864} \tag{8.2.5}$$

$$B_3 := B_1^3 + B_2^2 = (-\frac{c^2}{36})^2 - (\frac{27 + 4c^3}{864})^2. \tag{8.2.6}$$

Since $B_3 < 0$, the equation 8.2.2 has 3 real roots. We can find θ as follow,

$$\cos\theta = \frac{B_2}{\sqrt{-B_1^3}} = \frac{27 + 4c^3}{4c^3} \tag{8.2.7}$$

or

$$\theta = \arccos(1 + \frac{27}{4c^3}). \tag{8.2.8}$$

Now we consider the above equalities and the equations of the roots in the trigonometric method

$$r_1, r_2, r_3 = 2\sqrt{-B_1}(\cos\frac{\theta}{3} + \frac{2\pi}{3}T) - \frac{A_1}{3} \tag{8.2.9}$$

where $T = 0, 1, 2$. Therefore, the roots of the equation 8.2.2 are

$$r_1, r_2, r_3 = (\frac{c}{3}\cos(\frac{1}{3}\arccos(1 + \frac{27}{4c^3})) + \frac{2\pi}{3}T)) + \frac{c}{6}. \tag{8.2.10}$$

where $T = 0, 1, 2$. We assume the first root appears when $T = 1$. Then we have

$$r_1(c) = (\frac{c}{3}\cos(\frac{1}{3}\arccos(1 + \frac{27}{4c^3}) + \frac{2\pi}{3})) + \frac{c}{6} \tag{8.2.11}$$

Since the first weight W_1 in the SCTD $\mathcal{K}_c^b$ is the diameter of the isosceles rightangled triangles with the length of the side r_1, using the Pythagorean theorem we can write the first weight W_1 as a function of r_1 by

$$W_1(r_1(c)) = \sqrt{2}r_1(c), \tag{8.2.12}$$

or equivalently as a function of the energy c by the following equation

$$W_1(c) = \sqrt{2}((\frac{c}{3}\cos(\frac{1}{3}\arccos(1 + \frac{27}{4c^3}) + \frac{2\pi}{3})) + \frac{c}{6}) \tag{8.2.13}$$

Assume the roots of the cubic equation have order as $r_1' < r_2' < r_3'$. In the above, we have gotten the first r_1' that for convenience we denote by r_1. In the following we compute the second root r_2' of the cubic equation 8.2.1 via the first root r_1.

Recall: Given a cubic equation as

$$z^3 + a_1z^2 + a_2z + a_3 = 0 \tag{8.2.14}$$

and denote roots of that by b_1, b_2 and b_3. There are three relations between roots and coefficients of this equation as

$$\begin{cases} -b_1 - b_2 - b_3 = a_1 \\ b_1b_2 + b_1b_3 + b_2b_3 = a_2 \\ -b_1b_2b_3 = a_3. \end{cases} \tag{8.2.15}$$

Thus form the eq. 8.2.2,

$$a_1 = -\frac{1}{2}c, \qquad a_2 = 0, \qquad a_3 = -\frac{1}{16} \tag{8.2.16}$$

and denote the roots of the eq. 8.2.2 with r_1, r_2 and r_3. Let $r_1 = b_1$, form the first equation of 8.2.15.

$$-r_1 - b_2 - b_3 = -\frac{1}{2}c \tag{8.2.17}$$

$$\implies \qquad b_2 = \frac{1}{2}c - r_1 - b_3.$$

Since r_1 is a root of 8.2.15 we can express c with the help of r_1 by

$$c = \frac{16r_1^3 - 1}{8r_1^2}. \tag{8.2.18}$$

From 8.2.17

$$b_2 = \frac{-1}{16r_1} - b_3. \tag{8.2.19}$$

Now using second equation of 8.2.15

$$r_1(\frac{-1}{16r_1^2} - b_3) + r_1b_3 + (\frac{-1}{16r_1^2} - b_3)b_3 = 0 \tag{8.2.20}$$

$$\implies \frac{-1}{16r_1} - \frac{b_3}{16r_1^2} - b_3^2 = 0. \tag{8.2.21}$$

This is a quadratic equation in b_3 with coefficients

$$a_1' = 1, \qquad a_2' = \frac{1}{16r_1^2}, \qquad a_3' = \frac{1}{16r_1}. \tag{8.2.22}$$

Thus we have

$$\Delta = a_2^{2'} - a_1'a_3' = (\frac{1}{16r_1})^2 - 4(\frac{1}{16r_1}) = \frac{1 - 4^3r_1^3}{4^4r_1^4}. \tag{8.2.23}$$

Therefore

$$r_2', r_3' = \frac{-a_2' \pm \sqrt{\Delta}}{2a} \tag{8.2.24}$$

$$= \frac{\frac{-1}{16r_1^2} \pm \sqrt{\Delta}}{2} \tag{8.2.25}$$

$$= \frac{\frac{-1}{16r_1^2} \pm \frac{1}{16r_1^2}\sqrt{1-4^3r_1^3}}{2} \tag{8.2.26}$$

$$= \frac{-1 \pm \sqrt{1-4^3r_1^3}}{32r_1^2}. \tag{8.2.27}$$

Therefore the second root of the cubic equation 8.2.2 is

$$r_2' = \frac{-1+\sqrt{1-4^3r_1^3}}{32r_1^2}. \tag{8.2.28}$$

The root r_2' is the intersection point of the graph of equation 8.2.1 and the line $y = x$. If we want to have the intersection point of the graph of equation 8.1.1 and the line $y = -x$. We should multiply the root r_2' by -1. Hence we denote the intersection point of the equation 8.1.1 and the line $y = -x$ with r_2 which is $-r_2'$ and for convenience we call it the second root which is

$$r_2 = -\frac{-1+\sqrt{1-4^3r_1^3}}{32r_1^2}. \tag{8.2.29}$$

Now we have the intersection point of the graph of equation 8.1.1 and the line $y = -x$ which is denoted by r_2 and plays an important role to find the higher weights and computing the ECH capacities of the RKP.

We continue this chapter by computing the higher weights on the SCTD $\mathcal{K}_c^b$. Unlike the first weight W_1 which is always a smooth function of c, the higher weights of the ECH capacities of the rotating Kepler problem are not smooth. However in the nonsmooth points, the weights are continuous in c.

To determine continuous smooth functions of each weight and the domains of them, first we should find the domain that these functions are defined on. On the other hand, these domains are given by the critical energy values that for each weight is unique. The new tree which is introduced in Chapter 5 is very useful to find portions corresponding to each weights on the SCTD $\mathcal{K}_c^b$.

Using the new tree, we can compute the slopes and the critical energy values and each portion in the SCTD $\mathcal{K}_c^b$ correspond to each weight.

8.3 The Critical Energy Values and the Slopes of Weights

Recall given the CTD defined by Hutchings, we denoted the nodes of the Stern-Brocot tree with $\frac{k}{l}$ and related to each node like $\frac{k}{l}$ a slope equal to $S_{k,l}^{CTD} = -\frac{k}{l}$ in the Hutchings CTD.

Now we are going to introduce the above terms for the SCTD $\mathcal{K}_c^b$. The SCTD $\mathcal{K}_c^b$ is the CTD which is rotated by 45 degrees in clockwise direction that we defined in Chapter 5.

We now introduce a formula for computing critical energy values of portions of the SCTD $\mathcal{K}_c^b$. With this formula

we can obtain the critical value of a portion $\omega_{i_1\cdots i_j}$ uniquely which is important to find the weights of the ECH capacities in the SCTD $\mathcal{K}_c^b$.

For a portion $\omega_{i_1\cdots i_j}$, the critical energy value of that will be computed by the following formula

$$\begin{aligned} c^+_{k,l} &= -\frac{1}{2}(\frac{k}{l})^{\frac{2}{3}} - \frac{l}{k}(\frac{k}{l})^{\frac{2}{3}} \\ &= -(\frac{1}{2}+\frac{l}{k})(\frac{k}{l})^{\frac{2}{3}}. \end{aligned} \tag{8.3.1}$$

As we have seen in Chapter 3, some tori $T_{k,l}$ are assigned to asteroids. For instance, the tori $T_{2,1}$ and $T_{3,1}$ are assigned to the asteroids Hekuba and Hestia respectively.

The relation 8.3.1 gives us information about the energies for which the tori $T_{k,l}$ appear first. In the special cases that a torus has a special names we use the special name for it.

The slope of the torus $T_{k,l}$ in the SCTD $\mathcal{K}_c^b$ is given by the formula

$$S_{k,l} = \frac{k+l}{-k+l}. \tag{8.3.2}$$

The slope $S_{k,l}$ helps us to find the critical point of a portion $\omega_{i_1i_2\cdots i_j}$ for $i_1i_2\cdots i_j \in V$ on the SCDT $\mathcal{K}_c^b$ such that the portion corresponds to the torus $T_{k,l}$ in the SCTD $\mathcal{K}_c^b$ via the following relation

$$T_{k,l} = \mu^{-1}(\mu_{1\omega_{i_1\cdots i_j}}, \mu_{2\omega_{i_1\cdots i_j}}) \tag{8.3.3}$$

where $(\mu_{1\omega_{i_1\cdots i_j}}, \mu_{2\omega_{i_1\cdots i_j}})$ is the tangent point of the slope $S_{k,l}$ and the graph of the equation 8.1.1. We call them the critical points of the portion $\omega_{i_1i_2\cdots i_j}$.

Note that in Chapter 7, we computed the tori by the following relation on the CTD

$$T_{k,l} = \nu^{-1}(\nu_{1\Omega_{i_1\cdots i_j}}, \nu_{2\Omega_{i_1\cdots i_j}}) \tag{8.3.4}$$

such that these two equations give the same torus for the portion $\omega_{i_1i_2\cdots i_j}$ in the SCTD $\mathcal{K}_c^b$ and $\Omega_{i_1i_2\cdots i_j}$ in the CTD. Now we explain the equations of the critical points. First we take the derivative of equation 8.1.1 to get

$$\frac{d\mu_2}{d\mu_1} = -\frac{1}{8\mu_1^3}. \tag{8.3.5}$$

If we put the above equation equal to the slope $S_{k,l}$ then we will have the first critical value $\mu_{1\omega_{i_1i_2\cdots i_j}}$. Now we substitute $\mu_{1\omega_{i_1i_2\cdots i_j}}$ into the equation 8.1.1 and then get the second critical value $\mu_{2\omega_{i_1i_2\cdots i_j}}$. Therefore we have the critical points of the portions $\omega_{i_1i_2\cdots i_j}$ as $(\mu_{1\omega_{i_1i_2\cdots i_j}}, \mu_{2\omega_{i_1i_2\cdots i_j}})$. Since these portions correspond to tori and some of them have special name we will use the special name in the notation of the critical points. For example for the asteroid Hekuba (torus $T_{2,1}$) and the asteroid Hestia (torus $T_{3,1}$) we will use $(\mu_{1Hek}, \mu_{2THek})$ and (μ_{1Hes}, μ_{2Hes}) respectively.

8.4 The Higher Weights

Here we are going to compute the higher weights of the ECH capacities of the rotating Kepler problem. We start the computation of the higher weights with the second weight W_2 of the ECH capacities of the rotating Kepler problem in the SCTD $\mathcal{K}_c^b$.

8.4.1 The Second Weight W_2 for the portion ω_{11} in the SCTD $\mathcal{K}_c^b$

First we will obtain the portion ω_{11} of the SCTD $\mathcal{K}_c^b$. The portion ω_{11} is the biggest triangle in the rest part of the SCTD $\mathcal{K}_c^b$ that is bounded by the lines $x = r_1$, $y = -x$ and from the new tree we know that the slope corresponding to the portion ω_{11} is $S_{2,1} = -3$. In view of the formula 8.3.2, for the portion ω_{11}, the slope of ω_{11} in the SCTD $\mathcal{K}_c^b$ is

$$S_{k,l} = S_{2,1} = \frac{2+1}{-2+1} = -3 \tag{8.4.1}$$

which is the value of the node V_{11} on the new tree. In this chapter, we skip the formula 8.3.2 to compute the slopes of the portions in the SCTD $\mathcal{K}_c^b$ and we will only use the new tree to determine the slopes of the portions ω_{11} of the SCTD $\mathcal{K}_c^b$.

We compute the critical energy value of portion ω_{11} using the relation 8.3.1 as follows

$$c^+_{k,l} = c^+_{2,1} = -(\frac{1}{2} + \frac{l}{k})(\frac{k}{l})^{\frac{2}{3}} = -(\frac{1}{2} + \frac{1}{2})(\frac{2}{1})^{\frac{2}{3}} = -\sqrt[3]{4}. \tag{8.4.2}$$

Note that the critical energy value $c^+_{1,2} = -\sqrt[3]{4}$ is the energy which the asteroid Hekuba appears first.

Now we can find the critical point $(\mu_{1\omega_{11}}, \mu_{2\omega_{11}})$ for the portion ω_{11} in the SCTD $\mathcal{K}_c^b$. Let the slope $S_{2,1} = -3$ and put the relation 8.3.5 equal to -3.

$$\frac{d\mu_{2\omega_{11}}}{d\mu_{1\omega_{11}}} = -\frac{1}{8\mu^3_{1\omega_{11}}} = -3, \tag{8.4.3}$$

so we have

$$\mu_{1\omega_{11}} = \frac{1}{2\sqrt[3]{3}}. \tag{8.4.4}$$

Now for the second term of the critical point, assume the equation 8.1.1 and compute the value of $\mu_{2\omega_{11}}$

$$\mu_{2\omega_{11}} = \frac{1}{16\mu^2_{1\omega_{11}}} + \frac{c}{2} \tag{8.4.5}$$

$$= \frac{1}{16(\frac{1}{2\sqrt[3]{3}})^2} + \frac{c}{2} \tag{8.4.6}$$

$$= \frac{1}{4}\sqrt[3]{9} + \frac{c}{2}. \tag{8.4.7}$$

From the computation of the first weight and the equation 8.2.1, we can write the energy c as a function of the

first root r_1 by

$$c(r_1) = \frac{16r_1^3 - 1}{8r_1^2} \tag{8.4.8}$$

where r_1 is the first root of the equation 8.2.1. Therefore we write the critical point of the portion ω_{11} as function of r_1 by

$$(\mu_{1\omega_{11}}, \mu_{2\omega_{11}}) = (\frac{1}{2\sqrt[3]{3}}, \frac{1}{4}\sqrt[3]{9} + \frac{16r_1^3 - 1}{16r_1^2}). \tag{8.4.9}$$

Using the relation 8.3.3 and the above critical point, the torus corresponding to the portion ω_{11} is

$$T_{2,1} = \mu^{-1}(\mu_{1\omega_{11}}, \mu_{2\omega_{11}}). \tag{8.4.10}$$

The critical energy value gives us two different portions with the energies $c \leqslant c^+_{2,1}$ and $c^+_{2,1} \leqslant c \leqslant -\frac{3}{2}$. For these portions we have two different equations for the second weight W_2. Here we compute the weight W_2 for these two cases.

Case 1: Let $c \leqslant c^+_{2,1} = -\sqrt[3]{4}$. To compute the second weight W_2 in the case 1, we need to have the second root of the cubic equation 8.2.1. Because just in the second root r_2, there is a point that the slope $S_{2,1}$ in the SCTD $\mathcal{K}^b_c$ can be tangent to the graph of the equation 8.1.1. As we can see in Figure 8.4.1, the root r_2 is the length of the sides of the isosceles rightangle triangle.

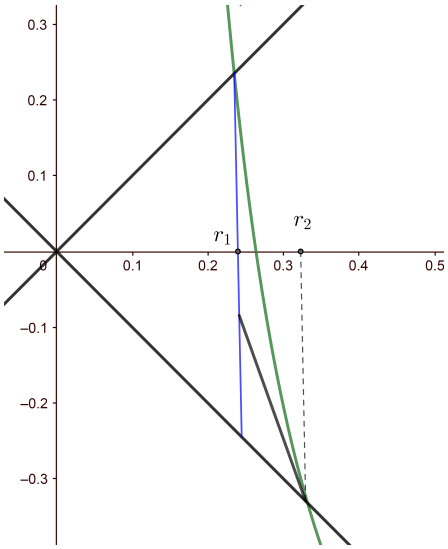

Figure 8.4.1: $c \leqslant c^+_{2,1} = -\sqrt[3]{4}$

Using the Pythagorean theorem, the diameter of this isosceles triangle is $\sqrt{2}r_2$. Therefore, by consider Figure 8.4.1, the relation of the second weight W_2 of ω_{11} of the ECH capacities of the rotating Kepler problem for the case 1 is

a smooth function of r_1 as follows,

$$W_2(r_1) = \sqrt{2}r_2 - W_1(r_1) = \sqrt{2}(r_2 - r_1) \tag{8.4.11}$$
$$= \sqrt{2}\left[(-\frac{-1+\sqrt{1-4^3r_1^3}}{32r_1^2}) - r_1\right].$$

Case 2: Let $-\sqrt[3]{4} = c_{2,1}^{+} \leqslant c \leqslant -\frac{3}{2}$. Given Figure 8.4.2 and consider the critical point $(\mu_{1\omega_{11}}, \mu_{2\omega_{11}})$ of Hekuba.

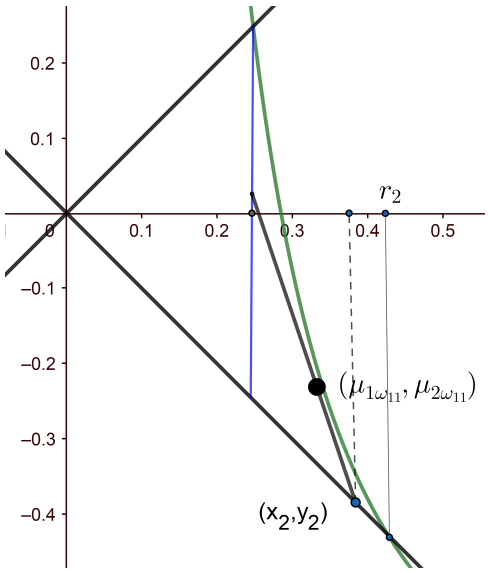

Figure 8.4.2: $-\sqrt[3]{4} = c_{2,1}^{+} \leqslant c \leqslant -\frac{3}{2}$

Since the slope $S_{2,1}$ is tangent to the graph of the equation 8.1.1 in the SCTD $\mathcal{K}_c^b$ just on the critical point $(\mu_{1\omega_{11}}, \mu_{2\omega_{11}})$, so this point is determined uniquely by the equation 8.1.1 and Hekuba.

Now consider Figure 8.4.2 and using the point $(\mu_{1\omega_{11}}, \mu_{2\omega_{11}})$, we write the function of a line through the point (x_2, y_2) with slope -3. Thus we have

$$y_2 - \mu_{2\omega_{11}} = 3(\mu_{1\omega_{11}} - x_2). \tag{8.4.12}$$

Since the point (x_2, y_2) is on the bisector of the fourth quadrant of the space $\mathbb{R}^2$, we have $y = -x$. Hence we can write

$$-x_2 - \mu_{2\omega_{11}} = 3(\mu_{1\omega_{11}} - x_2). \tag{8.4.13}$$

Therefore, if we compute the value of x_2 then we have an isosceles triangle whose side has length x_2. We can formulate the value of x_2 as a function of the first root r_1 as follow,

$$2x_2 = 3\mu_{1\omega_{11}} + \frac{1}{4}\sqrt[3]{9} + (\frac{16r_1^3 - 1}{16r_1^2}). \tag{8.4.14}$$

So we have

$$x_2(r_1) = \frac{3}{4\sqrt[3]{3}} + \frac{\sqrt[3]{9}}{8} + \frac{1}{2}(\frac{16r_1^3 - 1}{16r_1^2}). \tag{8.4.15}$$

Using the Pythagorean theorem, the hypotenuse of the rightangled triangle both of whose legs have length x_2 is $\sqrt{2}x_2$.

Now consider Figure 8.4.2, the second weight W_2 of the ECH capacities of the rotating Kepler problem in case 2 is given as a function of r_1 by

$$W_2(r_1) = \sqrt{2}x_2 - W_1(r_1) \tag{8.4.16}$$

$$= \sqrt{2}(x_2 - r_1) \tag{8.4.17}$$

$$= \sqrt{2}(\frac{3}{4\sqrt[3]{3}} + \frac{\sqrt[3]{9}}{8} + \frac{1}{2}(\frac{16r_1^3 - 1}{16r_1^2}) - r_1). \tag{8.4.18}$$

For convenience, we write the second weight W_2 as a function of the first root r_1 of the cubic equation 8.2.1 as

$$W_2(r_1) = \begin{cases} \sqrt{2}(r_2 - r_1) = \sqrt{2}(-\frac{-1 + \sqrt{1 - 4^3 r_1^3}}{32r_1^2} - r_1), & r_1 \leqslant \frac{1}{4}, \\ \sqrt{2}(\frac{3}{4\sqrt[3]{3}} + \frac{\sqrt[3]{9}}{8} + \frac{1}{2}(\frac{16r_1^3 - 1}{16r_1^2}) - r_1), & \frac{1}{4} \leqslant r_1 \leqslant \frac{1}{2}. \end{cases} \tag{8.4.19}$$

Observe that the function W_2 is piecewise analytic. It is continuous at $r_1 = \frac{1}{4}$ but it is not smooth at this point. Recall that the point $r_1 = \frac{1}{4}$ corresponds to the energy $c = -\sqrt[3]{4}$.

8.4.2 The Third Weight W_3 for the portion ω_{111} in the SCTD $\mathcal{K}_c^b$

In this step we are going to compute the third weight of the ECH capacities of the rotating Kepler problem. Given the SCTD $\mathcal{K}_c^b$. We should take the portions either ω_{110} or ω_{111} due to the indexes they are even or odd respectively. Note that we can take the portion ω_{110} and apply for the third weight W_3 when the both cases of the second weight W_2 are established. But if we have the third weight W_3 for the portion ω_{111}, then the second weight W_2 should only satisfy in the case 2. It means the energy should be $c_{2,1}^+ \leqslant c \leqslant -\frac{3}{2}$.

Here we assume the second weight W_2 satisfied in the case 2 and try to find an appropriate portion for the third weight W_3. From the above explanation and the assumption, we should compute the third weight for the portion ω_{111}.

The Stern-Brocot tree specifies the node $\frac{k}{l} = \frac{3}{1}$ on the Hutchings CTD for the portion ω_{111}. On the other hand, the node $\frac{3}{1}$ give us the torus $T_{3,1}$ which is determined by the critical point of the portion Ω_{111} with the relation 8.3.4 also we know that this torus is belong to the asteroid Hestia. Thus if we obtain the critical energy value $c_{3,1}^+$ for the torus $T_{3,1}$ then we know when the Hestia appears first.

Suppose the relation 8.3.1 and find the critical energy value of the portion ω_{111} as follow

$$c_{3,1}^+ = -\frac{1}{2}(\frac{1}{2} + \frac{1}{3})(\frac{3}{1})^{\frac{2}{3}} = -\frac{5}{6}\sqrt[3]{9}. \tag{8.4.20}$$

The energy $c^+_{3,1} = -\frac{5}{6}\sqrt[3]{9}$ is the energy that the Hestia appear first.

Via the new tree we can find the slope of the portion ω_{111}. The slope is $S_{3,1} = -2$.

For the next step, using the relation 8.3.5 and 8.1.1 and the slope $S_{3,1} = -2$, we are going to find the critical point $(\mu_{1\omega_{111}}, \mu_{2\omega_{111}})$ of the portion ω_{111}. This is the point that the slope $S_{3,1} = -2$ is tangent to the graph of the equation 8.1.1 in the region ω_{111}.

$$\frac{d\mu_2}{d\mu_1} = -\frac{1}{8\mu^3_{1\omega_{111}}} = -2, \tag{8.4.21}$$

$$\implies \mu_{1\omega_{111}} = \sqrt[3]{\frac{1}{16}}. \tag{8.4.22}$$

Also from the equation 8.1.1 we have

$$\mu_{2\omega_{111}} = \frac{1}{16\mu^2_{1\omega_{111}}} + \frac{1}{2}(\frac{16r_1^3 - 1}{8r_1^2}) \tag{8.4.23}$$

$$= \frac{1}{16(\sqrt[3]{\frac{1}{16}})^2} + \frac{16r_1^3 - 1}{16r_1^2}. \tag{8.4.24}$$

Note that with the relation 8.3.4 we can find the torus corresponds to the portion ω_{111} using this critical point as follow

$$T_{2,1} = \mu^{-1}(\mu_{1\omega_{111}}, \mu_{2\omega_{111}}). \tag{8.4.25}$$

If we consider the critical energy value $c^+_{2,1}$ and $c^+_{3,1}$. We can see the third weight W_3 has three different cases which each cases live in a certain energy level. We give these three cases in the following.

Case 1: Let $c \leqslant c^+_{2,1}$. In this case, the third weight W_3 of the ECH capacities of the rotating Kepler problem in the SCTD $\mathcal{K}^b_c$ is zero.

Case 2: Let $c^+_{2,1} \leqslant c \leqslant c^+_{3,1}$. In this case, we follow the method of the case 1 of the second weight W_2. Thus we need to compute the diameter of the isosceles rightangle triangle with the length of sides r_2 in Figure 8.4.3.

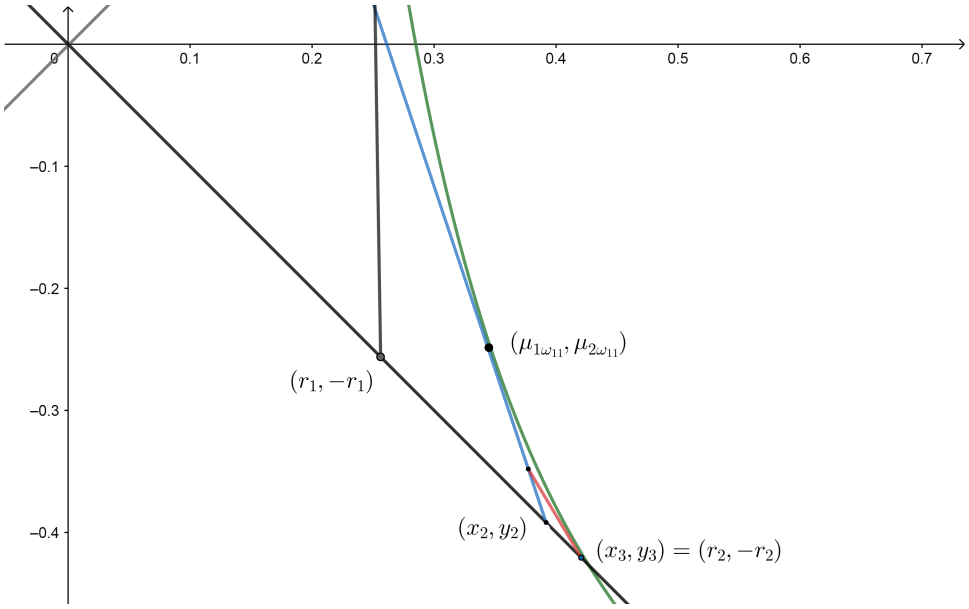

Figure 8.4.3: Case 2 for ω_{111} when $c^+_{2,1} \leqslant c \leqslant c^+_{3,1}$

Then we can get the third weight by following relation

$$W_3 = \sqrt{2}r_2 - W_2 - W_1. \tag{8.4.26}$$

We know that the second root r_2 is

$$r_2 = -\frac{-1 + \sqrt{1 - 4^3 r_1^3}}{32 r_1^2}. \tag{8.4.27}$$

Therefore the third weight W_3 for the case 2 is

$$W_3(r_1) = \sqrt{2}(-\frac{-1 + \sqrt{1 - 4^3 r_1^3}}{32 r_1^2}) - W_2(r_1) - \sqrt{2}r_1. \tag{8.4.28}$$

Case 3: Let $c^+_{3,1} \leqslant c \leqslant -\frac{3}{2}$. Consider Figure 8.4.4, we named the intersection point of the slope $S_{3,1} = -2$ and the line $y = -x$ with (x_3, y_3) on Figure 8.4.4.

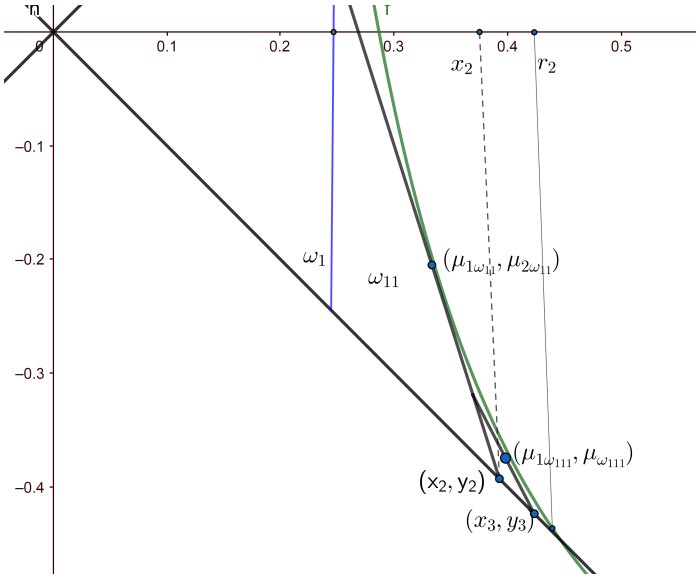

Figure 8.4.4: Case 3 for ω_{111} when $c^{+}_{3,1} \leqslant c \leqslant -\frac{3}{2}$

We computed the critical point $(\mu_{1\omega_{111}}, \mu_{2\omega_{111}})$ which is the tangent point of the slope $S_{3,1}$ and the graph of the equation 8.1.1. Now we assume the points $(\mu_{1\omega_{111}}, \mu_{2\omega_{111}})$ and (x_3, y_3) and then find the line function of these points with the slope $S_{3,1} = -2$.

We write

$$y_3 - \mu_{2\omega_{111}} = 2(\mu_{1\omega_{111}} - x_3). \tag{8.4.29}$$

Since the intersection point (x_3, y_3) lives in the line $y = -x$. Hence we have $(x_3, y_3) = (x_3, -x_3)$ and we can rewrite the above relation as

$$-x_3 - \mu_{2\omega_{111}} = 2(\mu_{1\omega_{111}} - x_3). \tag{8.4.30}$$

Therefore we have

$$x_3 = 2\mu_{1\omega_{111}} + \mu_{2\omega_{111}} = 2\sqrt[3]{\frac{1}{16}} + \frac{1}{16(\sqrt[3]{\frac{1}{16}})^2} + \frac{16r_1^3 - 1}{16r_1^2}. \tag{8.4.31}$$

Now we use the same way of the case 2 in the second weight weight W_2 and the get the third weight W_3 in the case 3 as a function of the first root r_1 by

$$W_3(r_1) = \sqrt{2}x_3(r_1) - (W_2(r_1) + W_1(r_1)). \tag{8.4.32}$$

Finally, we have the function of the third weight W_3 for the ECH capacities of the rotating Kepler problem in the

energy $c \leqslant -\frac{3}{2}$ is

$$W_3(r_1) = \begin{cases} 0 & r_1 \leqslant x_2 \\ \sqrt{2}r_2(r_1) - (W_2(r_1) + W_1(r_1)) = \sqrt{2}(r_2(r_1) - x_2(r_1)), & x_2 \leqslant r_1 \leqslant x_3, \\ \sqrt{2}x_3 - (W_2(r_1) + W_1(r_1)) = \sqrt{2}(x_3(r_1) - x_2(r_1)), & x_3 \leqslant r_1 \leqslant r_2. \end{cases} \tag{8.4.33}$$

8.4.3 The Fourth weight W_4 for the region ω_{110} in the SCTD $\mathcal{K}_c^b$

In this part, we compute the fourth weight W_4 of the ECH capacities for the rotating Kepler problem. For this goal, we assume the portion ω_{110} of the SCTD $\mathcal{K}_c^b$ which is bound by the line $x = r_1$, the graph of the equation 8.1.1 and the slope $S_{2,1}$. We denote this portion on Figures 8.4.5 and 8.4.6

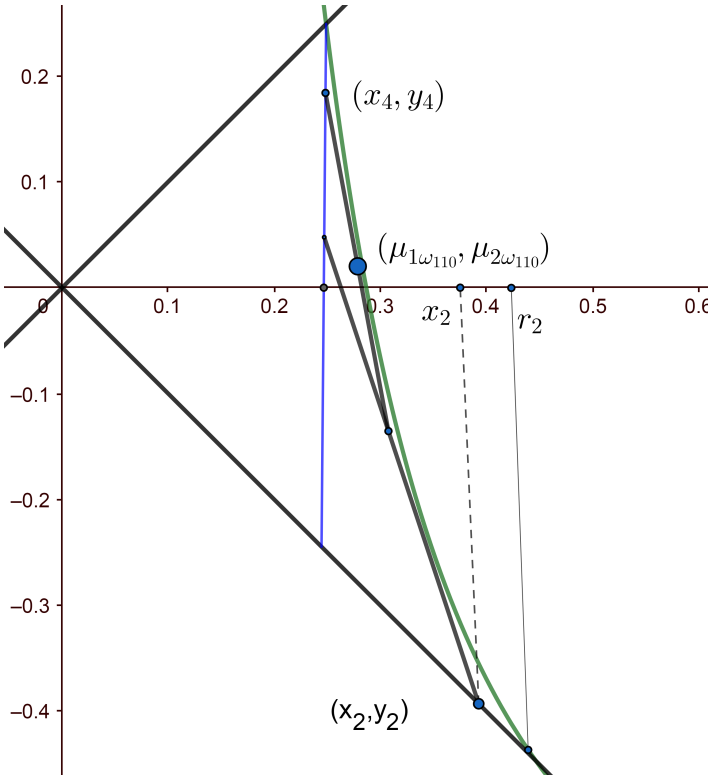

Figure 8.4.5: Fig. 1 for the weight W_4 when $c_{3,2}^+ < c_{2,1}^+$

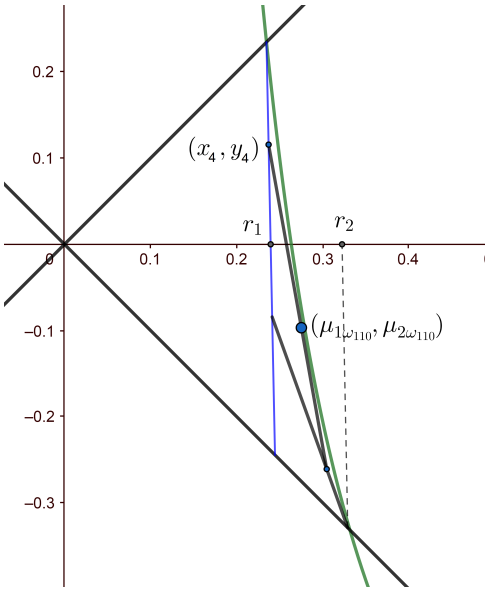

Figure 8.4.6: Fig. 2 for the weight W_4 when $c^+_{3,2} < c^+_{2,1}$

Using the new tree gives us the slope -5 for the portion ω_{110} in the SCTD $\mathcal{K}^b_c$.

Remark 60. For the computation of the third weight W_3, we took the portion ω_{111} and did our computation in this portion. This portion belongs to Case 2 of the second weight W_2. In other words, we can compute the third weight W_3 in the portion ω_{111} only when the second weight W_2 satisfy in the case 2. Unlike the portion ω_{111}, the portion ω_{110} appears for the both cases of the second weight W_2.

Here we assume the portion ω_{110} in the SCTD $\mathcal{K}^b_c$ and obtain the fourth weight W_4.

From the Stern-Brocot tree, we know that the node $\frac{k}{l} = \frac{3}{2}$ corresponds to the portion ω_{110}. Hence we can use the new tree to find the slope $S_{3,2} = -5$ for this portion ω_{110} in the SCTD $\mathcal{K}^b_c$. Also from the following relation we determine the torus corresponds to this node in the Hutchings CTD,

$$T_{3,2} = \nu^{-1}(\nu_{1\Omega_{110}}, \nu_{2\Omega_{110}}). \tag{8.4.34}$$

Now using the relations 8.3.1, we compute the critical energy $c^+_{3,2}$ as

$$c^+_{3,2} = -(\frac{1}{2} + \frac{2}{3})(\frac{3}{2})^{\frac{2}{3}} \tag{8.4.35}$$

$$= -(\frac{7\sqrt[3]{18}}{12}) \approx -1.528768. \tag{8.4.36}$$

We assume the relation 8.3.5 and the equation 8.1.1 and compute the critical point $(\mu_{1\omega_{110}}, \mu_{2\omega_{110}})$ for the fourth weight W_4 as follow

$$\frac{d\mu_2}{d\mu_1} = -\frac{1}{8\mu^3_{1\omega_{110}}} = -5 \tag{8.4.37}$$

$$\implies \mu_{1\omega_{110}} = \sqrt[3]{\frac{1}{40}}. \tag{8.4.38}$$

Also

$$\mu_{2\omega_{110}} = \frac{1}{16\mu_{1\omega_{110}}^2} + \frac{1}{2}\frac{16r_1^3 - 1}{8r_1^2}. \tag{8.4.39}$$

Therefore we have

$$(\mu_{1\omega_{110}}, \mu_{2\omega_{110}}) = (\sqrt[3]{\frac{1}{40}}, \frac{1}{16(\frac{1}{\sqrt[3]{40}})^2} + \frac{16r_1^3 - 1}{16r_1^2}). \tag{8.4.40}$$

From the above critical point, we can write

$$T_{3,2} = \mu^{-1}(\mu_{1\omega_{110}}, \mu_{2\omega_{110}}) \tag{8.4.41}$$

in the SCTD $\mathcal{K}_c^b$. We named the intersection point of the slope $S_{3,2} = -5$ and the line $x = r_1$ with (x_4, y_4) as we mentioned it on Figures 8.4.5 and 8.4.6.

We use this point and the critical point of the weight W_4 and write the the function line with them with eccentricity -5 as

$$\mu_{2\omega_{110}} - y_4 = -5(\mu_{1\omega_{110}} - x_4). \tag{8.4.42}$$

Since the point (x_4, y_4) lives in the line $x = r_1$, we assume the identity $(x_4, y_4) = (r_1, y_4)$ and obtain the value of y_4 as a function of r_1 as

$$\mu_{2\omega_{110}} - y_4 = -5(\mu_{1\omega_{110}} - r_1) \tag{8.4.43}$$

$$y_4 = \mu_{2\omega_{110}} + 5(\mu_{1\omega_{110}} - r_1). \tag{8.4.44}$$

Therefore we have the following equalities,

$$y_4(r_1) = \mu_{2\omega_{110}} + 5(\mu_{1\omega_{110}}) - 5r_1 \tag{8.4.45}$$

$$= \frac{1}{16(\frac{1}{\sqrt[3]{40}})^2} + \frac{16r_1^3 - 1}{16r_1^2} + 5(\sqrt[3]{\frac{1}{40}}) - 5r_1 \tag{8.4.46}$$

$$= \frac{1}{16(\sqrt[3]{\frac{1}{40}})^2} - \frac{1}{16r_1^2} - 4r_1 + 5(\sqrt[3]{\frac{1}{40}}). \tag{8.4.47}$$

Finally as we can see on Figures 8.4.5 and 8.4.6, we can write the relation of the fourth weight W_4 of the ECH capacities for the rotating Kepler problem as

$$\begin{aligned} W_4(r_1) =& (r_1 + y_4) - W_2(r_1) \\ =& (r_1 + \mu_{2\omega_{110}} + 5(\mu_{1\omega_{110}}) - 5r_1) - W_2(r_1) \\ =& \frac{1}{16(\sqrt[3]{\frac{1}{40}})^2} - \frac{1}{16r_1^2} - 3r_1 + 5(\sqrt[3]{\frac{1}{40}}) - W_2(r_1). \end{aligned} \tag{8.4.48}$$

Note that the necessary condition of the existence of the fourth weight W_4 is

$$S_{3,2} > \frac{1}{-8r_1^3} \tag{8.4.49}$$

or equivalently we can say the necessary condition is

$$r_1 < \mu_{1\omega_{110}} \qquad \text{or} \qquad r_1 > \mu_{2\omega_{110}}. \tag{8.4.50}$$

Remark 61. If we named the regions $\omega_{\dots 0}$ which is ended by zero on the SCDT $\mathcal{K}_c^b$ by the even region. Then we can generalize the above necessary condition of the existence of the weight for the even region as follow

$$S_{k,l} > \frac{1}{-8r_1^3}, \qquad \text{or} \qquad r_1 < \mu_{1\omega_{i_1\cdots i_j}} \qquad \text{or} \qquad r_1 > \mu_{2\omega_{i_1\cdots i_j}}. \tag{8.4.51}$$

where all of these three conditions are equivalent with each other and we consider the following figure for this case,

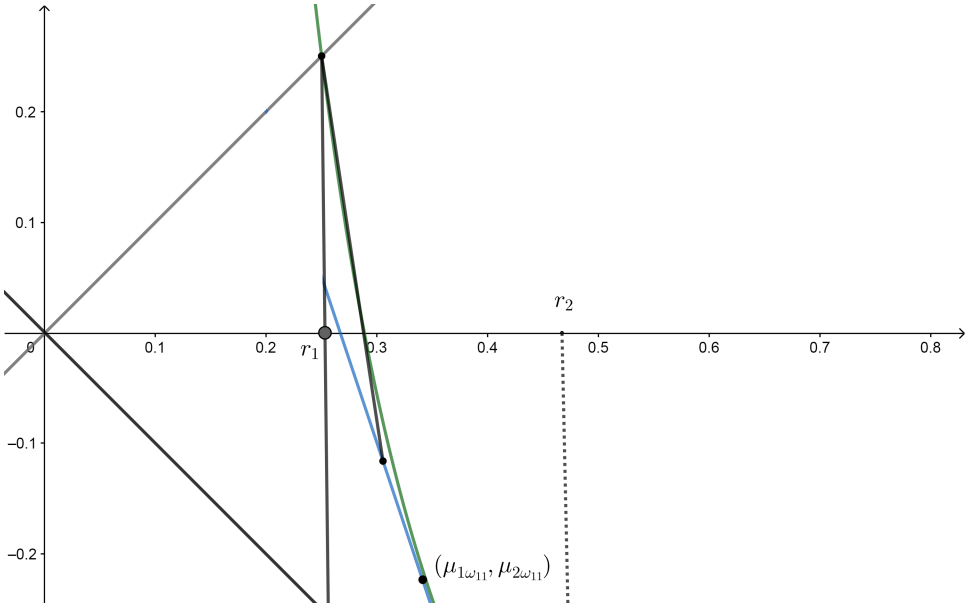

Figure 8.4.7: Fig. 3 for the weight W_4 when $c_{3,2}^+ < c_{2,1}^+$

Case 2: Let $c^+_{2,1} \leqslant c \leqslant -\frac{3}{2}$. Since the portion ω_{110} is not defined for $c^+_{2,1} \leqslant c \leqslant -\frac{3}{2}$. We have

$$W_4(r_1) = 0. \tag{8.4.52}$$

Now we abbreviate the fourth weight W_4 by

$$W_4(r_1) = \begin{cases} \dfrac{1}{16(\sqrt[3]{\frac{1}{40}})^2} - \dfrac{1}{16r_1^2} - 4r_1 + 5(\sqrt[3]{\frac{1}{40}}) - W_2(r_1), & c^+_{3,2} < c^+_{2,1}, \\ 0, & c^+_{2,1} \leqslant c \leqslant -\frac{3}{2}. \end{cases} \tag{8.4.53}$$

8.4.4 The Fifth weight W_5 for the portion ω_{1100} in the SCTD $\mathcal{K}^b_c$

In this section, we are going to compute the fifth weight W_5 of the SCTD $\mathcal{K}^b_c$ for the energy $c \leqslant -\frac{3}{2}$.

For this weight, we consider the portion ω_{1100} of the SCTD $\mathcal{K}^b_c$ and from the new tree we find the slope corresponds to this portion. The slope corresponds to the portion ω_{1100} is $S_{4,3} = -7$ which is the value of the node V_{1100} on the new tree.

Using the equations 8.3.5 and 8.1.1, we obtain the critical point $(\mu_{1\omega_{1100}}, \mu_{2\omega_{1100}})$ for the portion ω_{1100} which is the tangent point of the slope $S_{4,3} = -7$ and the graph of the function 8.1.1.

Let

$$\frac{d\mu_2}{d\mu_1} = -\frac{1}{8\mu^3_{1\omega_{1100}}} = -7 \tag{8.4.54}$$

$$\implies \mu_{1\omega_{1100}} = \sqrt[3]{\frac{1}{56}}, \tag{8.4.55}$$

and for the second component of the critical point we have

$$\mu_{2\omega_{1100}} = \frac{1}{16(\mu_{1\omega_{1100}})^2} + \frac{16r_1^3 - 1}{16r_1^2} \tag{8.4.56}$$

$$= \frac{1}{16(\sqrt[3]{\frac{1}{56}})^2} - \frac{1}{16r_1^2} + r_1. \tag{8.4.57}$$

Using the critical point $(\mu_{1\omega_{1100}}, \mu_{2\omega_{1100}})$ for the portion ω_{1100} and the relation 8.3.3, we can find the corresponding torus to the portion ω_{1100} as follows

$$\mu^{-1}(\mu_{1\omega_{1100}}, \mu_{2\omega_{1100}}) = T_{4,3}, \tag{8.4.58}$$

and by the equation 8.3.1 we can find the critical energy value for this portion as

$$c^+_{4,3} = (\frac{1}{2} + \frac{1}{4})(\frac{4}{3})^{\frac{2}{3}} \tag{8.4.59}$$

$$= (\frac{3}{4})(\frac{4}{3})^{\frac{2}{3}}. \tag{8.4.60}$$

This is the energy that the torus $T_{4,3}$ appears for first time.

The critical energy value give us two different relations for the weight W_5 such that these two relation are smooth and at the critical energy value $c^+_{4,3} = (\frac{3}{4})(\frac{4}{3})^{\frac{2}{3}}$ are continuous.

Now we can compute the fifth weight W_5 as the following cases.

Case 1: Let $c \leqslant c^+_{4,3}$. For this case we follow the method of the first case of the weight W_4 and try to find y_5 by using the slope $S_{4,3} = -7$ and the critical point $(\mu_{1\omega_{1100}}, \mu_{2\omega_{1100}})$. See Figure 8.4.8

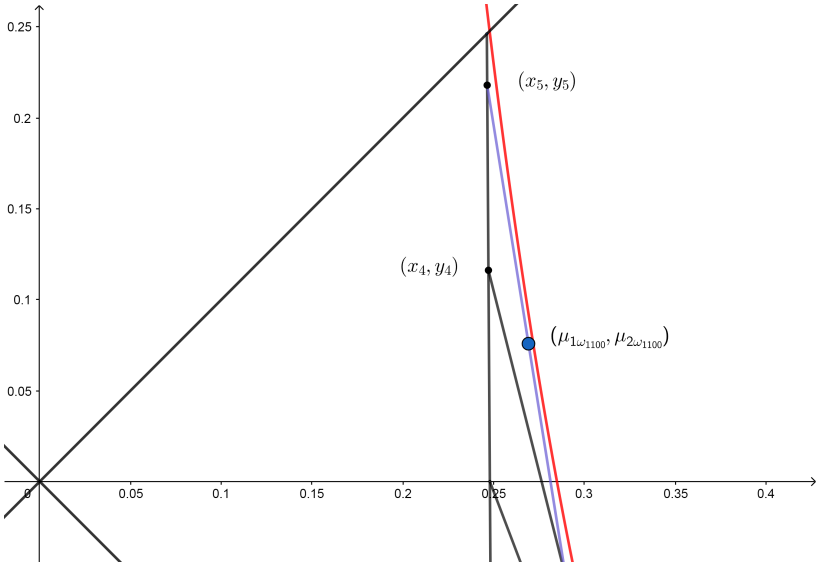

Figure 8.4.8: The portion ω_{1100} when $c \leqslant c^+_{4,3}$

Using the critical point $(\mu_{1\omega_{1100}}, \mu_{2\omega_{1100}})$ and the slope $S_{4,3} = -7$ we can write the following line function for the above figure.

$$y_5 - \mu_{2\omega_{1100}} = -7(x_5 - \mu_{1\omega_{1100}}). \tag{8.4.61}$$

Since the point (x_5, y_5) lies on the line $x = r_1$, we can rewrite the above relation as follows

$$\begin{aligned} y_5 &= -7(r_1 - \mu_{1\omega_{1100}}) + \mu_{2\omega_{1100}} \\ &= -7r_1 + 7(\sqrt[3]{\frac{1}{56}}) + \frac{1}{16(\sqrt[3]{\frac{1}{56}})^2} + \frac{16r_1^3 - 1}{16r_1^2} \\ &= -6r_1 + 7(\sqrt[3]{\frac{1}{56}}) + \frac{1}{16(\sqrt[3]{\frac{1}{56}})^2} - \frac{1}{16r_1^2}. \end{aligned} \tag{8.4.62}$$

Now by considering Figure 8.4.8. We can compute the fifth weight W_5 in case 1 for the SCTD $\mathcal{K}_c^b$ as follows

$$W_5(r_1) = r_1 + y_5 - (W_2(r_1) + W_4(r_1)) \tag{8.4.63}$$

$$= -5r_1 + 7(\sqrt[3]{\frac{1}{56}}) + \frac{1}{16(\sqrt[3]{\frac{1}{56}})^2} - \frac{1}{16r_1^2} - (W_2(r_1) + W_4(r_1)). \tag{8.4.64}$$

Case 2: Let $c_{4,3}^+ \leqslant c \leqslant -\frac{3}{2}$. Since the portion ω_{1100} is not defined for $c_{4,3}^+ \leqslant c \leqslant -\frac{3}{2}$. We have

$$W_5(r_1) = 0. \tag{8.4.65}$$

Therefore, we abbreviate the weight $W_5(r_1)$ for all energy $c \leqslant -\frac{3}{2}$ as follows

$$W_5(r_1) = \begin{cases} -5r_1 + 7(\sqrt[3]{\frac{1}{56}}) + \frac{1}{16(\sqrt[3]{\frac{1}{56}})^2} - \frac{1}{16r_1^2} - (W_2(r_1) + W_4(r_1)) & c \leqslant c_{4,3}^+, \\ 0 & c_{4,3}^+ \leqslant c \leqslant -\frac{3}{2}. \end{cases} \tag{8.4.66}$$

Note that for the portion ω_{1100} which is corresponding to the torus $T_{k,l} = T_{4,3}$. The conditions in Remark 61 holds for this weight, i.e.

$$r < \mu_{1\omega_{1100}}, \qquad \text{or} \qquad r_1 > \mu_{2\omega_{1100}}, \qquad \text{or} \qquad S_{4,3} > -\frac{1}{8r_1^3}. \tag{8.4.67}$$

Remark: We can see the weights $W_{i_1}, \cdots, W_{i_1,\cdots,i_k}$ of the SCTD $\mathcal{K}_c^b$ to computing the ECH capacities of the RKP are exactly sides of isosceles right-angled triangles in the standard coordinate.

To show the above claim, take the weight $W_{i_1,\cdots,i_k}$. There is a one-to-one correspondence between the Stern-Brocot tree and the new tree and also the portion $\Omega_{i_1,\cdots,i_k}$ and the the portion $\omega_{i_1,\cdots,i_k}$. Via the new tree and the SCTD $\mathcal{K}_c^b$, we can find the node $V_{i_1,\cdots,i_k}$ and the portion $\Omega_{i_1,\cdots,i_k}$ in the Stern-Brocot tree and the Hutchings CTD respectively such that the domain $\Omega_{i_1,\cdots,i_k}$ corresponds to the portion $\omega_{i_1,\cdots,i_k}$ in the SCTD $\mathcal{K}_c^b$.

If we rotate the portion $\omega_{i_1,\cdots,i_k}$ which corresponds to the weight $W_{i_1,\cdots,i_k}$ by 45 degrees in counter-clockwise direction and then multiplying it by $\begin{bmatrix} 1 & 0 \\ 1 & 1 \end{bmatrix} \in SL_2(\mathbb{Z})$ or $\begin{bmatrix} 1 & 1 \\ 0 & 1 \end{bmatrix} \in SL_2(\mathbb{Z})$. We will obtain an isosceles right-angled triangle with slope -1 corresponding to the portion $\Omega_{i_1,\cdots,i_k}$ in the Hutchings CTD. Note that the slope of the portion has a one-to-one relation with the node $V_{i_1,\cdots,i_k}$ in the Stern-Brocot tree. Hence sometimes we need to do the above multiplication several times to get the isosceles right-angles triangle with the slope -1.

Example 62. *Consider the second weight W_2 in the SCTD. By rotating the portion ω_{11} by 45 degrees in counter-clockwise direction we have the portion Ω'_{11} as follows such that its slope is $-\frac{1}{2}$*

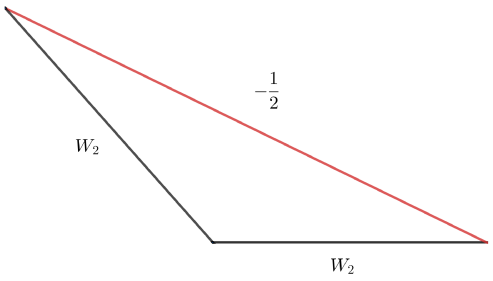

Figure 8.4.9: The portion Ω'_{11} in the CTD

Now by multiplying it by $\begin{bmatrix} 1 & 1 \\ 0 & 1 \end{bmatrix} \in SL_2(\mathbb{Z})$*, we obtain the portion* Ω_{11} *in the CTD with slope -1 as follows in the standard coordinate system.*

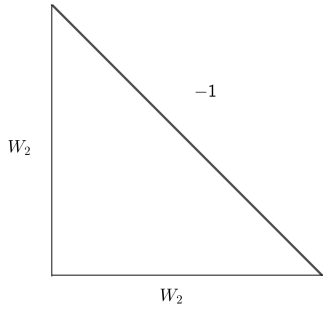

Figure 8.4.10: The portion Ω_{11} in the CTD

8.5 The Integrals of the Regions

As we have seen in Chapter 7, the necessary condition to compute the ECH capacities of the RKP. We have an order for weights form the biggest ones to lowest ones. Here we take the SCTD $\mathcal{K}_c^b$ and consider the order of the weights by computing the area of the regions that the weights are defined on those areas.

For the first weight W_1, we should compute the area of ω_1. Since it is an isosceles right-angle triangle, thus we have

$$Area(\omega_1) = \frac{1}{2}(\sqrt{2}r_1)^2 = r_1^2. \tag{8.5.1}$$

Now we take the rest part of the SCTD $\mathcal{K}_c^b$ that is the SCTD $\mathcal{K}_c^b$ minus ω_1 and obtain the area of it by computing

the following integral,

$$\begin{aligned}
\mathrm{Area}(\mathcal{K}_c^b - \omega_1) &= \int_{r_1}^{r_2} \mu_2 - (-\mu_1)\mathrm{d}\mu_1 \qquad (8.5.2)\\
&= \int_{r_1}^{r_2} \frac{1}{16\mu_1^2} + \frac{c}{2} - (-\mu_1)\mathrm{d}\mu_1\\
&= -\frac{1}{16\mu_1} + \frac{1}{2}c\mu_1 + \frac{1}{2}\mu_1^2|_{r_1}^{r_2}\\
&= \left(-\frac{1}{16(-\frac{-1+\sqrt{1-4^3r_1^3}}{32r_1^2})} + \frac{1}{2}(\frac{16r_1^3-1}{8r_1^2})(-\frac{-1+\sqrt{1-4^3r_1^3}}{32r_1^2}) + \frac{1}{2}(-\frac{-1+\sqrt{1-4^3r_1^3}}{32r_1^2})^2 \right)\\
&\quad - \left(-\frac{1}{16r_1} + \frac{1}{2}(\frac{16r_1^3-1}{8r_1^2})r_1 + \frac{1}{2}r_1^2 \right)\\
&= \frac{2r_1^2}{-1+\sqrt{1-4^3r_1^3}} + \frac{(1-\sqrt{1-4^3r_1^3}) - 2(-2+24r_1^3)}{32r_1} + \frac{4(-1+\sqrt{1-4^3r_1^3}) + 2 - 2\sqrt{1-4^3r_1^3} - 4^3r_1^3}{2\times 32^2 r_1^4}\\
&= \frac{2r_1^2}{-1+\sqrt{1-4^3r_1^3}} + \frac{5-\sqrt{1-4^3r_1^3} - 48r_1^3}{32r_1} + \frac{-2+2\sqrt{1-4^3r_1^3} - 64r_1^3}{2\times 32^2 r_1^4}.
\end{aligned}$$

Example 63. *If we let* $c = -\frac{3}{2}$. *Then we have* $r_1 = \frac{1}{4}$ *and* $r_2 = \frac{1}{2}$ *and also*

$$\mathrm{Area}(\omega_1) = (\frac{1}{4})^2 = \frac{1}{16} \qquad (8.5.3)$$

$$\mathrm{Area}(\mathcal{K}_c^b - \omega_1) = \int_{r_1=\frac{1}{4}}^{r_2=\frac{1}{2}} \mu_2 + \mu_1 \mathrm{d}\mu_1 = \frac{1}{32}. \qquad (8.5.4)$$

For the next step, we compute the area of the region ω_{11}. For this deal, first we find the line function through the point (μ_{1Hek}, μ_{2Hek}) with slope $S_{3,1} = -3$. Thus we have

$$\begin{aligned}
y_2 &= -3(x - \mu_{1Hek}) + \mu_{2Hek} \qquad (8.5.5)\\
&= -3x + 3\mu_{1Hek} + \mu_{2Hek}. \qquad (8.5.6)
\end{aligned}$$

Now we compute the following integral which is equal to the area of the region ω_{11} which is bounded by the functions y_2 and $y = -x$ from r_1 to x_2.

$$\begin{aligned}
\mathrm{Area}(\omega_{11}) &= \int_{r_1}^{x_2} y_2 - y\mathrm{d}x \qquad (8.5.7)\\
&= \int_{r_1}^{x_2} -3x + (3\mu_{1Hek} + \mu_{2Hek}) - (-x)\mathrm{d}x \qquad (8.5.8)\\
&= \int_{r_1}^{x_2} -2x + (3\mu_{1Hek} + \mu_{2ek})\mathrm{d}x. \qquad (8.5.9)
\end{aligned}$$

Since

$$x_2(r_1) = \frac{9}{8\sqrt[3]{3}} + \frac{16r_1^3 - 1}{32r_1^2}, \tag{8.5.10}$$

therefore

$$\begin{aligned} Area(\omega_{11}) &= -x^2 + (3\mu_{1Hek} + \mu_{2Hek})x|_{r_1}^{x_2} && (8.5.11)\\ &= (-(\frac{9}{8\sqrt[3]{3}} + \frac{16r_1^3 - 1}{32r_1^2})^2 + (3\mu_{1Hek} + \mu_{2Hek})(\frac{9}{8\sqrt[3]{3}} + \frac{16r_1^3 - 1}{32r_1^2})) - (-r_1^2 + (3\mu_{1Hek} + \mu_{2Hek})r_1) && (8.5.12)\end{aligned}$$

Example 64. *Let* $c = -\frac{3}{2}$. *For this energy er have* $r_1 = \frac{1}{4}$, $x_2 = r_2 = \frac{1}{2}$, $\mu_{1Hek} = \frac{1}{2\sqrt[3]{3}}$ *and* $\mu_{2Hek} = \frac{1}{4}\sqrt[3]{9} - \frac{3}{4}$. *Thus the area of the region* ω_{11} *is*

$$\begin{aligned} Area(\omega_{11}) &= \int_{\frac{1}{4}}^{\frac{1}{2}} -2x + (3\mu_{1Hek} + \mu_{2Hek})dx && (8.5.13)\\ &= -(\frac{1}{2})^2 + (3\frac{1}{2\sqrt[3]{9}} - \frac{3}{4})(\frac{1}{2}) - ((-\frac{1}{4})^2 + (3\frac{1}{2\sqrt[3]{9}} - \frac{3}{4})(\frac{1}{4})) && (8.5.14)\\ &= -\frac{3}{16} + (3\frac{1}{2\sqrt[3]{9}} - \frac{3}{4})(\frac{1}{4}) && (8.5.15)\\ &\approx 0.01501571682 && (8.5.16)\end{aligned}$$

In the example 63, we showed that for the first root $r_1 = \frac{1}{4}$, i.e. the energy $c = -\frac{3}{2}$, we have the following relation between the area of ω_1 and the rest part in the SCTD $\mathcal{K}_c^b$,

$$\frac{Area(\mathcal{K}_c^b - \omega_1)}{Area(\omega_1)} = \frac{1}{2}. \tag{8.5.17}$$

We define the function $\mathcal{F}$ as follow,

$$\begin{aligned} \mathcal{F} : (0, \frac{1}{4}] &\longrightarrow \mathbb{R} && (8.5.18)\\ \mathcal{F}(r) &= \frac{Area(\mathcal{K}_c^b - \omega_1)}{Area(\omega_1)}.\end{aligned}$$

Now we show that the function $\mathcal{F}$ for every $r_1 \in [0, \frac{1}{2}]$ or equivalently for all energy $c \leqslant -\frac{3}{2}$ is less than or equal to $\frac{1}{2}$.

Theorem 65. *Let* $c \leqslant -\frac{3}{2}$. *We have the following inequality,*

$$\mathcal{F}(r_1) = \frac{Area(\mathcal{K}_c^b - \omega_1)}{Area(\omega_1)} \leqslant \frac{1}{2} \qquad \forall r_1 \in [0, \frac{1}{4}]. \tag{8.5.19}$$

Proof. From the relations 8.5.2 and 8.5.1, we have the following identities

$$\begin{aligned} \mathrm{Area}(\mathcal{K}_c^b - \omega_1) =& \frac{2r_1^2}{-1+\sqrt{1-4^3r_1^3}} + \frac{5-\sqrt{1-4^3r_1^3}-48r_1^3}{32r_1} + \frac{-2+2\sqrt{1-4^3r_1^3}-64r_1^3}{2\times 32^2 r_1^4}, \\ \mathrm{Area}(\omega_1) =& r_1^2. \end{aligned} \tag{8.5.20}$$

We take these two identities and compute the following relation

$$\begin{aligned} \frac{\mathrm{Area}(\mathcal{K}_c^b - \omega_1)}{\mathrm{Area}(\omega_1)} &= \frac{\frac{2r_1^2}{-1+\sqrt{1-4^3r_1^3}} + \frac{5-\sqrt{1-4^3r_1^3}-48r_1^3}{32r_1} + \frac{-2+2\sqrt{1-4^3r_1^3}-64r_1^3}{2\times 32^2 r_1^4}}{r_1^2} \\ &= \frac{2}{-1+\sqrt{1-4^3r_1^3}} + \frac{5-\sqrt{1-4^3r_1^3}-48r_1^3}{32r_1^3} + \frac{-1+\sqrt{1-4^3r_1^3}-32r_1^3}{32^2r_1^6} \\ &= \frac{2}{-1+\sqrt{1-4^3r_1^3}} + \frac{5-\sqrt{1-4^3r_1^3}}{32r_1^3} - \frac{3}{2} + \frac{-1+\sqrt{1-4^3r_1^3}}{32^2r_1^6} - \frac{1}{32r_1^3}. \end{aligned} \tag{8.5.21}$$

For simplicity, we define $R := r_1^3$. Thus we have

$$\begin{aligned} \frac{\mathrm{Area}(\mathcal{K}_c^b - \omega_1)}{\mathrm{Area}(\omega_1)} =& \frac{2}{-1+\sqrt{1-4^3R}} + \frac{5-\sqrt{1-4^3R}}{32R} - \frac{3}{2} + \frac{-1+\sqrt{1-4^3R}}{32^2R^2} - \frac{1}{32R} \\ =& \frac{2}{-1+\sqrt{1-4^3R}} + \frac{4-\sqrt{1-4^3R}}{32R} - \frac{3}{2} + \frac{-1+\sqrt{1-4^3R}}{32^2R^2} \\ =& \frac{2}{-1+\sqrt{1-4^3R}} + \frac{-1-\sqrt{1-4^3R}}{-1-\sqrt{1-4^3R}} + \frac{4-\sqrt{1-4^3R}}{32R} + \frac{-1+\sqrt{1-4^3R}}{32^2R^2} - \frac{3}{2} \\ =& \frac{3-2\sqrt{1-4^3R}}{32R} + \frac{-1+\sqrt{1-4^3R}}{32^2R^2} - \frac{3}{2}. \end{aligned} \tag{8.5.22}$$

Now we take the first derivative of the equation 8.5.22 respect to R. Thus we have

$$\begin{aligned} \frac{d(\frac{\mathrm{Area}(\mathcal{K}_c^b - \omega_1)}{\mathrm{Area}(\omega_1)})}{dR} &= \frac{-64R - 3\sqrt{1-4^3R}+2}{32R^2\sqrt{1-4^3R}} + \frac{48R+\sqrt{1-4^3R}-1}{512R^3\sqrt{1-4^3R}} \\ &= \frac{-1024R^2 - 48R\sqrt{1-4^3R} + 80R + \sqrt{1-4^3R} - 1}{512R^3\sqrt{1-4^3R}}. \end{aligned} \tag{8.5.23}$$

If we put the nominator of the above equation equal to zero, then we can get the zeros of the nominator at the points $R = 0$ and $R = \frac{1}{64} = \frac{1}{4^3}$. From the definition, we have $r_1 = \sqrt[3]{R} = \frac{1}{4}$. Therefore the function $\mathcal{F}$ on its domain $(0, \frac{1}{4}]$ is monotone increasing. Note that the function $\mathcal{F}$ take its maximal value at the point $\frac{1}{4}$, i.e. $\mathcal{F}(\frac{1}{4}) = \frac{1}{2}$, which we have already obtained in the example 63. □

Corollary 66. *The weight $W_1(r_1) = \sqrt{2}r_1$ for the ECH capacities of the RKP in the SCTD in the first weight of the ECH capacities of the RKP.*

Example 67. *In this example we are going to compute the ECH capacities for the RKP, using the SCTD $\mathcal{K}_c^b$ for some k when the energy $c = -\frac{3}{2}$.*

First if we use the equations of weights which are introduced in this chapter, we can get the following values

$$\begin{aligned} W_1(c) \approx & \sqrt{2} r_1 = 0.353554 \\ W_2(r_1) \approx & 0.219247 \\ W_3(r_1) \approx & 0.0502325 \\ W_4(r_1) \approx & 0.223766 \\ W_5(r_1) \approx & 0.0514663 \end{aligned} \tag{8.5.24}$$

Note that for the energy $c = -\frac{3}{2}$*, we have* $r_1 = \frac{1}{4}$*,* $r_2 = \frac{1}{2}$ *and form examples 63 and 64 we know*

$$\begin{aligned} Area(\mathcal{K}_c^b) &= \frac{3}{32} \\ Area(\omega_1) &= \frac{1}{16} \\ Area(\mathcal{K}_c^b - \omega_1) &= \frac{1}{32} \\ Area(\omega) &\approx 0.01501571682 \end{aligned} \tag{8.5.25}$$

And also Theorem 65 says that $W_1(c)$ *is the first weight of the ECH capacities of the RKP.*

Therefore the above computations give us the following order of the weights $W_1, \cdots, W_5$*, and* W_j *when* $j \in \mathbb{N}$ *and* $j \geqslant 6$

$$W_1 > W_4 > W_2 > W_5 > W_3 > W_j, \qquad \forall j \geqslant 6. \tag{8.5.26}$$

Now consider the inequality

$$d^2 + d \leqslant 2k \tag{8.5.27}$$

Than we can have the following table.

Rank	The ECH cap. for $\mathcal{K}^b_c$	The ECH cap. for $c = -\frac{3}{2}$
$c_1(\mathcal{K}^b_c)$	W_1	0.353554
$c_2(\mathcal{K}^b_c)$	$W_1 + W_4 = c_1 + W_4$	0.57732
$c_3(\mathcal{K}^b_c)$	$2W_1 = 2c_1$	0.707108
$c_4(\mathcal{K}^b_c)$	$2W_1 + W_4 = c_3 + W_2$	0.930874
$c_5(\mathcal{K}^b_c)$	$2W_1 + W_4 + W_2 = c_4 + W_2$	1.150121
$c_6(\mathcal{K}^b_c)$	$2W_1 + 2W_4 = 2c_2$	1.15464
$c_7(\mathcal{K}^b_c)$	$3W_1 + W_4 = 3c_1 + W_4$	1.284428
$c_8(\mathcal{K}^b_c)$	$3W_1 + W_4 + W_2 = c_7 + W_2$	1.503675
$c_9(\mathcal{K}^b_c)$	$3W_1 + 2W_4 = c_7 + W_4$	1.508194
$c_{10}(\mathcal{K}^b_c)$	$3W_1 + 2W_4 + W_2 = c_9 + W_2$	1.727441
$c_{20}(\mathcal{K}^b_c)$	$5W_1 + W_4 + W_2 + W_5$	2.2622493

Table 8.1: ECH capacities for $c = -\frac{3}{2}$

Chapter 9

Appendix 1

9.1 The Restricted Three Body Problem

In this thesis, we focused on the Kepler problem and the RKP. But in this chapter, we are going to study about the restricted three body problem. The rotating Kepler problem is a limit case of the R3BP when the mass of one of the primaries vanishes.

Using the R3BP, we can explain the behaviour of a three body dynamical system when the mass of one body is zero. In the language of physic, we can describe the R3BP as the solar system, namely the Sun-Jupiter system. Since they are much heavier, we can assume all other bodies are massless in this dynamical system.

As we said in the last paragraph, the R3BP has two masses that we consider as the earth and the moon. We scale the total mass to one and if we denote the mass of the moon with $\mu \in [0, 1]$ then the mass of the earth will be $1 - \mu \in [0, 1]$.

We denote the moon by $m(t) \in \mathbb{R}^3$ and the earth by $e(t) \in \mathbb{R}^3$ for $t \in \mathbb{R}$ such that the earth and the moon move in 3-dimensional Euclidean space according to Newton's gravitational law.

This dynamical system has another part which consist of a massless object refereed to as the satellite. Note that the satellite does not influence the moon and the earth, but they attract the satellite according to Newton's gravitational law. One of the interesting parts of the R3BP is understanding the dynamics of the satellite. In this chapter, we denote the position of the satellite by q and its momentum by p. Thus we can give the Hamiltonian of the satellite in the inertial system by

$$\begin{aligned} E_t :&(\mathbb{R}^3 \setminus \{e(t), m(t)\}) \longrightarrow \mathbb{R} \\ E_t(q,p) =&\frac{1}{2}|p^2| - \frac{\mu}{|q - m(t)|} - \frac{1-\mu}{|q - e(t)|} \end{aligned} \tag{9.1.1}$$

where $e(t)$, $m(t) \in \mathbb{R}^3$ and this relation follows form Newton's gravitational law such that the Hamiltonian is the sum of kinetic energy and the Newton potential.

We assume that the satellite moves in the elliptic, i.e. the plane spanned by the orbits of the earth and the moon. By choosing a suitable coordinate system such that for every $t \in \mathbb{R}$, $e(t)$ and $m(t) \in \mathbb{R}^2$ we can have the

Hamiltonian

$$E_t : T^*(\mathbb{R}^2 \setminus \{e(t), m(t)\} \longrightarrow \mathbb{R}. \tag{9.1.2}$$

This domain is refereed to as the planar restricted three body problem while if the satellite moves in three dimensional space, this problem is called the spatial restricted three body problem.

From now, we only consider the planar case and assume in additional that the earth and the moon move on a circle about their common center of mass. Choosing coordinates such that $e(t) = -\mu(\cos(t), -\sin(t))$ and $m(t) = (1-\mu)(\cos(t), -\sin(t))$.

Using the above coordinate refereed our problem to the circular planar restricted three body problem and there is also a circular spatial restricted three body problem.

Note that the moon and the earth are moving in the Hamiltonian, so it is not autonomous, i.e. it depends on time. Even the domain of the Hamiltonian is time dependent. On the other hand, since the Hamiltonian depends on time it is not preserved under the flow of its time dependent Hamiltonian vector field, i.e. preservation of the energy does not hold.

In the above description, we said the Hamiltonian E_t even in the circular case is time dependent. But we can apply a time depend transformation such that the Hamiltonian of the circular restricted three body problem in the rotating coordinates becomes autonomous, i.e. independent of time and in particular, it is preserved along its flow.

In the next section, we explain the time transformation and its situations.

9.2 Time Dependent Transformation

Given (M, ω) a symplectic manifold and $E \in C^\infty(M \times \mathbb{R}, \mathbb{R})$ and $L \in C^\infty(M \times \mathbb{R}, \mathbb{R})$ two time dependent Hamiltonians. We abbreviate these Hamiltonians by $E_t = E(., t) \in C^\infty(M)$ and $L_t = L(., t) \in C^\infty(M)$. From these Hamiltonians we can have the Hamiltonian vector fields as X_{E_t} and X_{L_t}. We define the flow of the Hamiltonian vector fields ϕ_E^t and ϕ_L^t and assume that they exist for all times.

We define the time dependent Hamiltonian function as

$$L \diamondsuit E \in C^\infty(M \times \mathbb{R}, \mathbb{R}) \tag{9.2.1}$$

$$(L \diamondsuit E)(x, t) = L(x, t) + E((\phi_L^t)^{-1}x, t), \qquad x \in M, \quad t \in \mathbb{R}. \tag{9.2.2}$$

We show that the equality

$$\phi_{L\diamondsuit E}^t = \phi_L^t \circ \phi_E^t \tag{9.2.3}$$

holds for all $t \in \mathbb{R}$.

To show the above equality, let $x \in M$ and assume $\xi \in T_yM$ where $y = \phi_L^t(\phi_e^t))$. Since ϕ_E^t preserved the

symplectic form, we have

$$\begin{aligned}\omega(\xi, \frac{d}{dt}(\phi_L^t(\phi_E^t)(x)) &= \omega(\xi, X_{L_t}(y) + d\phi_L^t(\phi_E^t(x))X_{E_t}(\phi_E^t(x))) \\ &= dL_t(y)\xi + \omega(\xi, X_{E_t}((\phi_L^t)^{-1}(y)), (d\phi_L^t)^{-1}(y)) \\ &= dL_t(y)\xi + d(E \circ (\phi_L^t)^{-1})(y)\xi \\ &= d(L\diamondsuit E)_t(y)\xi.\end{aligned} \tag{9.2.4}$$

This is the proof of the above claim.

Note that in the above definition, we consider two time dependent Hamiltonians. But even if we take two autonomous Hamiltonian E and L, the function $L\diamondsuit E$ does not need to be autonomous, unless E is invariant under the flow of L.

9.3 The Circular Restricted Three Body Problem in the Rotating Frame

In this section we only consider the Hamiltonian 9.1.2 which is given with its condition in the first section of this chapter.

In the last section, we defined the transformation function. Now assume that function, L is the angular momentum which is given as follows

$$L \in C^\infty(T^*\mathbb{R}^2, \mathbb{R}), \qquad (q, p) \mapsto q_1p_2 - q_2p_1. \tag{9.3.1}$$

Define

$$E' := L\diamondsuit E. \tag{9.3.2}$$

We know that the angular momentum generates the rotation and if we let

$$e = (-\mu, 0), \qquad m = (1 - \mu, 0), \tag{9.3.3}$$

then we can write the Hamiltonian 9.3.2 as

$$E'(q, p) = \frac{1}{2}|p|^2 - \frac{\mu}{|q - m|} - \frac{1 - \mu}{|q - e|} + q_1p_2 - q_2p_1. \tag{9.3.4}$$

Observe that the above Hamiltonian is autonomous.

For simplicity, we denote the above Hamiltonian with E and omit the prime.

From the preservation property, the Hamiltonian E is preserved in the rotating frame. Note that the Hamiltonian 9.3.4 is autonomous only in the circular case.

Example 68. *If the primaries move on ellipses with positive eccentricity, it is called elliptical restricted three body problem and the Hamiltonian* E *does not become time dependent.*

Define Newton's potential for the earth and the moon as

$$V : \mathbb{R}^2 \setminus \{e, m\} \longrightarrow \mathbb{R} \tag{9.3.5}$$

$$q \mapsto -\frac{\mu}{|q-m|} - \frac{1-\mu}{|q-e|}. \tag{9.3.6}$$

Thus we have the equation of motion as

$$\begin{cases} q_1' = & p_1 - q_2 \\ q_2' = & p_2 + q_1 \\ p_1' = & -p_2 - \dfrac{\partial V}{\partial q_1} \\ p_2' = & p_1 - \dfrac{\partial V}{\partial q_2} \end{cases} \tag{9.3.7}$$

If we compute the second derivative of the above equation with respect to q, we have

$$\begin{aligned} q_1'' =& p_1' - q_2' = -p_2 - \frac{\partial V}{\partial q_1} - p_2 - q_1 = -2q_2' + q_1 - \frac{\partial V}{\partial q_1} \\ q_2'' =& p_2' + q_2' = p_1 - \frac{\partial V}{\partial q_2} + p_1 - q_2 = 2q_1' + q_2 - \frac{\partial V}{\partial q_2}. \end{aligned} \tag{9.3.8}$$

Then we can get that the first order ODE 9.3.7 is equivalent to the second order ODE

$$\begin{cases} q_1'' = & -2q_2' + q_1 - \dfrac{\partial V}{\partial q_1} \\ q_2'' = & 2q_1' + q_2 - \dfrac{\partial V}{\partial q_2} \end{cases} \tag{9.3.9}$$

We give a physical interpretation for the Hamiltonian 9.3.4. Complete the squares in 9.3.4 as

$$E(q, p) = \frac{1}{2}((p_1 - q_2)^2 + (p_2 + q_1)^2) - \frac{\mu}{|q-m|} - \frac{1-\mu}{|q-e|} - \frac{1}{2}q^2. \tag{9.3.10}$$

Form this Hamiltonian we can define the effective potential as follows which is a function of q only

$$U : \mathbb{R}^2 \setminus \{e, m\} \longrightarrow \mathbb{R} \tag{9.3.11}$$

$$q \mapsto -\frac{\mu}{|q-m|} - \frac{1-\mu}{|q-e|} - \frac{1}{2}q^2 = V(q) - \frac{1}{2}q^2. \tag{9.3.12}$$

Thus we can say the function is the sum of Newton's potential plus $-\frac{1}{2}q^2$, where the additional term give rise to the centrifugal force in the rotating coordinates.

This Hamiltonian is a magnetic Hamiltonian which contains a twist in the kinetic part that we can interpret in physics term as the Coriolis force. This force only depends on the velocity. But the gravitational force and the centrifugal force only depend on the position. Therefore we now can find the reason, why the Hamiltonian of the R3BP in the rotating coordinates becomes a magnetic Hamiltonian.

Now in this sense, the satellite is attract by four forces in the rotating system, the gravitation of forces of the

earth and the moon, the centrifugal force and the Coriolis force.

9.3.1 The Lagrangian Points

From the Chapters 2, 3 and the first section of this chapter, we got to know some basic definitions and the properties of the R3BP and the RKP. Here we assume the readers are familiar with them and explain the Lagrangian points.

Given the projection map

$$\pi : \mathbb{R}^4 = \mathbb{R}^2 \times \mathbb{R}^2 \longrightarrow \mathbb{R}^2 \tag{9.3.13}$$

$$(q, p) \mapsto q, \tag{9.3.14}$$

we restrict it to $\mathrm{crit}(E)$ and get a bijection map

$$\pi|_{\mathrm{crit}(E)} : \mathrm{crit}(E) \longrightarrow \mathrm{crit}(U) \tag{9.3.15}$$

where $\mathrm{crit}(E)$ is the critical set of the Hamiltonian E such that the inverse of this map at a critical point $(q_1, q_2) \in \mathrm{crit}(E)$ is

$$(\pi|_{\mathrm{crit}(E)})^{-1}(q_1, q_2) = (q_1, q_2, q_2, -q_1). \tag{9.3.16}$$

Now if we let $\mu \in (0, 1)$, the effective potential U has five critical points called Lagrangian points.

Suppose the axis x is the axis of the earth and the moon. Since the relation 9.3.16 maps the point (q_1, q_2) to the point $(q_1, -q_2)$, we can see that U is invariant under reflection at this axis.

This invariance property of U, gives us two different cases of the critical points of U. The first case has three critical points that lie on the axis of the earth and the moon, i.e. they are fixed under reflection. These are saddle points of U. These collinear points were discovered by Euler. There are two other critical points which are maxima of U. The reflection at the x-axis interchanges them. They were discovered by Lagrange. These points make an equilateral triangle with the earth and the moon.

We first explain the collinear points and give some properties of them. Given the effective potential U restricted to $\mathbb{R} \setminus \{-\mu, 1-\mu\}$ we define a new function as

$$u : U|_{\mathbb{R}\setminus\{-\mu,1-\mu\}} : \mathbb{R} \setminus \{-\mu, 1-\mu\} \longrightarrow \mathbb{R} \tag{9.3.17}$$

$$r \mapsto \frac{-\mu}{|r+\mu-1|} - \frac{1-\mu}{|r+\mu|} - \frac{r^2}{2}. \tag{9.3.18}$$

We know that U is invariant under the reflection at the axis earth-moon. Hence the critical points of u are the same as the critical points of U on the axis. On the other hand, the critical points of U are the same as the critical points of E. Therefore we can use the critical point of u to find these collinear Lagrangian points of the Hamiltonian E.

The function u has singularities at $-\mu$, $1-\mu$, $-\infty$ and $+\infty$ and in these points the function u goes to $-\infty$.

Take the second derivative of u,

$$u''(r) = \frac{-2\mu}{|r+\mu-1|^3} - \frac{2(1-\mu)}{|r+\mu|^3} - 1 < 0. \tag{9.3.19}$$

This inequality says that u is a strictly convex function. Hence there are precisely three maxima of the function u such that if we denote the maximal points by l_1, l_2 and l_3 they live in the intervals as $\mu < l_1 < 1-\mu$, $l_2 < 1-\mu$ and $l_3 > -\mu$.

The maxima points l_1, l_2 and l_3 are called the Lagrangian collinear points. Therefore we can give the following lemma.

Lemma 69. *The three collinear Lagrange points are saddle points of the effective potential* U.

Proof. We will proof the Lemma later when we introduced the Lagrangian points l_4 and l_5. □

In this part, we explain the equilateral points of Lagrange. For this purpose, we only consider the upper half-space $\mathbb{R}\times(0,\infty)$. Since we can use the reflection symmetry for the lower half-space of $\mathbb{R}\times(0,\infty)$, we skip the lower part.

Note that the distance between earth and the moon is one, i.e., $|e-m|=1$ and define

$$\Theta := \{(\rho,\sigma)\in(0,\infty)^2 : \rho+\sigma>1, |\rho-\sigma|<1\} \tag{9.3.20}$$

and also a diffeomorphism

$$\phi : \mathbb{R}\times(0,\infty) \longrightarrow \Theta \tag{9.3.21}$$

$$\phi(q) = (|q-m|, |q-e|), \qquad q\in\mathbb{R}\times(0,\infty). \tag{9.3.22}$$

If we define a smooth function $\varphi : \Theta \longrightarrow \mathbb{R}$ by

$$\varphi := U\circ\phi^{-1}, \tag{9.3.23}$$

then we can see the critical points of φ to correspond to the critical points of U in upper half-space. Let $q\in\mathbb{R}\times(0,\infty)$, we can write

$$q^2 = \mu q^2 + (1-\mu)q^2 \tag{9.3.24}$$

$$= \mu(\rho^2 + 2<m,q> - m^2) + (1-\mu)(\sigma^2 + 2<e,q> - e^2) \tag{9.3.25}$$

$$= \mu\rho^2 + 2\mu(1-\mu)<1,q> - \mu(1-\mu)^2 + (1-\mu)\sigma^2 \tag{9.3.26}$$

$$\quad - 2\mu(1-\mu)<1-q> - (1-\mu)\mu^2 \tag{9.3.27}$$

$$= \mu\rho^2 + (1-\mu)\sigma^2 - \mu(1-\mu). \tag{9.3.28}$$

Thus the the function φ satisfies the equality

$$\varphi(\rho,\sigma) = -\frac{\mu}{\rho} - \frac{1-\mu}{\sigma} - \frac{1}{2}(\mu\rho^2 + (1-\mu)\sigma^2 - \mu(1-\mu)). \tag{9.3.29}$$

and its first derivative is

$$d\varphi(\rho,\sigma) = \frac{\mu(1-\rho^3)}{\rho}d\rho + \frac{(1-\mu)(1-\sigma^3)}{\sigma^2}d\sigma. \tag{9.3.30}$$

If we put the above equation equal to zero we get a unique critical point at $(1,1) \in \Theta$ for φ and the Hessian of φ at the point $(1,1)$ is

$$H_\varphi(1,1) = \begin{bmatrix} -3\mu & 0 \\ 0 & -3(1-\mu) \end{bmatrix} \tag{9.3.31}$$

That says the function φ at this point is a maximum.

Denote the fourth Lagrangian point by l_4 and define it by

$$l_4 = \phi^{-1}(1,1) := (\frac{1}{2} - \mu, \frac{\sqrt{3}}{2}). \tag{9.3.32}$$

The Lagrangian point l_4 is defined in the upper half-space, so by reflection at the axis of earth and moon, we can define the Lagrangian point l_5 by

$$l_5 := (\frac{1}{2} - \mu, -\frac{\sqrt{3}}{2}). \tag{9.3.33}$$

Using the reflection symmetry, the Lagrangian point l_5 is a maxima of U as well which is related to the unique critical point in the lower half-space $\mathbb{R} \times (-\infty, 0)$.

The complement of the axis earth-moon is $\mathbb{R}^2 \setminus (\mathbb{R} \times \{0\})$. So we can summarize the above result by the following lemma.

Lemma 70. *The only critical points of* U *on* $\mathbb{R}^2 \setminus (\mathbb{R} \times \{0\})$*, are* l_4 *and* l_5 *and they are also maxima of* U*.*

Corollary 71. *The effective potential have global maximum precisely at the two equilateral Lagrange points, namely*

$$\max U = U(l_4) = U(l_5) = -\frac{3}{2} - \frac{\mu(\mu-1)}{2}. \tag{9.3.34}$$

Proof. We compute the value of $U(l_4)$ by using the relation 9.3.30,

$$U(l_4) = \phi(1,1) = -\mu - (1-\mu) - \frac{1}{2}(\mu + 1 - \mu - \mu(1-\mu)) = -\frac{3}{2} + \frac{\mu(1-\mu)}{2}. \tag{9.3.35}$$

□

Now we can proof the lemma 69.

Proof. First we need to show that

$$\det \begin{bmatrix} \frac{\partial^2 U}{\partial q_1^2}(l_i) & \frac{\partial^2 U}{\partial q_1 \partial q_2}(l_i) \\ \frac{\partial^2 U}{\partial q_1 \partial q_2}(l_i) & \frac{\partial^2 U}{\partial q_2^2}(l_i) \end{bmatrix} < 0, \qquad 1 \leqslant i \leqslant 3. \tag{9.3.36}$$

To compute this determinate, we compute all of the component of the matrix separately. We know that U is invariant under reflection at the q_1 axis and the three collinear Lagrange points are fixed points by this reflection. So

$$\frac{\partial^2 U}{\partial q_1 \partial q_2}(l_i) = 0, \qquad 1 \leqslant i \leqslant 3. \tag{9.3.37}$$

and

$$\frac{\partial^2 U}{\partial q_1^2}(l_i) < 0, \qquad 1 \leqslant i \leqslant 3. \tag{9.3.38}$$

Therefore we need to check just the following inequality,

$$\frac{\partial^2 U}{\partial q_1^2}(l_i) > 0, \qquad 1 \leqslant i \leqslant 3. \tag{9.3.39}$$

Assume the collinear Lagrange points are nondegenerate. In this sense, the kernel of the Hessian of them is trivial. So this equivalent to the assumption

$$\frac{\partial^2 U}{\partial q_1^2}(l_i) \neq 0, \qquad 1 \leqslant i \leqslant 3. \tag{9.3.40}$$

The Euler characteristic of the two fold punched plane satisfies

$$\chi(\mathbb{R} \setminus \{e, m\}) = -1. \tag{9.3.41}$$

Denote the number of maxima of U, the number of the saddle points of U and the number of minima of U by ν_2, ν_1 and ν_0 respectively. Since U goes to $-\infty$ at infinity as well as at the singularities e and m and from the Poincare'-Hopf index theorem, we can write

$$\nu_2 - \nu_1 - \nu_0 = \chi(\mathbb{R}^2 \setminus \{e, m\}) = -1. \tag{9.3.42}$$

By Lemma 70 we know that l_4 and l_5 are maxima, so that

$$\nu_2 \geqslant 2. \tag{9.3.43}$$

Three colinear Lagrange points are maxima of u, if we restrict U to the axis through earth and moon. It follows that they are either saddle points or maxima of U. In particular

$$\mu_0 = 0 \tag{9.3.44}$$

and therefore

$$\mu_1 + \mu_2 = 5. \tag{9.3.45}$$

Now from 9.3.42, 9.3.44 and 9.3.45, we have

$$\nu_2 = 2, \qquad \nu_1 = 3. \tag{9.3.46}$$

Thus the lemma is established in the nondegenerate case. □

Consider the projection map $\pi|_{\mathrm{crit}(E)}$. Via this projection , the critical points of the Hamiltonian E and the critical points of the effective potential have a one-to-one correspondence, and we know that the value of E at a critical point coincides with the value of U of its projection. It is interesting to compute that with the rotating Kepler problem. Now if we denote the Hamiltonian of the rotating Kepler problem by K, it has a unique critical value $-\frac{3}{2}$ that will determine the boundary of the concave toric domain for the rotating Kepler problem in Chapter 3, and we use this critical point when we want to compute the ECH capacities for the rotating Kepler problem in Chapter 8.

The saddle points of U have some properties that we find in the following lemma.

Lemma 72. *If $\mu \in (0, \frac{1}{2})$ the critical values of the collinear Lagrange points are ordered as follows*

$$U(l_1) < U(l_2) < U(l_3), \tag{9.3.47}$$

and for $\mu = \frac{1}{2}$, we have

$$U(l_1) < U(l_2) = U(l_3). \tag{9.3.48}$$

If $\mu \in (\frac{1}{2}, 1)$ by interchanging the roles of the earth and the moon. We get

$$U(l_1) < U(l_3) < U(l_2). \tag{9.3.49}$$

Proof. Let $\mu \in (0,1)$ and $-\mu < q < 1-\mu$ and show that $U(l_1) < U(l_2)$. We abbreviate $\rho := 1-\mu-q > 0$ and set $q' := 1-\mu+\rho$ and identify $\mathbb{R}$ with $\mathbb{R} \times \{0\} \subset \mathbb{R}^2$. We can write

$$U(q') - U(q) = -\frac{\mu}{\rho} - \frac{1-\mu}{1+\rho} - \frac{1}{2}(1-\mu+\rho)^2 + \frac{\mu}{\rho} + \frac{1-\mu}{1-\rho} + \frac{1}{2}(1-\mu-\rho)^2 \tag{9.3.50}$$

$$= (1-\mu)\left(\frac{1}{1-\rho} - \frac{1}{1-\rho} - 2\rho\right) \tag{9.3.51}$$

$$= \frac{2(1-\mu)\rho^3}{1-\rho^2} \tag{9.3.52}$$

$$> 0. \tag{9.3.53}$$

In particular, for $q = l_1$ we have

$$U(l_1) < U(l_1') \leqslant U(l_2), \tag{9.3.54}$$

where for the last inequality we use the maximum of the restriction of U to $(1-\mu, \infty)$.

For the second step, we will show that $U(l_2) < U(l_3)$ for $0 < \mu < \frac{1}{2}$. Let $q > 1-\mu$, we estimate

$$\begin{aligned}
U(-q) - U(q) &= -\frac{\mu}{1-\mu+q} - \frac{1-\mu}{q-\mu} - \frac{q^2}{2} + \frac{\mu}{q-1+\mu} + \frac{1-\mu}{q+\mu} + \frac{q^2}{2} && (9.3.55)\\
&= \mu\left(\frac{1}{q-(1-\mu)} - \frac{1}{q+(1-\mu)}\right) + (1-\mu)\left(\frac{1}{q+\mu} - \frac{1}{q-\mu}\right) && (9.3.56)\\
&= \frac{2\mu(1-\mu)}{q^2-(1-\mu)^2} - \frac{2\mu(1-\mu)}{q^2-\mu^2} && (9.3.57)\\
&= \frac{2\mu(1-\mu)((1-\mu)^2-\mu^2)}{(q^2-(1-\mu)^2)(q^2-\mu^2)} && (9.3.58)\\
&= \frac{2\mu(1-\mu)(1-2\mu)}{q^2-(1-\mu)^2)(q^2-\mu^2)} && (9.3.59)\\
&> 0. && (9.3.60)
\end{aligned}$$

Now for $q = l_2$ and l_3 are the maximum of the restriction of U to $(-\infty, -\mu)$. So we have

$$U(l_2) < U(-l_2) \leqslant U(l_3). \tag{9.3.61}$$

Finally let $\mu = \frac{1}{2}$, the effective potential U is invariant under reflection at the y-axis $(q_1, q_2) \mapsto (-q_1, q_2)$ as well and l_2 is mapped to l_3 under reflection at the x-axis. □

We showed the projection map

$$\pi|_{crit(E)} : crit(E) \longrightarrow crit(U) \tag{9.3.62}$$

is a bijection. We now denote the preimages of the projection map $\pi|_{crit(E)}$ as follows

$$L_i = \pi|^{-1}_{crit(E)}(l_i) \in crit(E) \tag{9.3.63}$$

for $i \in \{1, 2, 3, 4, 5\}$.

For $l_i = (q_1^i, q_2^i)$, we have

$$L_i = (q_1^i, q_2^i, -q_2^i, q_1^i) \tag{9.3.64}$$

and

$$H(L_i) = U(l_i). \tag{9.3.65}$$

Using the above notation, denote the Morse index of L_i by $\mu(L_i)$. The Morse index $\mu(L_i)$ at a critical point of H

is the number of negative eigenvalues of the Hessian of H at L_i, therefore we have

$$\mu(L_i) = \mu(l_i). \tag{9.3.66}$$

Theorem 73. *For $\mu \in (0,1)$ the Morse indices of the five critical points of H satisfy the following equalities*

$$\mu(L_1) = \mu(L_2) = \mu(L_3) = 1, \qquad \mu(L_4) = \mu(L_5) = 2. \tag{9.3.67}$$

If $\mu \in (0, \frac{1}{2})$ the critical values of H are ordered as

$$H(L_1) < H(L_2) < H(L_3) < H(L_4) = H(L_5). \tag{9.3.68}$$

If $\mu = \dfrac{1}{2}$, then the critical values satisfy

$$H(L_1) < H(L_2) = H(L_3) < H(L_4) = H(L_5). \tag{9.3.69}$$

9.4 Hill's Region

Given the Hamiltonian of the planar circular R3BP E in the rotating coordinates as

$$E(q,p) = \frac{1}{2}((p_1 - q_2)^2 + (p_2 - q_2)^2) + U(q), \tag{9.4.1}$$

where $U(q)$ is the effective potential. We showed that the Hamiltonian E is autonomous, so for a fixed energy $c \in \mathbb{R}$, the energy hypersurface or level set is as follow

$$\Sigma_c = E^{-1}(c) \subset T^*(\mathbb{R}^2 \setminus \{e, m\}) \tag{9.4.2}$$

which is preserved under the flow of the Hamiltonian vector field of E.

Consider the footpoint projection

$$\pi : T^*(\mathbb{R}^2 \setminus \{e, m\}) \longrightarrow \mathbb{R}^2 \setminus \{e, m\} \tag{9.4.3}$$

$$(q,p) \mapsto q. \tag{9.4.4}$$

Using this projection map, the Hill's region of Σ_c is defined as the shadow of Σ_c under the footpoint projection map, i.e. we can define the Hill's region as follows

$$\mathfrak{K}_c : \pi(\Sigma_c) \subset \mathbb{R}^2 \setminus \{e, m\}. \tag{9.4.5}$$

The first two quadratic terms of the Hamiltonian of E say that they are nonnegative. This is a guarantee, that we can write the Hill's region as the sublevel set of the effective potential.

In other words, the Hill's region $\mathcal{K}_c$ is

$$\mathcal{K}_c = \{q \in \mathbb{R}^2 \setminus \{e, m\} \mid U(q) \leqslant c\}. \tag{9.4.6}$$

Until now, we defined the Hill's region as the sublevel of the effective potential U. Now we are going to explain, what happens for the Hill's region $\mathcal{K}_c$ when the energy c is changing.

Let the energy be less than the first critical value, i.e. $c < E(L_1)$. In this case, the Hill's region is divided into three connected components as follows

$$\mathcal{K}_c = \mathcal{K}_c^e \cup \mathcal{K}_c^m \cup \mathcal{K}_c^u \tag{9.4.7}$$

where the earth e lies in the closure of $\mathcal{K}_c^e$ and the moon m lies in the closure oh $\mathcal{K}_c^m$. Note that the connected components $\mathcal{K}_c^e$ and $\mathcal{K}_c^e$ are bounded but the connected component $\mathcal{K}_c^u$ is unbounded.

Consider the connected components of $\mathcal{K}_c$, we can decompose the energy hypersurface of the R3BP into the three connected components as follow

$$\Sigma_c = \Sigma_c^e \cup \Sigma_c^m \cup \Sigma_c^u, \tag{9.4.8}$$

where

$$\Sigma_c^e := \{(q, p) \in \Sigma_c, \quad q \in \mathcal{K}_c^e\} \tag{9.4.9}$$

and similarly we can define Σ_c^u and Σ_c^m as well.

Bibliography

[1] U. Frauenfelder, O. v. Koert, The Restricted Three-Body Problem and Holomorphic Curves, Birkhäuser (2019).

[2] P. Albers, J. W. Fish, U. Frauenfelder and O. v. Koert, The Conley-Zehnder indices of the rotating Kepler problem, Mathematical Proceedings of the Cambridge Philosophical Society 154, 243-260 (2012).

[3] K. Choi, D. Cristofaro-Gardiner, D. Frenkel, M. Hutchings, V. G. B. Ramos, Symplectic embeddings into four-dimensional concave toric domains, Journal of Topology 7 (2014), 1054-1076.

[4] T. Ligon, M. Schaaf, On the Global Symmetry of the Classical Kepler Problem, Reports on Math. Phys. 9 (1976), 281-300.

[5] R. Cushman, J. Duistermaat, A Characterization of the Ligon-Schaaf Regularization Map, Comm. Pure Appl. Math. 50 (1997), 773-787.

[6] D.McDuff, D. Salamon, Introduction to Symplectic Topology 2nd edition, Oxford University Press (1998).

[7] B. Bates, M. Bunder, K. Tognetti, Linling the Calkin-Wilf Tree and the Stern-Brocot tree, European Journal of Combinatorics (2010).

[8] D. McDuff, The Hofer conjecture on embedding symplectic ellipsoids, J. Differential Geom. 88 (2011), 519-532.

[9] G. Heckman, T. de Laat, On the Regularization of the Kepler Problem, Jour. Symp. Geom. 10, vol. 3 (2012), 463-473.

[10] E. A. Belbruno, U. Frauenfelder, O. v. Koert, A Family of Periodic Orbits in the Three-Dimensional Lunar Problem, Celestial Mechanics and Dynamical Astronomy, 131, no. 7, Feb.. 2019.

[11] E. A. Belbruno, A new regularization of the restricted three-body problem and an application, Celestial Mechanics, vol. 25, Dec. 1981, p. 397-415.

[12] T. Levi-Civita, Sur la régularisation du probléme des trois corps, Acta Math. 42 (1920), 99-144.